Vol. 63 • No. 7
July 2020

Microwave Journal

ARTIFICIAL INTELLIGENCE

horizon house®
Founded in 1958
mwjournal.com


ANALOG DEVICES
AHEAD OF WHAT'S POSSIBLE™
COMMUNICATIONS
RADAR
ELECTRONIC WARFARE
We Have You Covered from Alpha to Zulu
The industry's most complete portfolio of ICs and modules—from RF to bits.
RF/µW Amplifiers/ TR Modules
Analog Beamforming
Frequency Conversion
Converters and Transceivers
ADC
DAC
Power
Find your competitive advantage at analog.com/ADEF

Designed For
5G MIMO Active Antenna!!!
The World First SMT Microstrip Patented Isolator/Circulator at 28GHz & 38GHz

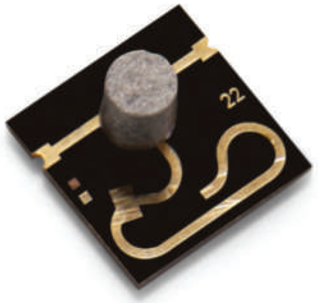

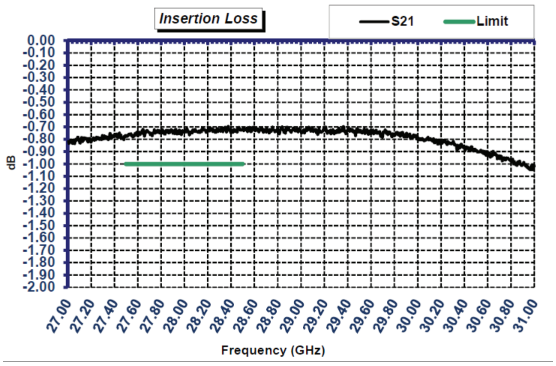

- *No Metal Bias Needed*
- *Easy Reflow Assembly*
- *No Expensive Wire Bonding*

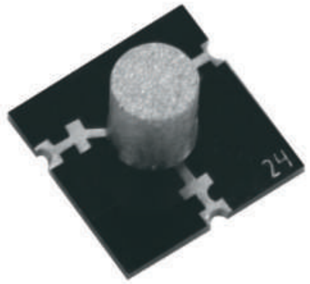

- *200kpcs Sold For Similar Array Application*
- *Proven Technology*

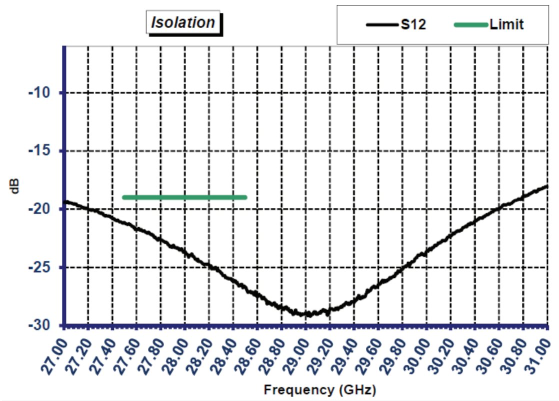

JQL

Tel:1(888)236-9828(US&Canada)

www.jqlelectronics.com sales@jqlelectronics.com

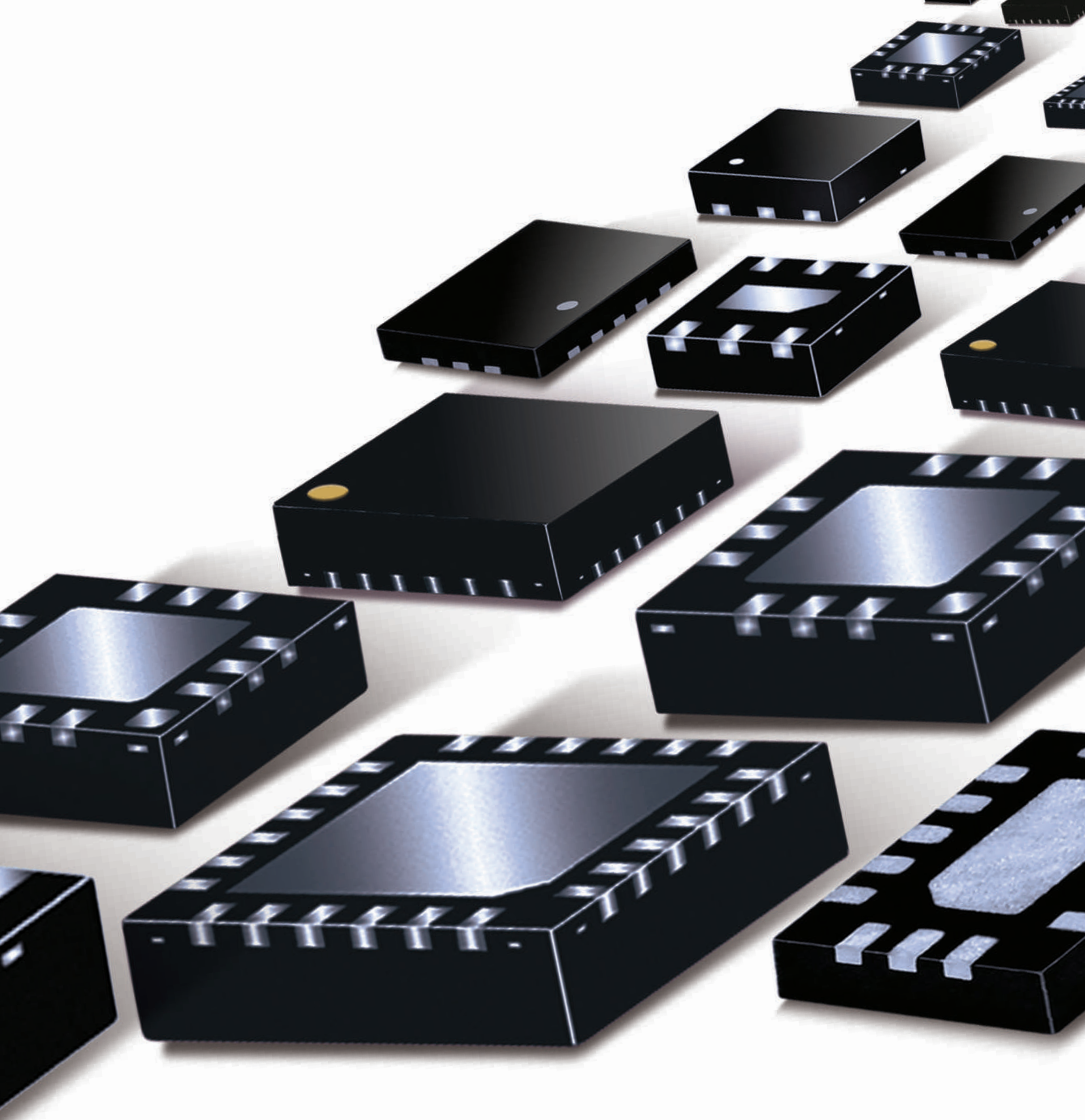

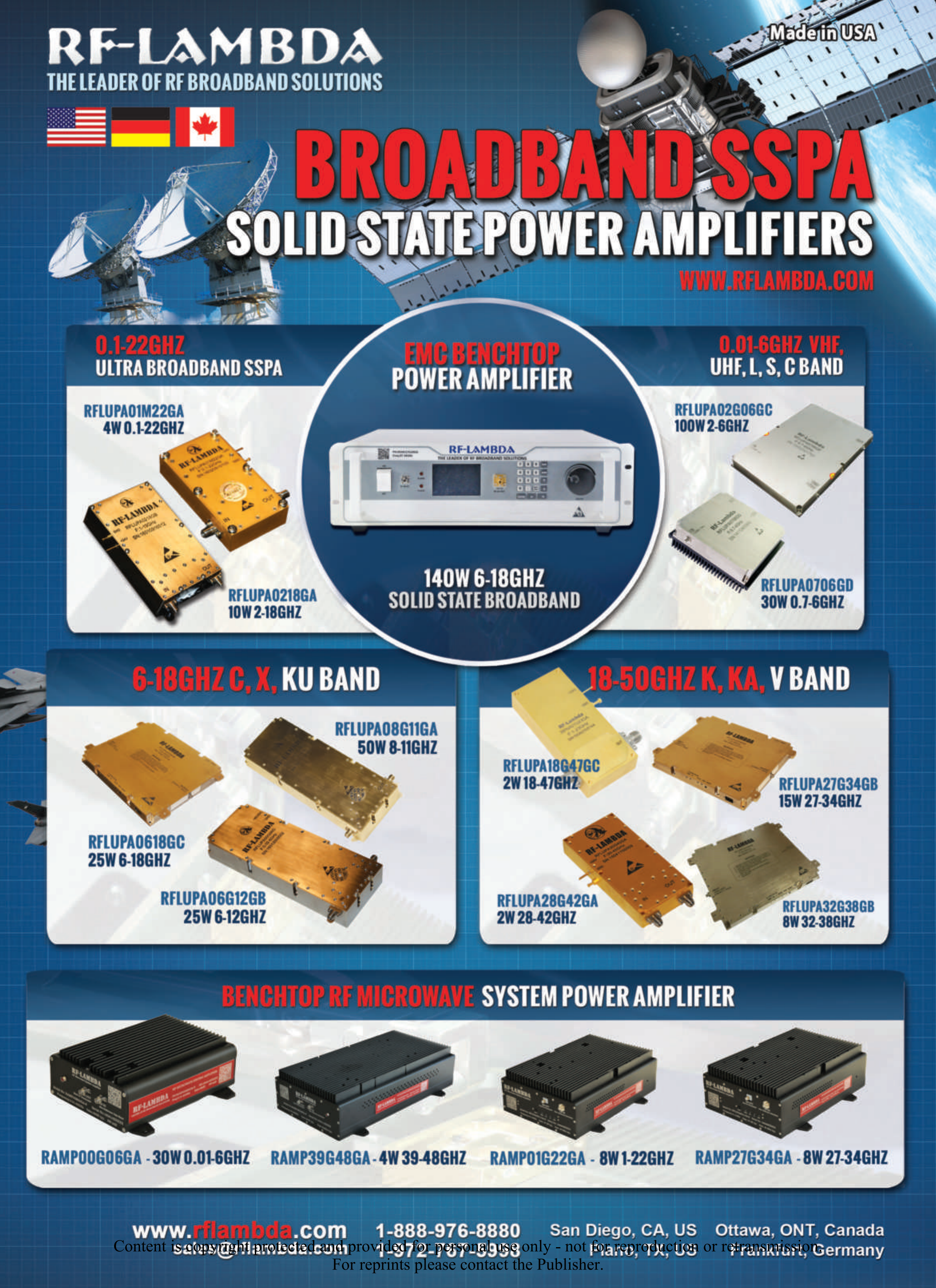
RF-LAMBDA
THE LEADER OF RF BROADBAND SOLUTIONS
Made in USA
BROADBAND SSPA
SOLID STATE POWER AMPLIFIERS
WWW.RFLAMBDA.COM
0.1-22GHZ
ULTRA BROADBAND SSPA
RFLUPA01M22GA
4W 0.1-22GHZ
RFLUPA0218GA
10W 2-18GHZ
EMC BENCHTOP
POWER AMPLIFIER
140W 6-18GHZ
SOLID STATE BROADBAND
0.01-6GHZ VHF,
UHF, L, S, C BAND
RFLUPA02G06GC
100W 2-6GHZ
RFLUPA0706GD
30W 0.7-6GHZ
6-18GHZ C, X, KU BAND
RFLUPA08G11GA
50W 8-11GHZ
RFLUPA0618GC
25W 6-18GHZ
RFLUPA06G12GB
25W 6-12GHZ
18-50GHZ K, KA, V BAND
RFLUPA18G47GC
2W 18-47GHZ
RFLUPA27G34GB
15W 27-34GHZ
RFLUPA28G42GA
2W 28-42GHZ
RFLUPA32G38GB
8W 32-38GHZ
BENCHTOP RF MICROWAVE SYSTEM POWER AMPLIFIER
RAMP00G06GA - 30W 0.01-6GHZ
RAMP39G48GA - 4W 39-48GHZ
RAMP01G22GA - 8W 1-22GHZ
RAMP27G34GA - 8W 27-34GHZ
www.rflambda.com
1-888-976-8880
San Diego, CA, US
Ottawa, ONT, Canada
Plano, TX, US
Frankfurt, Germany

mpG K&L® MICROWAVE
a DOVER company

Filter Wizard®

K&L's On-Line Filter Synthesis Tool

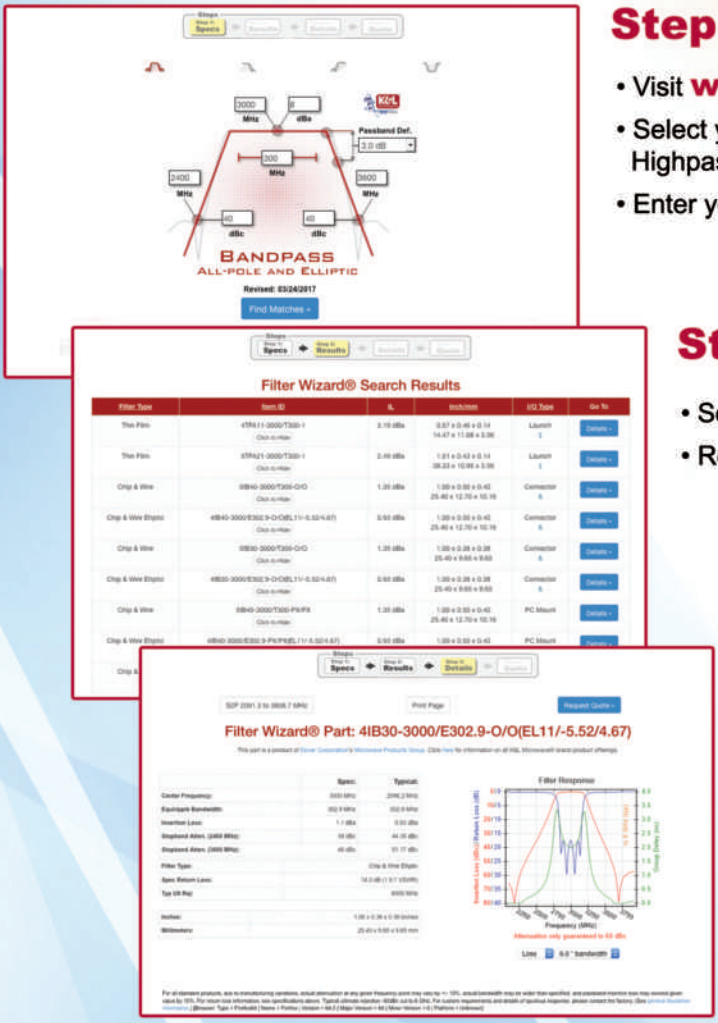

Step 1:

- Visit **www.klfilterwizard.com**
- Select your specific filter type from Bandpass, Lowpass, Highpass or Bandstop
- Enter your custom performance requirements.

Step 2:

- Select from a list of potential filter offerings.
- Review key parameters and size.

Step 3:

- Download S-parameter data for your system simulation.
- Receive detailed specifications.
- Print data sheets including outline drawings.

Step 4:

- Submit a request for quote and receive a quotation within 48 hours.

Microwave Products Group a DOVER company

ENABLING COMMUNICATION AND SIGNAL CONTROL

www.klmicrowave.com • www.klfilterwizard.com • 410-749-2424 • sales@klmicrowave.com •


AMPLICAL
Let Amplical
Jump Those Hurdles for You
with our Complete In-House Design, Manufacturing and Test Capabilities
Customers can depend on us for quick order fulfillment, competitive pricing and dedicated service.
Let us prove our commitment to you today.
High performance standard and custom Control Components and Amplifiers to 40GHz.
• EW Systems
• Communications Systems
• Radar
• Test
• Simulation
Products:
• Switches
• Attenuators
• Phase Shifters
• Limiters
• Switch Matrices
• Broadband Amplifiers
• Low Noise Amplifiers
• High Power Amplifiers
• Custom Components and Sub-assemblies
Phone: 973-386-1119
Fax: 973-386-1131
E-mail: info@amplical.com
web: www.amplical.com


Proven mmWave RF Solutions that Connect and Protect™
Unmanned Vehicles
Space and Satcom
Electronic Warfare
Phased Array Radar
QORVO CMD299K4
QORVO QPA3070
QORVO QPA2211
For Mission Critical Aerospace and Defense Applications
Since its inception, Qorvo® has focused on helping our customers overcome their toughest design challenges in aerospace and defense applications. Our MMIC design experience, portfolio of GaN/GaAs solutions combined with our extensive knowledge of the entire RF/microwave signal chain enable us to make your next system design a reality.
To find out how Qorvo solutions are All Around You®, visit www.qorvo.com
Custom MMIC Is Now
QORVO®
© 06-2020 Qorvo US, Inc. | QORVO, ALL AROUND YOU and CONNECT AND PROTECT are registered trademarks of Qorvo US, Inc.

Microwave Journal

CONTENTS

July 2020
Vol. 63 • No. 7
RF/Microwave Software & Design
mwjournal.com

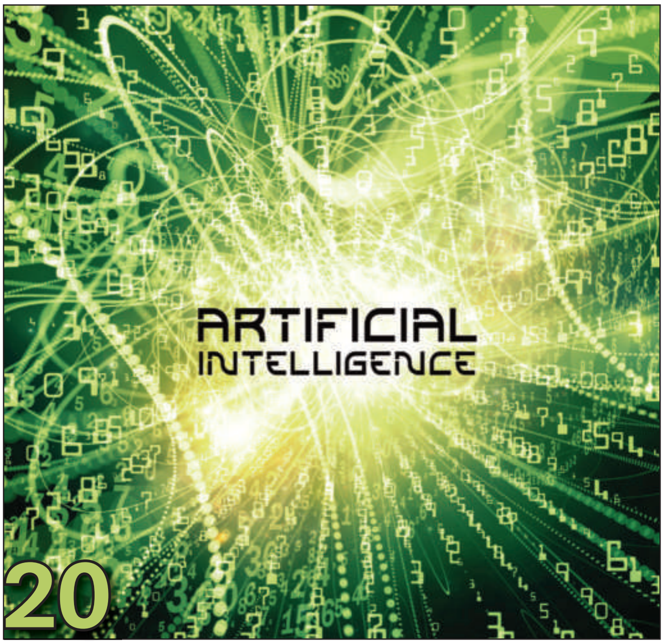

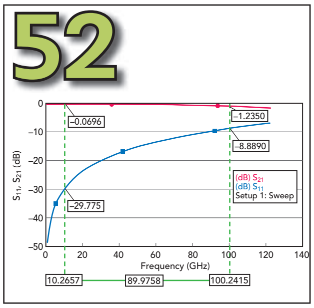

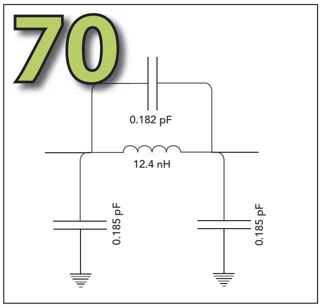

Look for this month's exclusive article online at mwjournal.com

Wideband Retrodirective Arrays for Wireless Charging of Portable Devices

Telecommunication and Navigation Institute, Kuwait and Texas Tech University, Lubbock, Texas

Cover Feature

Technical Feature

Application Note

63 YEARS OF PUBLISHING EXCELLENCE

Has Amplifier Performance or Delivery Stalled Your Program?

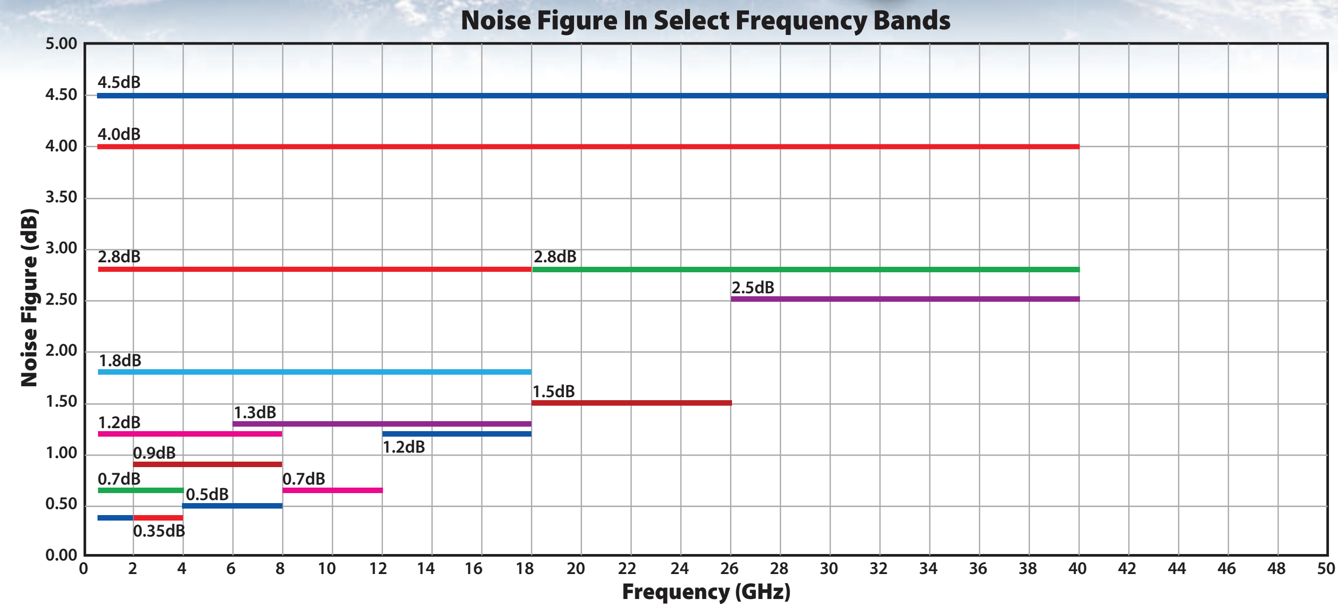

B&Z TECHNOLOGIES
Innovating to Excel

www.bnztech.com

CONTENTS

mwjournal.com

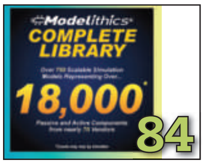

Product Features

Tech Briefs

Departments

Microwave Journal (USPS 396-250) (ISSN 0192-6225) is published monthly by Horizon House Publications Inc., 685 Canton St., Norwood, MA 02062. Periodicals postage paid at Norwood, MA 02062 and additional mailing offices.

POSTMASTER: Send address corrections to Microwave Journal, PO Box 1028, Lowell, MA 01853 or e-mail mwj@e-circ.net.com. Subscription information: (978) 671-0446. This journal is issued without charge upon written request to qualified persons working in the RF & microwave industry. Other subscriptions are: domestic, $120.00 per year, two-year subscriptions, $185.00; foreign, $200.00 per year, two-year subscriptions, $370.00; back issues (if available) and single copies, $10.00 domestic and $20.00 foreign. Claims for missing issues must be filed within 90 days of date of issue for complimentary replacement.

EXECUTIVE EDITORIAL OFFICE
685 Canton Street, Norwood, MA 02062
Tel: (781) 769-9750
FAX: (781) 769-5037
e-mail: mwj@mwjournal.com

EUROPEAN EDITORIAL OFFICE
16 Sussex Street, London SW1V 4RW, England
Tel: Editorial: +44 207 596 8730 Sales: +44 207 596 8740
FAX: +44 207 596 8749

SUBSCRIPTION SERVICES
Send subscription inquiries and address changes to:
Tel: (978) 671-0446
e-mail: mwj@e-circ.net

www.mwjournal.com

Printed in the USA

Microwave Journal Online

Visit us @ mwjournal.com

E LEARNING CENTER

Access webinars on-demand from the archived webinars and events page at www.mwjournal.com/events

Executive Interview

Samuel Cho, founder and CTO of **RFHIC**, discusses the motivation to start the company, his early adoption of GaN and RFHIC's plans for growth.

Hear From Industry Experts

WHITE PAPERS

AMCAD Engineering — Behavioral Modelling Challenges for RF System Simulation

ANALOG DEVICES (AHEAD OF WHAT'S POSSIBLE™) — Analog Devices Advances RF/mW in The Space Industry

COPPER MOUNTAIN TECHNOLOGIES — Time Domain Analysis with a VNA

ROHDE & SCHWARZ — Ensuring Performance of Connected Home Electronics Products

Wolfspeed — Power Design With Wolfspeed's GaN Large-Signal Models

Join Us Online

Follow us
@Pathindle
@MWJGary
@MWJEditor

Join us at the RF and Microwave Community

Become a fan at facebook.com/microwavejournal

Catch *Frequency Matters*, the industry update from *Microwave Journal*,
microwavejournal.com/FrequencyMatters

COM

AUGUST

MARK YOUR CALENDAR

4-6 VIRTUAL

IMS — Connecting Minds. Exchanging Ideas.

IMS2020 and Microwave Week, scheduled for June 21-26, 2020 in Los Angeles, Calif., is transitioning to a virtual event. IMS2020 is the flagship conference of Microwave Week, the world's largest event for RF and microwave technology which brings 10,000 attendees from 48 countries and over 600 exhibiting companies. The virtual event will continue with the theme of "Connectivity Matters," built on five pillars that link the world; 5G and 6G networks, aerospace and defense programs, autonomous vehicles, the digital economy and ensuring the connection of under-represented communities. Events featured include the technical sessions, technical lectures, panel sessions, 5G Summit, industry workshops, MicroApps, virtual exhibition and several notable keynote speakers. **https://ims-ieee.org**

VIRTUAL 4-6

RFIC

Also occurring during Microwave Week, the Radio Frequency Integrated Circuits (RFIC) Symposium features workshops and a tutorial event, the Technical Lecture, two Plenary Speakers, the Plenary Reception, presentations of contributed papers, special lunch-time panel sessions and awards will be presented to authors of three selected student papers, as well as to authors of three selected industry papers. **www.rfic-ieee.org**

11-13

EXPO ELECTRONICA

For 23 years, ExpoElectronica has been a leading exhibition in the electronic industry. It is widely represented by electronic, semiconductor, electromechanical, passive components, printed circuit boards and microcircuits, displays, embedded systems and more. ExpoElectronica 2020 focuses on leading global trends including 5G, IoT and AI. **www.expoelectronica.ru**

4-6 VIRTUAL

ARFTG

Held as part of Microwave Week, in conjunction with IMS and RFIC 2020, the 95th ARFTG Microwave Measurement Conference will cover RF/digital mixed-signal measurement and calibration, nonlinear/large-signal measurement and modeling techniques, Terahertz measurement techniques, calibration methods, materials measurement approaches and other topical areas of RF, microwave and mmWave measurements. **www.arftg.org**

26 VIRTUAL

5G ANTENNA SYSTEMS

Attend 5G Antenna Systems to learn about market opportunities, new 5G Antenna technology and the endless emerging application trends. Topics will include antenna design, integration, 5G developments and insights and supporting technologies for the 5G ecosystem. **www.antennasonline.com**

FOR DETAILS, VISIT MWJOURNAL.COM/EVENTS

Coming**Events**

CALL FOR PAPERS

2020 IEEE BiCMOS and BCICTS
July 17

AOC International Symposium & Convention
July 31

COMSOL Conference 2020 North America
August 14

IEEE Women in Engineering Forum USA East
September 1

mwjournal.com

JULY

SEMICON WEST 2020
July 20–23 • Virtual
www.semiconwest.org

IEEE EMC+SIPI 2020
July 29–August 28 • Virtual
www.emc2020virtual.emcss.org

AUGUST

IEEE MTT-S IMS 2020
August 4-6 • Virtual
https://ims-ieee.org

95th ARFTG Microwave Measurement Symposium
August 4-6• Virtual
www.arftg.org

RFIC Symposium
August 4-6• Virtual
www.rfic-ieee.org

Expo Electronica
August 11-13 • Moscow, Russia
www.expoelectronica.ru

5G Antenna Systems
August 26 • Virtual
www.antennasonline.com

SEPTEMBER

IEEE RFIT 2020
September 2-4 • Hiroshima, Japan
www.rfit2020.org

PCB West 2020
September 8–11 • Santa Clara, Calif.
www.pcbwest.com

GNU Radio Conference
September 14–18 • Virtual
www.gnuradio.org

OCTOBER

AUVSI's Xponential
October 5–8 • Dallas, Texas
www.xponential.org

EDICON Online
October 6, 13, 20 & 27 • Virtual
www.ediconoline.com

COMSOL Conference 2020
October 7–8 • Virtual
www.comsol.com/conference/north-america

EDI CON China 2020
October 13–14 • Beijing, China
www.ediconchina.com

NOVEMBER

AMTA 2020
November 1–6 • Newport, R.I.
www.amta2020.org

Global MilSatCom
November 3–5 • London, U.K.
www.globalmilsatcom.com

2020 IEEE BiCMOS and BCICTS
November 8–11 • Monterey, Calif.
www.bcicts.org

APMC 2020
November 10–13 • Hong Kong, China
www.apmc2020.org

IEEE Women in Engineering Forum USA East 2020
November 12–14 • Providence, R.I.
https://attend.ieee.org/wie-forum-usa-east-2020/

Space Tech Expo Europe 2020
November 17–19 • Bremen, Germany
www.spacetechexpo.eu

DECEMBER

WAMICON 2020
December 1–3 • Clearwater Beach, Fla.
www.wamicon.org

AOC International Symposium & Convention
December 8–10 • Washington D.C.
www.crows.org/mpage/2020HOME

Cover Feature
Invited Paper

Artificial Intelligence and Machine Learning Add New Capabilities to Traditional RF EDA Tools

Contributions by Altair, ANSYS, Cadence/AWR, Keysight and MathWorks

Altair Antenna Design Optimization with Machine Learning

Altair, Troy, Mich.

Altair's simulation-driven approach to innovation is powered by an integrated suite of software which optimizes design performance across multiple disciplines. Encompassing structures, motion, fluids, thermal management, electromagnetics, system modeling and embedded systems, the suite also provides data analytics and true-to-life visualization and rendering. Altair's vision is to transform decision making by applying simulation, data analytics and high performance computing.

Altair has been pioneering artificial intelligence (AI) and machine learning (ML) using their design exploration (DoE) tool, Altair HyperStudy™, for many years. HyperStudy automatically creates intelligent design variants, manages runs and collects data. Users are then guided to understand data trends, perform trade-off studies and optimize design performance and reliability. Taking advantage of design exploration methodology in HyperStudy, ML has been incorporated for antenna design optimization and electromagnetic compatibility problems using electromagnetic simulation tool, Altair Feko™. ML approaches are applied to complex antenna designs with many design variables. The complete workflow of the ML approach for antenna design optimization is detailed in these steps:

- Generate training and test data with an appropriate DoE study and numerical simulation
- Build a ML model based on the generated training data
- Validate the ML model using the generated test data
- Use ML model to optimize antenna design

Antenna design with ML helps in understanding data trends, perform trade-off studies and optimize design performance and reliability. Two examples are provided to illustrate advantages of applying ML for antenna design process using Feko and HyperStudy.

Example 1: Dual port LTE antenna (see ***Figure 1***)

- Antenna simulation model with 12 design variables and two responses (S11, S21)
- Use ML regression model for fast optimization. Comparison of processing times:

Data generation with DoE: 14.7 hrs

Training of ML regression model: 2 sec

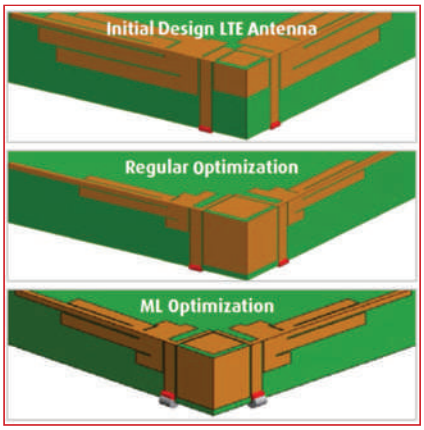

Fig. 1 **Optimization of dual port LTE antenna.**

RF & MICROWAVE FILTERS

RLC has the customized filter solutions you need.

RLC manufactures a complete line of RF and Microwave filters covering nearly every application in the DC to 50 GHz frequency range. We offer different filter types, each covering a specific engineering need.

In addition, our large engineering staff and high volume production facility give RLC the ability to develop and deliver both standard and custom designed filters at competitive costs, within days or a few weeks of order placement.

- Band Pass, Low Pass, High Pass & Band Reject
- Connectorized, Surface Mount, PCB Mount or Cable Filters
- Wave Guide Bandpass and Band Reject
- 4th Order Bessel Filters
- Spurious Free, DC to 50 GHz, Low Loss, High Rejection
- Custom Designs

For more detailed information, or to access ***RLC's exclusive Filter Selection Software****, visit our web site.*

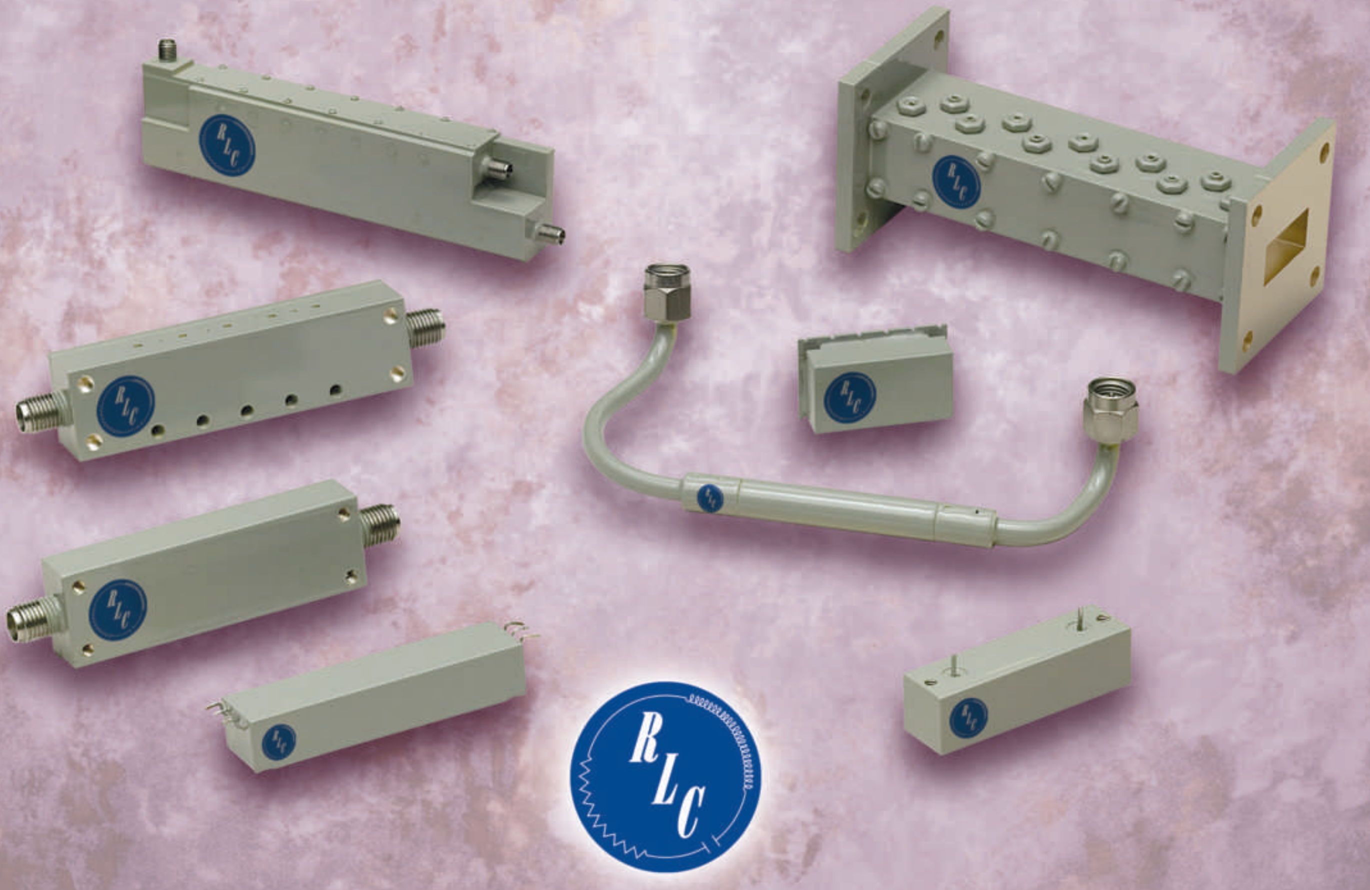

RLC ELECTRONICS, INC.

83 Radio Circle, Mount Kisco, New York 10549 • Tel: 914.241.1334 • Fax: 914.241.1753
E-mail: sales@rlcelectronics.com • www.rlcelectronics.com

ISO 9001:2000 CERTIFIED

VISA MasterCard

RLC is your complete microwave component source...
Switches, Filters, Power Dividers, Terminations, Attenuators, DC Blocks, Bias Tees & Detectors.

Optimization based on ML model: 10 sec

Regular optimization based on simulation model: 40.4 hrs

Speed up factor 2.75 by using ML approach

Example 2: Optimization of WLAN antenna with evolutionary learning (see ***Figure 2***)

- Antenna simulation model with 112 (binary) design variables and two responses
- Design variable indicates if honeycomb element is metallic or not
- Number of possible design combinations: $2^{112} \approx 5.2 \cdot 1{,}033$
- Find optimal antenna topology using evolutionary learning
- Optimization goal: Minimize S11 at 2.44 and 5.2 GHz
- Optimization constraint: Sum of metallic honeycomb elements < 50

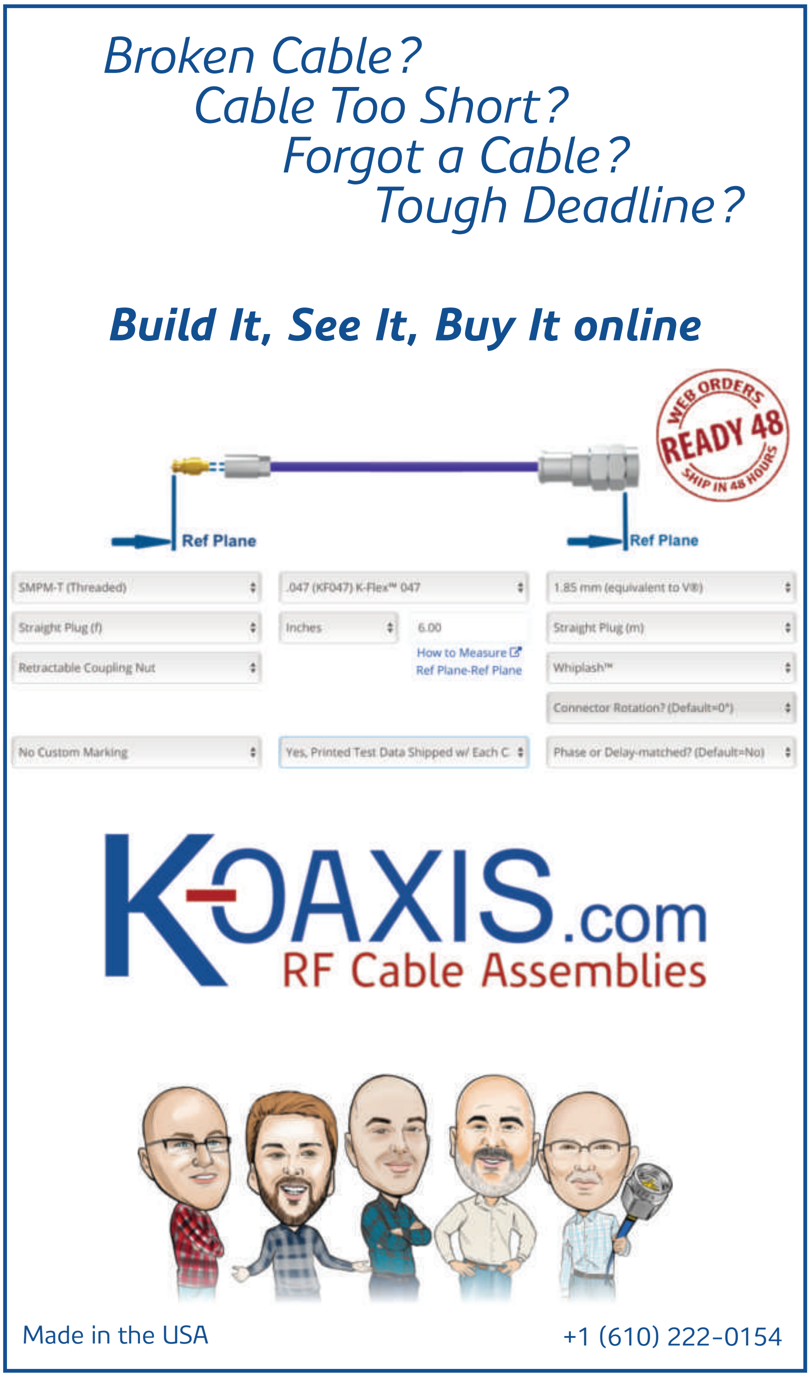

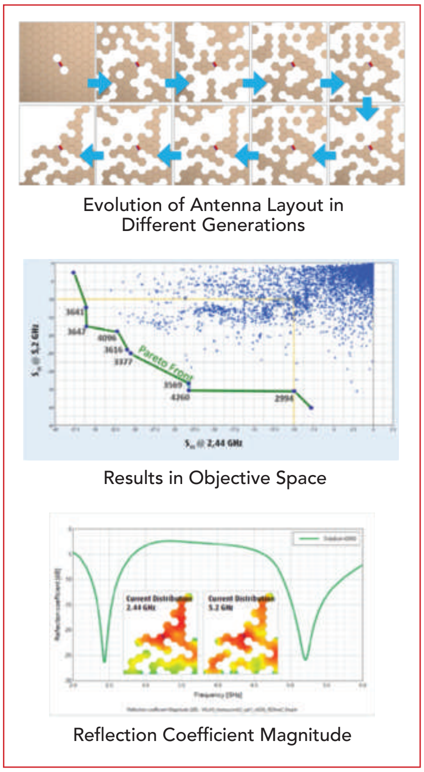

Fig. 2 **Optimization of WLAN antenna with evolutionary learning.**

- After 4,300 iterations and 12 generations the multi-objective genetic algorithm has identified a set of Pareto-optimal solutions

Altair has been using regression type ML algorithms for design exploration and optimization for many years and now also applies this approach to antenna and related electromagnetic problems. Altair has recently expanded its ML portfolio with new products that address data analytics to include ML and predictive analytics. Application of Altair's modern ML tools to antenna design will revolutionize development of new and innovative antennas for current and future wireless devices and products.

Machine Learning with Ansys Physics-Based Simulation

Ansys Inc., Canonsburg, Pa.

Ansys has embraced and used ML methods and tools for quite some time with the goal of advancing the capabilities of physics-based engineering simulation. An early example is the automated methods that Ansys HFSS uses during the adaptive meshing solution process. The method uses previous finite element solutions

to predict where more elements should be placed for more accurate solutions. Although not ML in the modern sense, making predictions or decisions without being explicitly programmed to do so, automated adaptive meshing leverages the computer to perform the work of finding an optimal mesh for accuracy and speed based on previous observations.

In semiconductors, the RedHawk-SC product leverages big data and ML to enable rapid design iterations of exceedingly large and complex integrated circuit designs. ML provides actionable analytics to identify and prioritize design fixes. Ansys is also making use of ML methods in specific simulation capabilities such as inference of optical properties of materials, designing smart assistants for gauging high performance computing (HPC) resource usage prior to simulation and automatic road scenario generation for advanced driver-assistance systems and automotive radar.

ML FOR AUTOMOTIVE RADAR DETECTION

Ansys has demonstrated the use of the Ansys HFSS Shooting and Bouncing Ray (SBR+) asymptotic electromagnetic solver to predict radar returns in a complex driving scenario. Ansys HFSS SBR+ is used to predict the Doppler response for a vehicle-mounted radar as it travels through a moving scene that includes the road and combinations of stationary, moving vehicles and persons, buildings, road signs and foliage.

Using that capability, the software may apply ML algorithms to provide radar-based object localization and classification. In ML, the goal is to detect and infer certain patterns from complex data by generating a mathematical model that can be used to quickly make decisions on new data. It is generally rare for pre-trained models or datasets to exist that can be utilized in ML training; thus, the method of this work is to generate the datasets and training using the Ansys HFSS SBR+ computation.

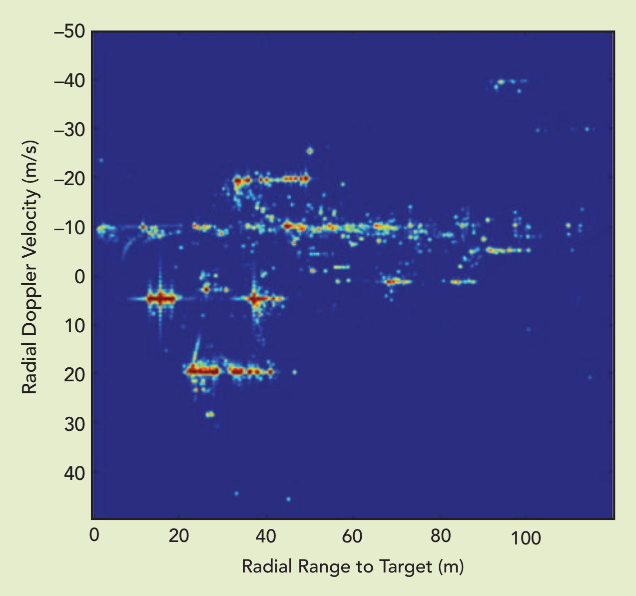

Fig. 3 Typical range-Doppler plot.

Advantages of using this simulation-based approach is that the data may be generated automatically using any driving scenario that may not be possible empirically. More importantly, the objects in the scene were placed there when creating the scenario providing the unique ability to self-annotate and label the data. We know if there is another automobile or pedestrian because we placed it there. This is in significant difference to empirical methods that require massive and painstaking hand annotation. Of course, dataset creation is accelerated using HPC especially considering the highly parallel simulation requirement.

Velocity of an object is effectively determined by Doppler shift in the returned signal and distance (range) from the radar is effectively determined by time delay. A typical radar return (see ***Figure 3***) provides magnitude of scattered fields in a color shaded image, with range and range rate indicated in the plot via location along the Range and Doppler axis, respectively. Everything in the environment scatters fields so automobiles, pedestrians, signs, buildings and trees all contribute and may show up in radar image.

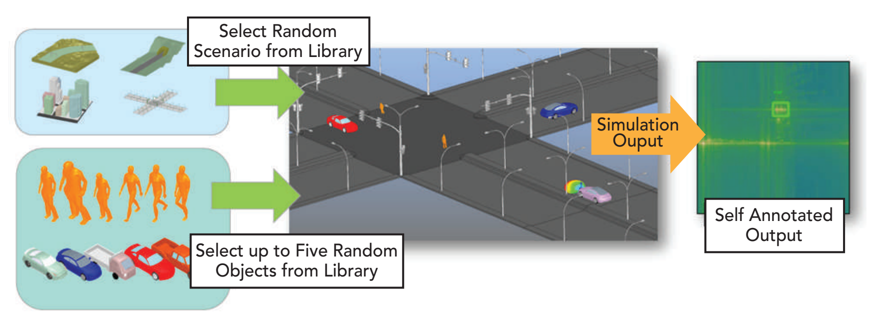

Fig. 4 **Radar scenario is built by placing components from a library for stationary and moving objects. Simulations result in range-Doppler plot with self-annotation.**

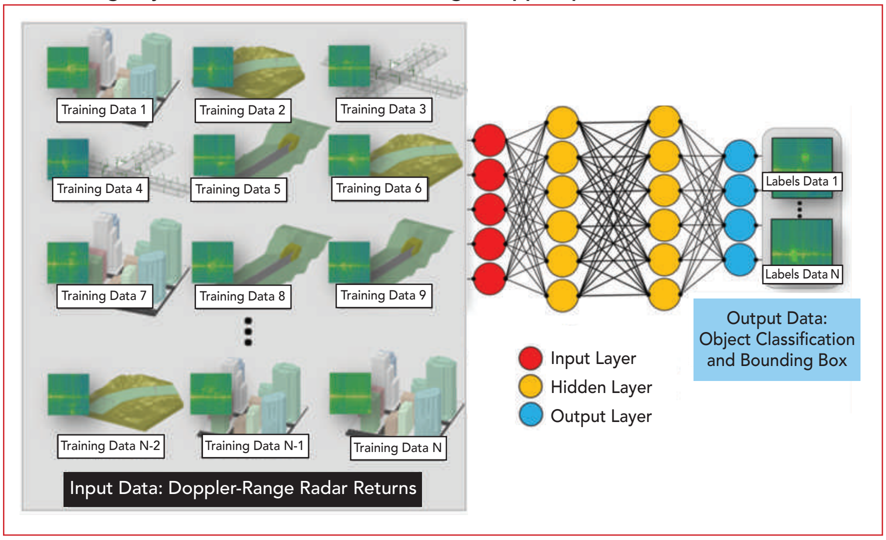

Fig. 5 **Multiple scenarios are used to train a neural network which can then provide inference for object classification.**

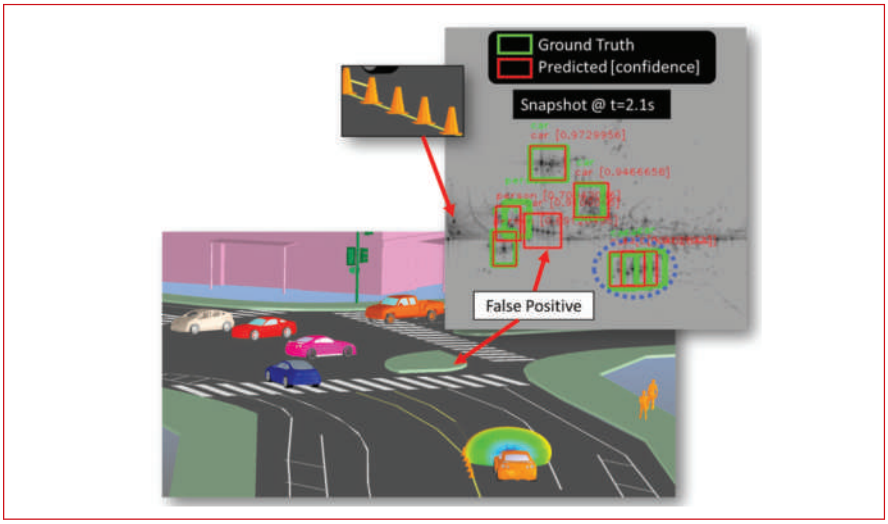

Fig. 6 **Highly complex radar scenario used for validation.**

SIMULATION ENABLED ML

In the Ansys ML approach, they follow a three-step process to generate data, train the ML algorithm and then run detection on scenarios and compare with ground truth. ***Figure 4*** illustrates the automated process to generate the data. They first create the radar scene by combining library components to generate full scenario with velocity and location randomly placed within environment limits. Automated results are generated as range-Doppler returns for a radar module, and fully annotated range-Doppler plots are produced using an XML file with locations and object identifiers.

For the training, they implemented a deep learning model based on a YOLO v3 architecture, a convolutional neural network-based approach used in many image-based object detection classifiers and trained from scratch using radar results obtained from physics-based simulation. ***Figure 5*** illustrates the overall neural network training using labeled data that may include upwards of 9,000 scenarios. The software then proceeds to test and validate the model by testing against a new radar scenario that was not used during the training. Ansys found an 83 percent mean average precision (mAP), a metric used to quantify accuracy of object detection. Pedestrian detection accuracy improvement was observed with more training data, increasing from 61 percent to 74 percent, when using 3,000 to 9,000 training scenarios, respectively.

Ansys attempted an extremely complex radar scenario that also

included a concrete road structure, not included as part of the training, and a very tight three vehicle cluster (see ***Figure 6***). The mAP of this scenario was a lower 52 percent, with a false positive detection of an automobile at the concrete road structure and an inability to isolate one of the three closely spaced vehicles.

Ansys has shown that it is possible and desirable to leverage physics-based simulation to train ML algorithms for automotive radar applications. Ansys HFSS SBR+ was used for dataset generation with up to 9,000 unique scenario simulations. Each scenario requires one to two GB of RAM, with an average solve time of 20 minutes using a single core. The method is parallel with near linear scaling with compute cores. 6,000 scenarios can be computed in half a day on a 128-core machine. Results show that objects can be located and classified in a real-world environment with good confidence.

Cadence AWR Uses Machine Learning to Accelerate Designs

Cadence AWR, San Jose, Calif.

Today's RF systems are largely developed with software tools that provide engineering teams with ready access to compact and electromagnetic (EM)-based models, as well as to a broad range of simulation and optimization technologies that address all stages of electronic product computer-based design. Yet, as each new, next generation of electronic systems grows more complex, design work and fabrication likewise grow more challenging and expensive. There is real concern that engineering and economic hurdles threaten the pace of the More than Moore (MtM) law for the development of microelectronics and for non-digital functions such as RF to mmWave front ends and the integration of multi-fabric technologies.

ML, AI and cloud computing (CC) are all avenues being explored to help to mitigate these concerns. Performing various engineering tasks through learned decision making and optimized design flows for greater productivity, as well as enhanced speed/capacity of simulation technologies, are a few examples where ML, AI and CC are being employed. In general, convolution and recurrent neural networks along with machine and deep learning algorithms will be significant drivers in the development of 5G communication systems and beyond. These systems include RF through mmWave electronics and the electronic components within them. As such, decision making design automation will be essential to the development of future communication and wireless detection systems.

Cadence® AWR Design Environment® software uses genetic optimization algorithms to explore a greater range of design candidates for wireless product development by applying ML to accelerate the design of antennas, filters and impedance matching networks, all key components within 5G wireless communication and radar systems. The software operates from performance criteria set by the designer and is enhanced by the designer's knowledge in defining the goals/search limits, after which the tool assumes the task of empirical topology/parameter design space optimization.

NETWORK SYNTHESIS

The AWR Design Environment network synthesis wizard creates optimized two-port matching networks composed of discrete and distributed components using ML and AI (see ***Figure 7***). The designer specifies the maximum number of sections and the types of components to include in the search space and the wizard explores for the best circuit topologies and optimizes the component parameter values.

The wizard's optimization goals are specified by the designer using a dedicated set of synthesis measurements, much like optimization goals are normally defined within AWR software. Specialized measurements are provided for input noise matching, amplifier output power matching and inter-stage matching. The optimum reflection coefficients are specified over frequency and can be provided in the form of load pull data, network parameter data files or even circuit schematics.

When generating possible network topologies, the wizard begins by creating all the possible topologies for a single component. The number of such topologies is generally equal to the number of checked boxes on the software's components page. For example, to create a two-section topology, the wizard takes each one-section topology and goes through the list of components allowed to follow the first one. The process repeats, producing an exponential growth in the number of topologies as a function of the number of sections. This setting, which is referred to as "M" and has a default of 1,000, provides a way to constrain the exponential growth by limiting the number of N-section topologies that will be used to create the topologies with N+1 sections. Only the "M" best topologies will be propagated.

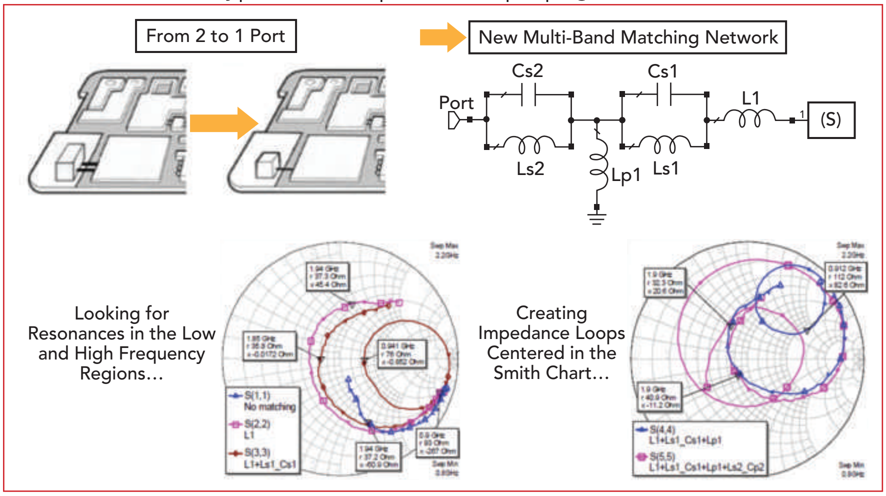

Fig. 7 **Multi-band impedance-matching circuits with minimal components (six-element case shown) using the AWR Design Environment network synthesis wizard to support antenna integration** ***(Source: Fractus Antennas).***

This search-based method determines candidate circuit topologies based upon user specification of capacitor, inductor and transmission line element types to be used in series and shunt slots. The wizard then performs an exhaustive search, exploring all possible topologies by expanding the solution up to a user-defined maximum number of sections.

Heuristic methods then determine what element can follow an existing element. Through a self-learning (or ML) process, the synthesizer understands which elements can be placed serially, such as two different width transmission lines to form a stepped-impedance transformer or a fully distributed transmission line network for higher frequencies. It also understands what cannot be placed serially, such as two capacitors from a matching perspective.

In addition to network synthesis, AWR software products also employ evolutionary algorithms to create novel antenna structures in which AI employs genetic optimization and EM analysis for exploration of designs. Whether designers are focused on developing impedance matching networks for broadband amplifiers or next generation antenna design, AWR software capitalizes on advances offered by ML, AI and CC. The ability to support different classes of design, as well as simulation technologies, with a variety of such computational techniques will become more and more critical to the future of RF to mmWave design and preserve MtM.

Keysight's AI/Machine Learning Optimizations in Design Software

Keysight Technologies, Santa Rosa, Calif.

Keysight Technologies has a long history in AI/ML research as well as applying AI/ML techniques in modeling, simulation and test environments. Keysight Labs and application teams conduct this research, often partnering with select universities and individual researchers on specific exploration opportunities. Keysight is well known for the successful adoption of AI/ML techniques in simulation and modeling of field effect transistors using neural networks and in inference engines for manufacturing analytics and test plan optimization.

Keysight's focus when combining AI/ML techniques with EM simulation is finding improved solutions to optimization and EM design problems. For example, a traditional

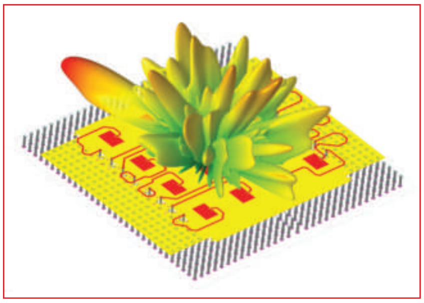

Fig. 8 Antenna array far field gain pattern from 16 array elements *(Source: Global Foundries and Fraunhofer IIS/EAS/IZM).*

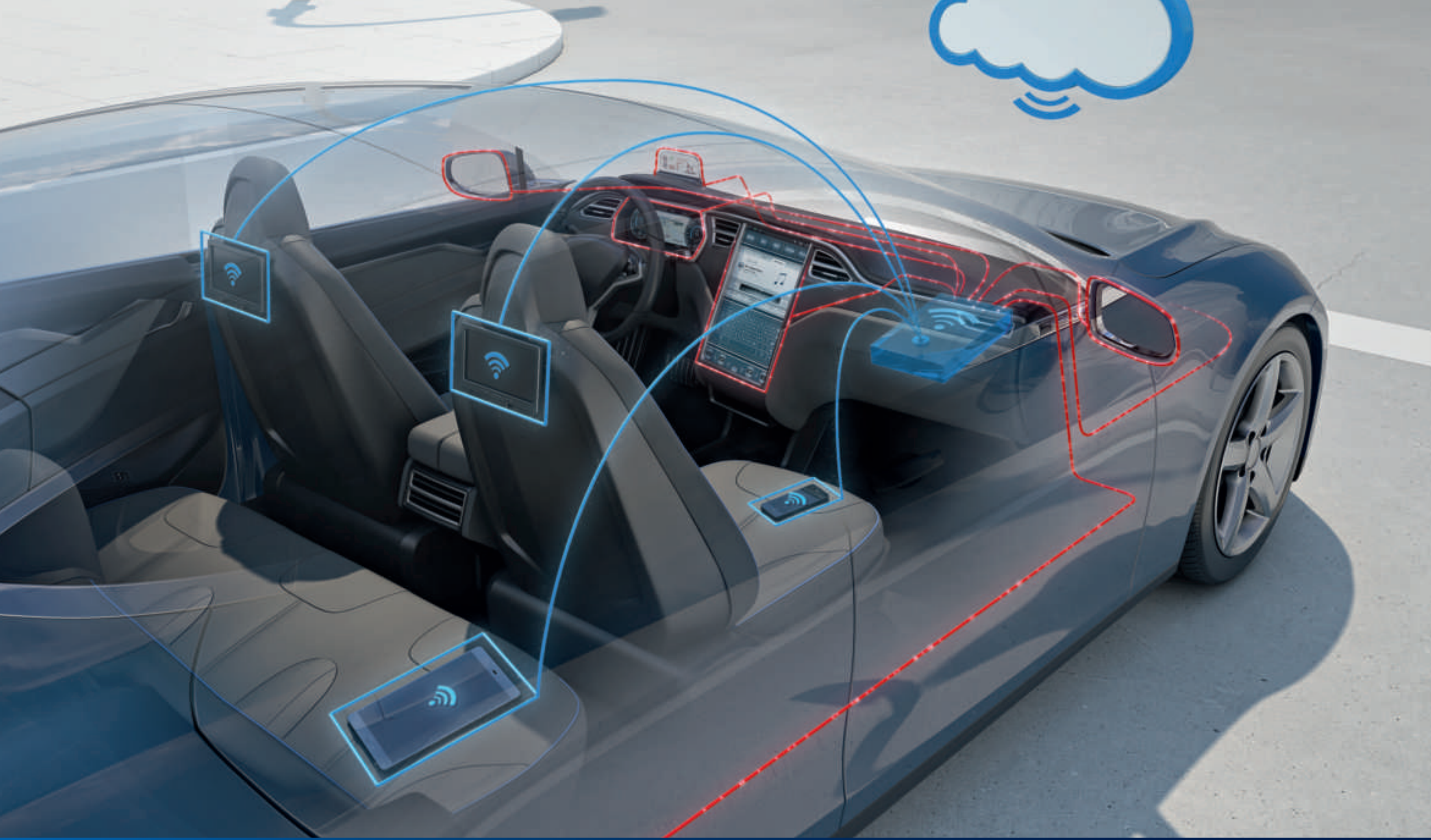

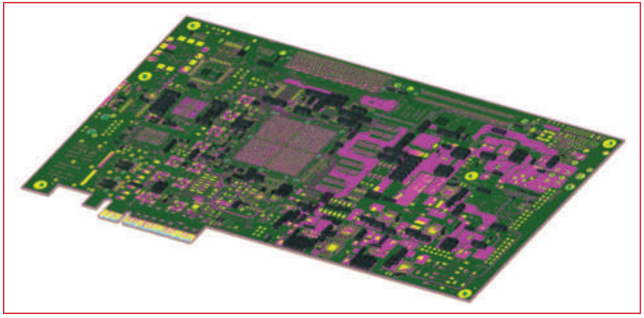

Fig. 9 A Xilinx Kintex UltraScale FPGA Evaluation PCB showing AI/ML-aided decap placements.

application of AI/ML techniques is searching for an optimal antenna shape within a set of physical constraints imposed by cost or available area (see ***Figure 8***).

To create an optimal antenna, designers start by selecting a base design described by a large set of parameters with a wide range of values. The effect of those parameters, or their combination, is typically hard to predict or model. Sweeping through the entire parameter space and selecting the best configuration is not practical. Each new configuration also requires an EM simulation that can take a significant amount of time to complete. Any technique that reduces the number of EM simulations will have a large impact on the time it takes to produce the optimal antenna.

Traditional optimization techniques frequently produce unsatisfactory results as they tend to become stuck in local optima. Using evolutionary algorithms to search the continuous design parameter space enables both limitation of the number of EM simulations needed and avoidance of local minima in an efficient way.

Keysight has also had success in application of AI/ML techniques to EM simulation for finding the optimal number of decoupling capacitors (decaps) needed on a PCB for power delivery from the voltage regulator to the chips. Power distribution networks require placement of decaps between power and ground rails. Determining the optimal number of decaps is key to PCB performance and reducing costs. For a complex PCB, there can easily be 100 decap placements and for each of them a wide set of available choices. Sequencing through all possible combinations to find the optimal number of decaps is again impractical, and would take hundreds of years, even taking advantage of parallel simulations (see ***Figure 9***).

Given a choice between five decap models for each location, the number of combinations is 6,100, including the option not to place one. Deciding against decap placement is a valid choice as it reduces PCB cost. Keysight looked at how experts in the field approached the decap problem and combined it with AI/ML techniques that reduce search spaces. The AI/ML algorithm quickly dismisses areas in the parameter space that are unlikely to yield a good solution. It uses the techniques of experts to find solutions in areas that stand a good chance to provide a solution. The algorithm accelerates each evaluation of a potential solution by precomputing the EM part of the problem, so that it leverages a previous solution efficiently and does not require starting the EM simulation from the beginning.

MathWorks Seamlessly Integrates AI into Their Tools

MathWorks, Natick, Mass.

MathWorks has a range of tools built on MATLAB and Simulink that are widely used to model, simulate and deploy wireless and radar systems. Tools such as Antenna Toolbox, RF Toolbox, Phased Array System Toolbox and Sensor Fusion and Tracking Toolbox span across the RF, antenna, phased array, signal processing and data processing disciplines. Modeling building blocks, algorithms and system simulators are also available in standards-based toolboxes including 5G Toolbox, LTE Toolbox and WLAN Toolbox.

MATLAB supports a broad range of AI algorithms and training workflows for deep learning, ML and

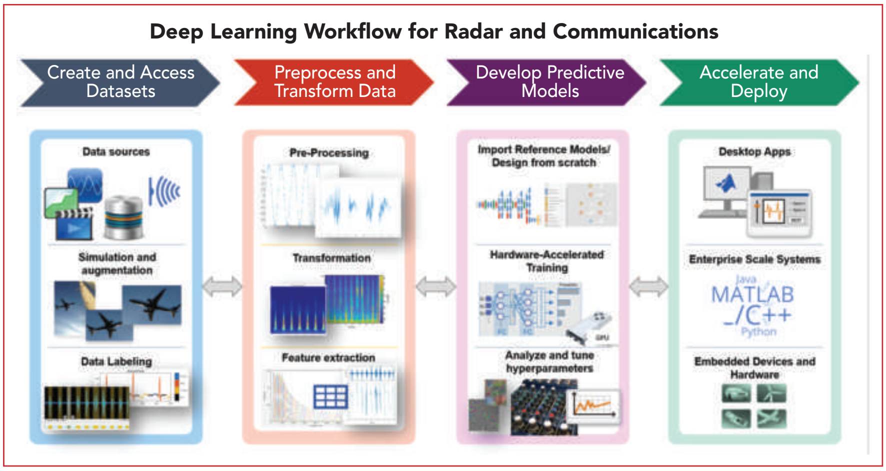

Fig. 10 MathWorks tools span the AI workflow for radar and wireless communications from data acquisition to deployment.

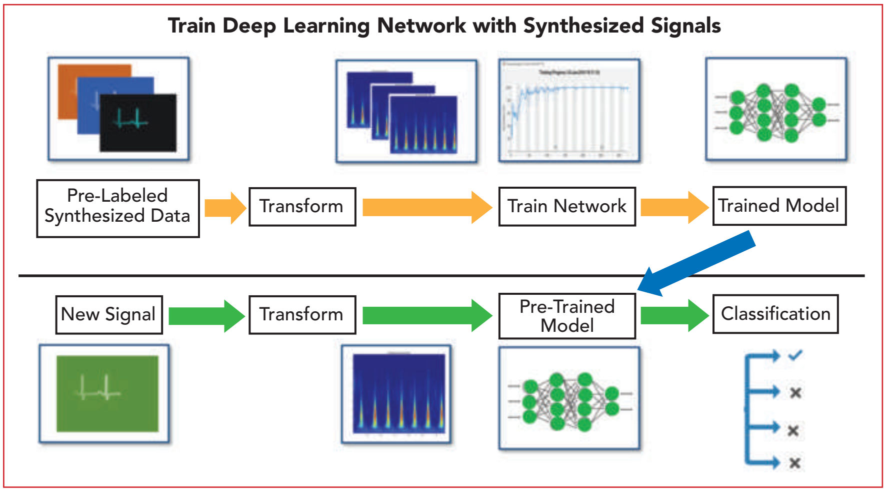

Fig. 11 Train AI networks with synthesized radar or wireless data and test with real-world data.

reinforcement learning. These are part of the integrated environment that includes their wireless and radar tools including Communications Toolbox and Phased Array System Toolbox, enabling system designers to apply these AI techniques directly in their applications. This could include labeling baseband data to train a network for supervised learning. Modulation ID and target classification are good examples of this type of supervised learning. In other applications, AI techniques are used to improve the performance of the system. For example, a wireless system may learn how channels vary over time or how to perform optimally in the presence of interference.

5G wireless systems and multifunction radar systems operate in such complex environments and perform tasks that previous generation systems never had to address. There are many system-level challenges that are hard to solve. AI can be applied to these systems to solve problems and improve system performance. The good news is that a lot of the foundation for AI that evolved for vision-based systems can be leveraged. Algorithms and workflows specific to signals are also available to make AI possible for RF applications. System engineers can now integrate AI into their workflow seamlessly using MATLAB and Simulink and supporting toolboxes.

In wireless and radar applications, this spans the following steps in system design workflows (see ***Figure 10***):

- Connecting to radios and radars directly
- Managing large data sets including the process of labeling baseband signals (with Signal Processing Toolbox)
- Extracting features from signals

to use with ML networks (with Signal Processing Toolbox and Wavelet Toolbox)

- Synthesizing realistic data to train deep learning networks
- Designing AI networks that are specific to wireless and radar applications (with Deep Learning Toolbox)
- Connecting to networks in the larger AI ecosystem (with Deep Learning Toolbox)
- Deploying code to a processor, GPU or FPGA

The workflow spans from the earliest prototyping stage to deployment which ensures that the systems that get delivered match the system models built at the earliest project phases. System engineers can generate great amounts of data using channel models, impairments and environmental conditions in system simulations.

Having this data can reduce the amount of field testing required to train a deep learning network. Even when data exists, data synthesis can be invaluable to augment data with corner case conditions. This helps to ensure system developers deliver more robust systems. Robustness in this case translates to better results in areas such as improved classification or better target recognition. This could also mean higher performance in the presence of interference or recognizing trusted RF sources.

The most common AI applications in wireless and radar include areas like modulation identification, spectrum management, channel estimation and target classification. An RF fingerprinting application example that MathWorks recently modeled was delivered with the R2020a release. This is an example that was widely requested by their customers and is especially interesting for cyber security applications. The idea is that a network can be trained to recognize an RF fingerprint between a trusted transmitter and receiver. If spoofing is attempted to interfere with operations or to gain unauthorized connections, the trained AI network can recognize this condition. Using Communications Toolbox and WLAN Toolbox, MathWorks developed the algorithms and trained the AI system with purely synthesized data. They were then able to obtain the same results when they tested the system with data collected with off-the-shelf radios (see ***Figure 11***).

OVERALL SUMMARY

AI and ML have been implemented into many EDA tools and platforms to automate many design processes and obtain results faster and more accurately as shown by Altair, Ansys, Cadence AWR, Keysight and MathWorks. They have also enabled the simulation of scenarios that were previously too complex or data intensive to execute without AI and ML. The implementation of these capabilities is only just beginning and expect many new improvements in the near future with AI and ML.■

ATC 531Z Broadband Multilayer Capacitors

Low Insertion Loss from 16 KHz to 30 GHz

Advantages:

- Broadband Performance
- Low insertion Loss
- Flat Frequency Response
- Excellent Return Loss
- Unit-to-Unit Performance Repeatability
- Rugged Ceramic Construction

Features:

- EIA 0201Case Size
- Capacitance: 100 nF
- Operating Frequency: 16 KHz to 30 GHz
- Insertion Loss: <0.5 dB typ.
- Low Loss X5R Dielectric
- Voltage Rating: 16 WVDC
- Solderable SMT Terminations
- RoHS Compliant

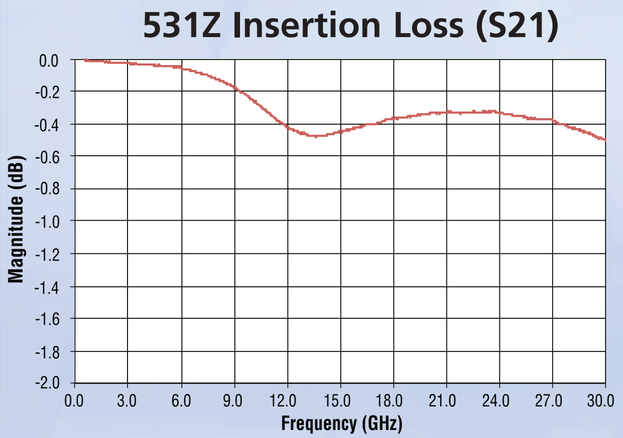

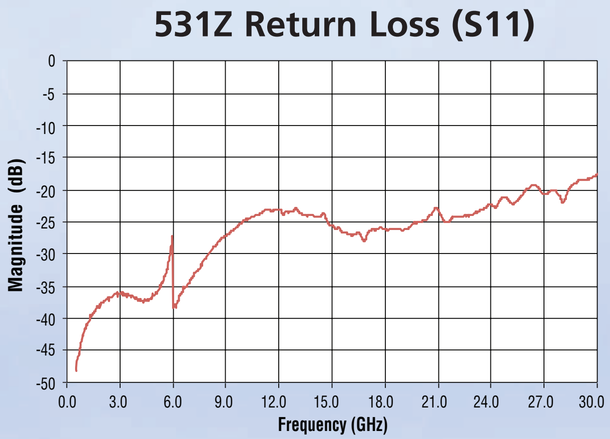

RoHS Compliant

www.atceramics.com

AMERICAN TECHNICAL CERAMICS
AN AVX GROUP COMPANY

THE ENGINEERS' CHOICE® ISO 9001 REGISTERED COMPANY

THE ENGINEERS' CHOICE®

Advanced Air and Missile Defense, in the Hands of Soldiers

It is a cold December morning at White Sands Missile Range in New Mexico, and two surrogate cruise missile targets have just been launched, one after the other. They are flying separate courses among the jagged San Andres and Sacramento mountains toward soldiers in a U.S. Army Air and Missile Defense unit at a test site called TAC-2 – Tactical Command Post.

These sophisticated targets precisely mimic real cruise missile threats and can take advantage of this terrain to hide from the radars and sensors commanders have positioned in the area. This can create gaps in tracking that make the job of interceptor missiles or other defensive weapons more difficult.

Today, though, their maneuvers will not enable them to evade detection. This is Flight Test 5 (FT-5), the most sophisticated and difficult development test yet for the Army's Integrated Air and Missile Defense Battle Command System (IBCS), developed by Northrop Grumman.

IBCS Launch (Source: Northrop Grumman)

High above the range, sensors aboard U.S. Air Force F-35 fighter aircraft see and acquire the two surrogate missiles. IBCS integrates the aircraft sensor data with that of available ground sensors, including Sentinel, Patriot weapon system and U.S. Marine Corps TPS-59 radars. All share information via the IBCS Integrated Fire Control Network (IFCN). As one sensor loses sight of the threats—and each will at some point—the targets are acquired by other sensors on the IFCN, enabling IBCS to create a precise, uninterrupted composite track of each missile's movements.

With data from every sensor, IBCS produces a single integrated air picture on the screens of the air defense soldiers at TAC-2. They see every change in altitude and direction as the two surrogate missiles paint tracks across their screens. Because IBCS enables joint weapons as well as joint sensors, the defenders at the controls can select the best effector to use against these targets. Now, the soldiers are about to launch two Patriot Advanced Capability 2 (PAC-2) interceptor missiles.

"Without IBCS, all those different sensors operate independently, creating opportunities for threats to avoid detection as they fly to a target," explained Northrop Grumman IBCS Program Director Mark Rist. "Without being integrated onto a network, these sensors produce a more ambiguous, less-clear air picture, making engagements of threat systems more challenging."

He is monitoring FT-5 from miles away, in the test's mission control room. The soldiers at TAC-2 can be heard on the radio, calm but urgent voices reporting "target acquired" by airborne sensor, and talking of the "IP" or intercept point, and "kill box." It has only been moments since the threats were launched, but now comes "Free to engage…Missile away…Missile away…"

One, then another PAC-2 interceptor missile is launched by the soldiers. IBCS is not only able to launch the missiles, but also plays a critical role in the engagement by actively closing the fire control loop and providing in-flight updates as the PAC-2s converge on their targets. The surrogate cruise missile targets are closing in and can now be seen on video in the control room—and then suddenly they cannot: One, then the other disappears in a ball of fire as the PAC-2s destroy them.

IBCS enables soldiers to be even more effective by integrating all the systems' data and providing a common command and control (C2). Soldiers will only need to learn to use the IBCS C2, instead of spending time becoming specialists on only one or two of a dozen different sensor and weapon systems. That enhances IBCS's already impressive battlefield survivability because soldiers will be capable of using any of the available sensors with any available weapon systems at any command post connected to the self-connecting, self-healing IFCN.

Also, less time will be spent in recurrent training, making more time available for teaching operators defense strategy and how to fight. The IBCS "every sensor; best effector" concept gives commanders greater flexibility in defense design, allowing them to position resources for greatest coverage in far less time essentially helping to change the way soldiers see and fight air battle.

The open-architecture system-of-systems approach to IBCS eases integration of any new or legacy sensor and effector systems, which is important for U.S. joint operations and to foreign governments. Poland has an agreement with the U.S. Army to purchase IBCS for modernization of the nation's WISLA medium-range air defense system and other countries have expressed interest as well.

With the success of FT-5, Northrop Grumman will now focus on the Army's Limited User Test planned for later this year, followed by the low-rate initial production and full-rate production phases of the system, to field IBCS to Army air defenders in fiscal year 2021.

Blackjack Focuses on Risk Reduction Flights and Simulations to Prepare for Full Demonstration

In partnership with the U.S. Space Force and the Space Development Agency, DARPA's Blackjack program is targeting flights to low-

For More Information Visit mwjournal.com for more defense news.

Earth orbit (LEO) later this year and 2021. Using a series of small risk reduction satellites, the program aims to demonstrate advanced technology for satellite constellation autonomy and space mesh networks. Blackjack seeks to develop and validate critical elements of global high-speed autonomous networks in LEO, proving a capability that could provide the Department of Defense with highly connected, resilient and persistent overhead coverage.

The upcoming demonstration flights are all planned as rideshares, catching a ride to LEO on a launch with other missions. The first demonstration, Mandrake 1, is a cubesat that will carry supercomputer processing chips. Mandrake 2 is a pair of small satellites that will carry optical inter-satellite links for broadband data. These could form the basis of future optically meshed computer networks in LEO.

The program also is targeting a risk reduction payload called Wildcard, a software-defined radio that will experiment with links from LEO to tactical radios. A data fusion experiment with the ability to host advanced third party algorithms, known as massless payloads, is intended for an upcoming Loft Orbital mission.

Blackjack aims to demonstrate sensors that are low in size, weight and power and that can be mass produced to fit on many different buses from many different providers, for less than $2 million per payload.

The agency is evaluating buses from Airbus, Blue Canyon Technologies and Telesat, all of which have progressed through preliminary design review. The final selection of buses will happen in 2020. The program recently completed a preliminary design review for Pit Boss, selecting SEAKR as the primary performer for the on-orbit autonomy system. The agency also awarded a contract to Lockheed Martin as the satellite integrator.

Several sensor payloads are under consideration for the Blackjack demonstration sub-constellation, including overhead persistent infrared from Collins Aerospace and Raytheon; radio frequency systems from Northrop Grumman Mission Systems, Trident and Systems & Technology Research; position, navigation and timing from Northrop Grumman; optical inter-satellite links from SA Photonics and electro-optical/infrared from L3Harris. The program also recently completed a small business innovation research contract with Augustus Aerospace to work on an Army Space and Missile Defense Command-related payload.

Over the next few months, the program will run simulations to test payloads in virtual constellations of all types of missions. The goal is to show interoperability between the commoditized buses and the various payloads being considered.


Reactel, Incorporated
Reacting First to All Your Filter Needs.
REACTEL, INC.
Let our Engineers show you what we can do in tight spaces!
High Performance, Rugged Packaging, Small Size and Weight
Great things *can* come in small packages. Reactel filters are ideally suited for the demanding environments that unmanned vehicles encounter.
Many manufacturers rely on Reactel to provide units which are:
• High performance
• Lightweight
• Low profile
Contact a Reactel engineer with your filter or multiplexer requirements. We can create a unit which will be the perfect fit for your applications.
REACTEL, INC.
REACTEL, INC
8031 Cessna Avenue • Gaithersburg, Maryland 20879 • Phone: (301) 519-3660 • Fax: (301) 519-2447
For general inquiries, please email reactel@reactel.com • Follow us on Twitter: @reacteljim
Go online to www.reactel.com to download your Reactel catalog today.
RoHS Compliant 2002/95/EC
Intertek
@reacteljim

LOW NOISE AMPLIFIERS

0.5 to 18 GHz

- 50Ω Matched over Multi-Octave Bandwidths
- Excellent Gain Flatness
- Low Noise Figure, 1.3 dB
- High IP3, up to +35 dBm

Mini-Circuits®

(718) 934-4500 sales@minicircuits.com **www.minicircuits.com**

578 Rev B_P

GaN RF Continues Growing

"In the past few years, RF applications have received a boost from the implementation of GaN technology," asserted Ezgi Dogmus, PhD. Technology and Market Analyst at Yole Développement (Yole). "The main GaN RF market drivers remain telecom and defense applications." The total GaN RF market will increase from US$740 million to more than US$2 billion by 2025, with a CAGR of 12 percent.

Yole recently released its annual RF GaN technology and market report, GaN RF Market: Applications, Players, Technology and Substrates 2020. The report includes an updated packaged device and bare die market segmentation as well as an extensive analysis of 5G wireless infrastructure and competitive analysis of GaN versus other existing technologies. This report also delivers an analysis of the military GaN RF market.

In telecom infrastructure, the aftermath of U.S. sanctions related to Huawei slowed the GaN-based remote radio head market in 2019 and pushed OEMs to restructure their supply chain for the coming years. Nevertheless, GaN deployment will remain the same for the long-term. In advanced antenna systems, the increase in bandwidth will favor increasing GaN implementation. Also, small cells and backhaul connections will see an impressive deployment of GaN in the coming years. In military applications, with investments from governments to improve their national security by replacing TWT-based systems, defense will remain one of the GaN RF market's main drivers.

"Radar is the main driver in military applications, mainly due to the increase of T/R modules in new GaN-based AESA systems and stringent requirements for lightweight devices for airborne systems," detailed Technology and Market Analyst at Yole, Ahmed Ben Slimane, PhD. "The total GaN RF military market will surpass US$1.1 billion in 2025, at a 22 percent CAGR."

For handsets, GaN's high performance and small form factor could attract OEMs. The adoption of GaN PAs will depend on the evolution over the next five years of GaN's technology maturity, supply chain and cost, as well as OEM strategies. This is analyzed in Yole's GaN RF report with a detailed treatment of GaN implementation in different market segments. It also includes an extensive overview of 5G's impact on the wireless infrastructure and RF front ends, along with the GaN-based military market.

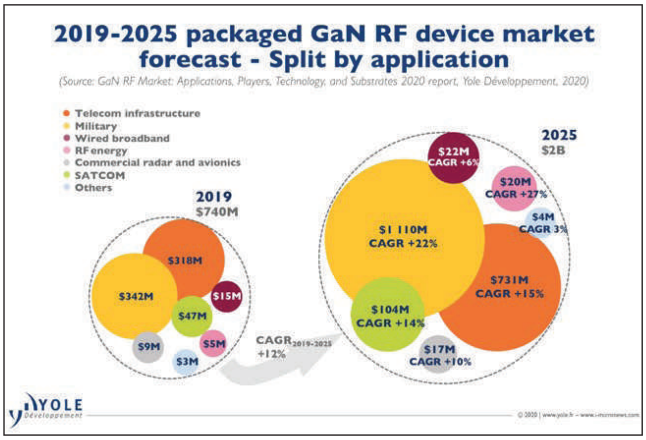

GaN Device Market Forecast (Source: Yole Développement).

It is not possible today to deliver a comprehensive and relevant picture of the RF GaN industry without considering the U.S.–China conflict and COVID-19 outbreak. Indeed, both events have started to deeply modify the semiconductor industry landscape. This analysis is also part of the 2020 RF GaN report. China is the largest market for antenna systems and will remain so for the next several years. Due to U.S. sanctions related to Huawei, the OEM's supply chain has been restructured with a positive impact on Asian integrated device manufacturers and foundries, as well as European players. For example, the European foundry UMS doubled its GaN RF business in 2019, owing mainly to the base transceiver station market. The U.S.-China trade war also makes it more urgent for Huawei and ZTE to have domestic suppliers.

"According to industry feedback, despite the virus outbreak, leading Chinese telecom operators' 5G construction goals remain unchanged and development continues," said Ezgi Dogmus from Yole. Thus, the virus outbreak is likely to have minor consequences for GaN deployment in 2020. "And we could also expect a market adjustment starting from H2-2020 in China as well as the rest of the world…" added Dogmus.

The GaN-based military market, which is the second major segment will likely follow the same trend. Yole's team expects only minor changes long term as the defense market is "on demand." However, in the short-term, some disruptions in the supply chain may slow the global military market.

EV Connected Services to Reach US$378 Million in Revenues by 2030

Subscriptions of connected services for consumer and commercial electric vehicles (EV), such as charging-station locator, eco-routing and EV telematics, will grow 270 percent from 2020 to 2024, reaching 7 million subscribers by 2024. According to ABI Research, the combined revenue opportunity of connected services for consumer and commercial EVs will reach US$378 million by 2030.

"EV sales have presented slow market growth in past years. However, the increasing number of countries setting up deadlines to end the sale of internal combustion engine (ICE) vehicles will propel higher EV adoption. While Norway voiced its intention to end the sales

For More Information Visit mwjournal.com for more commercial market news.

of new ICE vehicles by 2025, Germany, Sweden, India, China, among other countries, seek to ban the sales of ICE vehicles from 2030. Moreover, with an increasing number of cities in Europe enforcing emission rules, only EVs will be able to run in urban areas in the next years," explained Maite Bezerra, smart mobility and automotive analyst at ABI Research. "In fact, 27 million of consumer and 1 million of commercial plug-in electric vehicles (PEV) will be sold by 2030."

Lack of charging infrastructure and range anxiety are still the main factors hindering extensive EV adoption. The quantity of charging stations presented a substantial growth in the past years. China and Japan, for instance, now have over 40 thousand charging stations each. "Yet, there is a general perception of deficient charging infrastructure due to a lack of communication between vehicles and charging stations," said Bezerra. Connected services, such as HERE's EV Charging Stations and TomTom's EV Routing Services, can help change that perception by displaying information such as charging-station location, compatibility and real-time availability to drivers or fleet managers. Existing Horizon applications, which have yet to gain substantial market traction, can also be used by EVs to optimize acceleration and break events, saving energy and increasing the range of EVs considerably. Tesla, Nissan and Peugeot lead the way by offering a comprehensive suite of connected services for EVs.

The rapid adoption of EVs will pose challenges for utilities as the increased capacity creates overload peaks that compromise the stability of the grid. Therefore, communication between charging stations and utilities is also highly relevant for sustained EV adoption. Smart energy management solutions monitor, control and restrict the use of chargers for optimal energy consumption. Meanwhile, vehicle-to-grid (V2G) communication, offered by companies such as Nuvve and Virta, balance the grid by reading the frequency of power production and adjusting charging and discharging. This way, EVs can smooth the increase in electricity demand and sell energy back to the national grid or use the stored energy to reduce energy consumption from houses or buildings. Presently, Nissan and Mitsubishi are at the forefront of V2G.

Passenger EVs are often used for commuting and are charged at home or at work. Therefore, services that offer convenience and reduce range anxiety find greater traction among consumer EVs. Connected services for consumer EVs will reach 26.37 million subscribers by 2030, with a revenue opportunity of US$222 million. ABI Research anticipates 2 million subscribers by 2030 and a revenue opportunity of US$ 156 million.

When RF test and calibration become a bottleneck in your IC design process.

FormFactor delivers a hands-free solution to RF test cycles that minimizes labor, improves accuracy, cuts costs and optimizes time to market.

IC testing in the RF frequency domain demands continuous attention to performance parameters and frequent hands-on recalibration.

FormFactor now provides autonomous calibration throughout the RF test cycle. It continually monitors performance drift and automatically recalibrates when necessary. No need for an operator to be present, even when testing at multiple temperatures.

The result? More test data with higher accuracy. All at minimum time and cost.
For more information visit formfactor.com/go/RF.

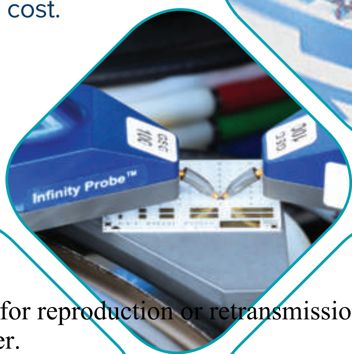

FormFactor™
Test insight from lab to fab.

Around the **Circuit**

Barbara Walsh, Multimedia Staff Editor

MERGERS & ACQUISITIONS

National Instruments Corp. (NI) announced it has entered into a definitive agreement to acquire **OptimalPlus Ltd**. The acquisition will expand NI's enterprise software capabilities to provide customers with business-critical insights through advanced product analytics across their product development flow and supply chain. NI and OptimalPlus serve highly complementary positions in the semiconductor, automotive and electronics industries. NI test systems are used in semiconductor manufacturing with OptimalPlus serving as a leading supplier of semiconductor manufacturing data analytics. Similarly, the NI automotive and electronics production test offerings are complementary to OptimalPlus' growing automotive and electronics analytics business.

Cobham Advanced Electronic Solutions announced the sale of its Cobham RAD Inc. radiation testing business in Colorado Springs, Colo. to **Radiation Test Solutions, Inc.** (RTS). Cobham RAD is a provider of military standard radiation effects test services, heavy ion single event effects testing, device preparation services prior to test, device screening and element evaluation, and quick turn prototype integrated circuit assembly.

COLLABORATIONS

ZTE Corp. announced that ZTE, along with the Guangdong branch of **China Mobile** and Migu, China Mobile's entertainment and data service subsidiary, has completed the industry's first pre-commercial trial of 8K VR field of vision (FoV) service based on 5G MEC on the live network of China Mobile. By deploying vCDN on the 5G MEC platform, the pre-commercial trial has adopted advanced FoV encoding technology, video transcoding, intelligent CDN and other edge capabilities to save more than 70 percent of bandwidth, thereby significantly improving the VR service experience and promoting the development of 5G video services.

ACHIEVEMENTS

Analog Devices (ADI) recently received a **BAE Systems** Partner 2 Win Supplier of the Year Award for "Original Component Manufacturer of the Year," based on exceptional performance and contributions to supply chain success in 2019 for BAE Systems' Electronic Systems sector. ADI was selected from a pool of more than 2,200 suppliers that worked with the sector in 2019. BAE Systems' Partner 2 Win program is designed to achieve operational excellence and eliminate defects in its supply chain by raising the bar of performance expectations to meet the demand of current and future customers.

Anritsu Corp. announced that it has achieved approval for the world's first 5G new radio (NR) standalone test for carrier aggregation. The tests are based on 3GPP TS 38.523 and were approved by 3GPP RAN5 working group in frequency range 1 (FR1). Anritsu has subsequently also achieved the 3GPP approval for carrier aggregation testing for 5G NR non-standalone in FR1. All these tests are available on the Anritsu 5G NR Mobile Device Test Platform ME7834NR. The ME7834NR is registered with both the Global Certification Forum and PCS Type Certification Review Board as Test Platform 251.

RFMW has been recognized by **BAE Systems** with their 2019 Silver Tier Award for exceptional performance and contributions to supply chain success. RFMW was one of only 26 suppliers earning this prestigious status by providing a 99.85 percent quality and 98 percent delivery rating for all of 2019.

Keysight Technologies Inc. announced that **Audix Technology Corp.**, a Taiwanese-based test laboratory, has selected Keysight's 5G solutions to verify safe levels of RF and microwave emissions from wireless devices. Audix wants to ensure that new 5G devices, operating in either sub-6GHz and mmWave frequency bands, meet electromagnetic radiation safety standards. Keysight's wide range of 5G solutions, including 5G network emulators, signal sources and analyzers, enable test houses such as Audix to validate the performance and safety compliance of devices transmitting RF and mmWave electromagnetic fields.

HaiLa Technologies Inc., a Canadian start-up that has been working to develop a low power communication technology for IoT, has now raised US$5 million in an oversubscribed seed round led by **Chrysalix Ventures**. HaiLa's technology enables the use of existing ambient signals in the air as the carrier to ride its data on.

Verkotan has selected PWC technology from **Rohde & Schwarz** for 5G NR OTA base station testing. Rohde & Schwarz has expanded its 5G NR testing portfolio with the R&S PWC200, developed for 5G massive MIMO base station testing for both production and R&D. For Verkotan, another important criterion for choosing the R&S PWC200 was the possibility to combine the solution with their own existing in-house OTA software applications and test chambers, making their investment more cost-effective. In addition to the Verkotan software, their R&S PWC200 is using software-based functionality provided by Rohde & Schwarz, including pretransfer calibration, field simulation and calibration as well as self-test.

CONTRACTS

The **U.S. Navy** has awarded **Boeing** a combined $3.1 billion in contracts for Harpoon and Standoff Land Attack Missile Expanded Response (SLAM ER) weapon systems in support of foreign military sales. About $2.6 billion of that was contracted on May 13, 2020 while the remainder had been previously awarded. Boeing

For More Information For up-to-date news briefs, visit mwjournal.com

Exceptional
Phase Noise Performance
Dielectric Resonator Oscillator

Now Available In Surface Mount!

SDRO Series
0.75" x 0.75 x 0.53"

RoHS Patented Technology

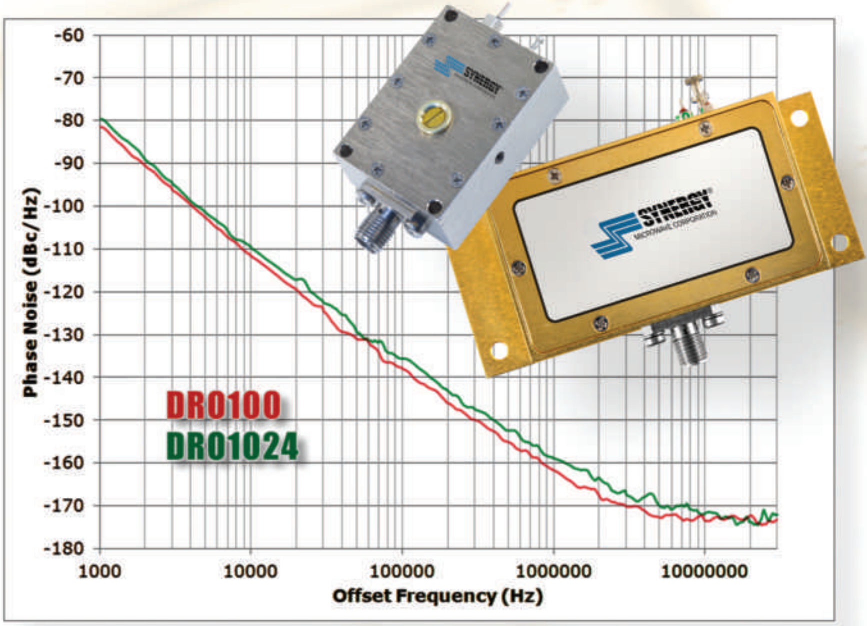

Model	Frequency (GHz)	Tuning Voltage (VDC)	DC Bias (VDC)	Typical Phase Noise @ 10 kHz (dBc/Hz)
Surface Mount Models				
SDRO800-8	8.000	1 - 10	+8.0 @ 25 mA	-114
SDRO900-8	9.000	1 - 10	+8.0 @ 25 mA	-114
SDRO1000-8	10.000	1 - 15	+8.0 @ 25 mA	-107
SDRO1024-8	10.240	1 - 15	+8.0 @ 25 mA	-105
SDRO1118-7	11.180	1 - 12	+5.5 - +7.5 @ 25 mA	-104
SDRO1121-7	11.217	1 - 12	+5.5 - +7.5 @ 25 mA	-104
SDRO1130-7	11.303	1 - 12	+5.5 - +7.5 @ 25 mA	-104
SDRO1134-7	11.340	1 - 12	+5.5 - +7.5 @ 25 mA	-104
SDRO1250-8	12.500	1 - 15	+8.0 @ 25 mA	-105
Connectorized Models				
DRO80	8.000	1 - 15	+7.0 - +10 @ 70 mA	-114
DRO8R95	8.950	1 - 10	+7.0 - +10 @ 38 mA	-109
DRO100	10.000	1 - 15	+7.0 - +10 @ 70 mA	-111
DRO1024	10.240	1 - 15	+7.0 - +10 @ 70 mA	-109
DRO1024H	10.240	1 - 15	+7.0 - +10 @ 70 mA	-115
KDRO145-15-411M	14.500	*	+7.5 @ 60 mA	-100

* Mechanical tuning only ±4 MHz

Talk To Us About Your Custom Requirements.

SYNERGY® MICROWAVE CORPORATION

Phone: (973) 881-8800 | Fax: (973) 881-8361
E-mail: sales@synergymwave.com
Web: WWW.SYNERGYMWAVE.COM
Mail: 201 McLean Boulevard, Paterson, NJ 07504

Around the **Circuit**

last delivered the SLAM ER weapon system in 2008. In October 2019, Boeing began construction on a new 35,000 sq. ft. manufacturing facility to support increased production for the Harpoon and SLAM ER programs. Construction is expected to be complete in 2021.

Kratos Defense & Security Solutions Inc. announced that it had been awarded a $4.9 million contract to modernize the infrastructure and systems that interconnect the **Air Force Satellite Control Network** (AFSCN) sites under the AFSCN Network Edge Transport System (ANETS) program. The ANETS program will enable the AFSCN to meet the growing needs of its user community. Kratos will provide CACI, the prime contractor for this program, and the government a modular, low-risk, turnkey, integrated solution based on mature commercial off-the shelf technology.

Integra Technologies was awarded a $3 million contract from **Northrop Grumman**. Integra Technologies' Wichita manufacturing facility will utilize upwards of one hundred current employees to service the new order. Integra Wichita will supply the value-added services required for the components to properly function for their final destination in military applications. With the new Northrop Grumman contract and over 290 active aerospace and defense customers, Integra's 250 Wichita employee owners are working at full capacity to meet customer demands.

Comtech Telecommunications Corp. announced that during its third quarter of fiscal year 2020, its Mission-Critical Technologies group, which is part of Comtech's Government Solutions segment, was awarded orders consisting of $1.6 million of additional funding on the previously announced three-year $124.2 million contract to provide ongoing sustainment services for the AN/TSC-198A SNAP (secret internet protocol router and non-classified internet protocol router access point) and baseband equipment. The contract has been funded $88.6 million to date.

PEOPLE

▲ *Vahid Manian*

Morse Micro, an Australian developer and innovator that is reinventing Wi-Fi for IoT and other advanced wireless technologies, has named **Vahid Manian** as their chief operating officer, responsible for overseeing Morse Micro's new U.S. headquarters. In his new position, Manian will lead its key sales, marketing, applications and operations teams. They are designing the industry's first Wi-Fi HaLow /802.11ah silicon chip—a wireless solution that securely connects smart devices over long distances using minimal power.

Our “S” Series Amplifiers Are Designed For Demanding Applications

Our “S” Series amplifier provides a wide, instantaneous frequency range from 0.7 to 6 GHz, and 15 to 500 Watts power. This capability is delivered without compromise. Consider these standard features:

- Single-band
- Class A
- High linearity
- Flatness over frequency range
- Operate in extreme VSWR
- Replicate complex modulation

The performance integrity of the “S” Series amplifier makes them ideal for use as a driver amplifier for telecom system device testing, EMC testing, and more. And as with all amplifiers from AR, these are Built to Last.

At AR, innovative solutions just keep coming. To learn more, call us at 215-723-8181 or visit www.arworld.us/SSeries.

AR Bargain Corner
Low Prices, High Quality! Visit
www.arworld.us/bargain-corner

We’re with you all the way

rf/microwave instrumentation

Other ar divisions: modular rf • sunar rf motion • ar europe

Around the **Circuit**

▲ *Neal Coching*

dB Control, an international defense electronics manufacturer and wholly owned subsidiary of HEICO Corp., has appointed **Neal Coching** as director of quality. Prior to joining dB Control, Coching was the director of operations at Teledyne Microwave Solutions. He has also served as Teledyne Cougar's director of contract manufacturing, and as quality manager for Cougar Components and V-Packet.

▲ *John D. McClellan*

Anokiwave Inc. announced that **John D. McClellan** has joined the company's Board of Directors, effective February 1, 2020. McClellan joins the Anokiwave Board of Directors with over 30 years of experience in corporate leadership, private equity and strategy consulting. He is a partner at Pear Tree Partners, L.P, which provides investment and advisory services to early stage and growth capital companies. His previous positions include CEO of Palladium, Inc., managing director at Thomas H. Lee Partners, CEO of Sprague Energy Corp. and president of EPIK Communications, which he founded.

REP APPOINTMENTS

AR RF/Microwave Instrumentation has named **Scientific Devices** as its distributor for Australia and New Zealand. Scientific Devices has expertise in a number of technologies and currently serves several markets. Scientific Devices represents manufacturers throughout Australia and New Zealand from its headquarters in Melbourne with a field office in Sydney.

Ranatec announced it has entered an agreement with **Signal Solutions Nordic** to distribute Ranatec products. Headquartered in Finland, Signal Solutions will sell Ranatec's niche portfolio of test and measurement tools in Finland, Poland and the U.S. through its regional sales offices. Signal Solutions is a provider of hardware, services and total solutions for R&D labs, test sites, manufacturing facilities and data centers with a focus on RF, microwave, fiber optics, EMC and shielding technology.

Richardson RFPD announced that it has entered into a global franchise agreement with **AVX Corp**. AVX's newest division, AVX RF Solutions, manages and works to expand the already extensive portfolio of leading-edge microwave and RF components. AVX RF Solutions encompasses AVX's RF products along with RF products from two additional AVX brands—American Technical Ceramics and Ethertronics®. The global agreement between Richardson RFPD and AVX covers the products managed by the AVX RF Solutions division, as well as AVX's power film capacitors and SuperCapacitors.

AMCOM COMMUNICATIONS
The RF Power House

New Driver Amplifiers

ISO 9001

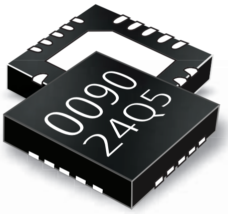

AM009024WM-QN5-R
is an ultra-broadband GaAs MMIC power amplifier. It has 22dB gain, and 24dBm output power over the 0.05 to 9GHz .

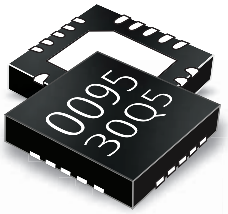

AM009530WM-QN5-R
is an ultra-broadband GaAs MMIC power amplifier. It has 20dB gain, and 30dBm output power over the 0.05 to 9.5GHz .

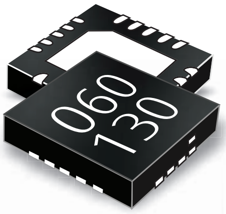

AM06013033WM-QN5-R
is a broadband GaAs MMIC which operates between 6 and 13 GHz with 28 dB gain and 33 dBm output power.

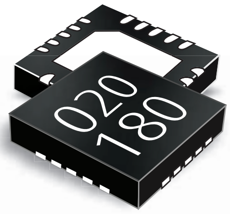

AM02018026WM-QN5-R
Broadband GaAs MMIC Distributed Power Amplifier which operates between 2 and 18 GHz with 23 dB gain, and 26 dBm output power.

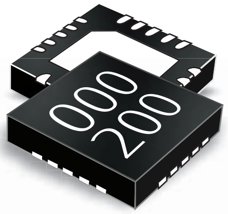

AM00020026WM-QN5-R
Broadband GaAs MMIC Distributed Power Amplifier which operates between DC and 20 Ghz with 13 dB gain, and 26 dBm output power.

Custom MMIC Circuit Design and Production

We offer custom design of MMIC circuits with output power from a few watts to over fifty watts. Power amplifiers, Low Noise Amplifiers, Phase Shifters, Attenuators, Up-converters, Down-converters, and Switches. Smart compact design in ceramic or plastic packages. Frequencies up to 40GHz. Our design team has successfully developed over 100 MMIC circuits.

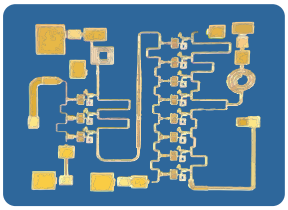

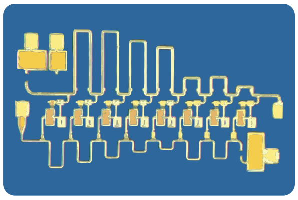

IMS
Connecting Minds. Exchanging Ideas.

Visit us Virtually

We are excited to participate in this years International Microwave Symposium (IMS) show that will be held virtually due to the COVID-19 pandemic. We are still looking forward to a great show in August!

GaAs MMIC PAs

Model	Freq(GHz)	Gain(dB)	P1dB(dBm)	Psat(dBm)	Eff(%)	Vd(V)
AM003536WM-XX-R	0.01-3.5	23	35	36	20	20
AM002535MM-XX-R	0.03-2.5	24	34	35	25	20
AM012535MM-XX-R	0.03-2.5	20	33	33.5	20	20
AM009023WM-XX-R	0.05-9	21	21	23	20	12
AM008030WM-XX-R	0.05-10	18	30	31	20	12
AM012020WM-XX-R	0.1-2	30	16	17	8	8
AM011037WM-XX-R	0.2-1.0	31	37	37.5	40	8
AM103026MM-XX-R	0.9-3.2	22	25	26	10	14
AM132740MM-XX-R	1.3-2.7	26	38	39	30	14
AM142540MM-XX-R	1.4-1.8	25	39	40	35	14
AM153040WM-XX-R	1.4-3.4	18	37	38	30	12
AM143440WM-XX-R	1.5-1.8	20.5	38.5	39	35	12
AM143438WM-XX-R	1.5-1.8	20.5	37.5	38	30	12
AM153540WM-XX-R	1.5-3.5	18	39	39.5	35	14
AM183030WM-XX-R	1.6-3.3	30.5	30.5	31.5	20	8
AM183031WM-XX-R	1.6-3.3	31.5	31.5	32.5	25	8

GaN MMIC PAs

Model	Freq(GHz)	Gain(db)	Psat(dBm)	Eff(%)	Vd(V)
AM00010037WN-00-R	DC-10	13	37	25	28
AM00010037WN-SN-R	DC-10	13	37	23	28
AM003042WN-00-R	0.05-3	24	42	35	40
AM003042WN-XX-R	0.05-3	23	42	33	40
AM206041WN-00-R	1.8-6.5	32	42	27	28
AM206041WN-SN-R	1.8-6.5	30	41	23	28
AM408041WN-00-R	3.75-8.25	33	42	27	28
AM408041WN-SN-R	3.75-8.25	31	41	23	28
AM07512041WN-00-R	7.75-12.25	28	42	27	28
AM07512041WN-SN-R	7.75-12.25	27	41	22	28
AM08012041WN-00-R	7.5-12	22	42	20	28
AM08012041WN-SN-R	7.5-12	21	41	20	28

Visit our website today to view our full product line.

www.amcomusa.com

Phone 301.353.8400 - www.amcomusa.com - info@amcomusa.com

CELEBRATING 23 YEARS OF BUSINESS

Editor's Note: In Part III, the authors describe methods to reduce stiction effects in the capacitive (metal-insulator-metal) contact MEMS switch for applications in low SNR signal routing application in modern electronics circuits including 5G communication. Also, experimental results to validate simulation results presented earlier for DSG structure-based metamaterial switch are also included in this paper. As described in Part I (May Issue), the combination of a primary shunt switch, DGS structures and secondary shunt switches, is shown to behave like a metamaterial. In Part II, the authors have shown new ways to reduce stiction effects in the Resistive MEMS switch (metal-to-metal contact) using artificially created metamaterial structure.

INVITED PAPER

A Microelectromechanical Switch with Metamaterial Contacts, Part III: Reducing Stiction

Shiban K. Koul and Pranav K. Srivastava
C.A.R.E, Indian Institute of Technology, Delhi, India

Ajay K. Poddar and Ulrich L. Rohde
Synergy Microwave, N.J., U.S.

The theory of a repulsive Casimir force and application in a resistive contact MEMS switch is discussed in detail in Part II (June Issue). In this article, a new method to reduce the stiction effects in the capacitive (metal-insulator-metal) contact MEMS switch that has applications in low SNR signal routing application in modern electronics circuits including 5G communication is described.[1-8] In addition, experimental results to validate simulated results presented earlier for DSG structure-based metamaterial switch are included.

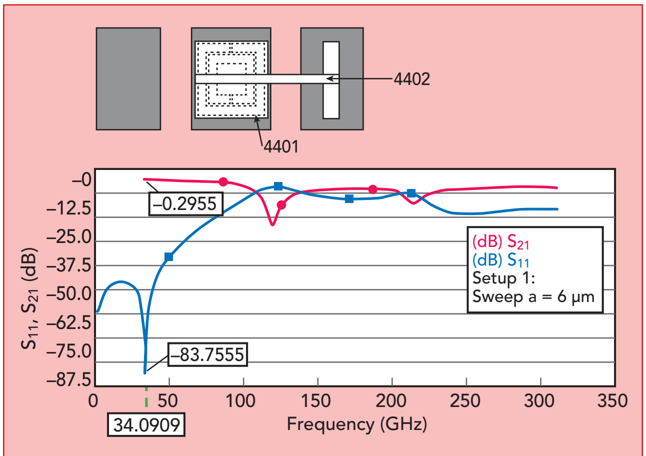

Fig. 1 Transmission and reflection characteristics of composite structure described by 4401 and 4402.

CASIMIR REPULSIVE FORCE INSPIRED CAPACITIVE MEMS SWITCH

The metamaterial unit cell described in reference[9] and realized using a composite engineered structure, provides promising characteristics in the relevant band of frequencies for the MEMS switch (e.g., between 60 to 130 GHz). ***Figures 1*** to ***3*** provide results for transmission and reflection characteristics for a respective unit cell structure. The composite structure, 4401 illustrated in Figure 1, is included in a metal layer

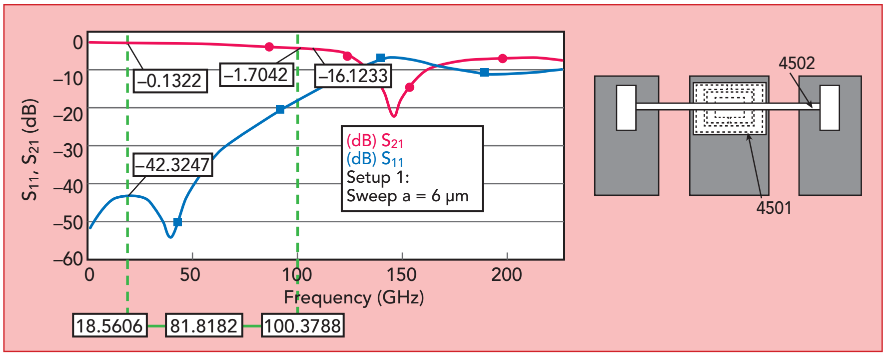

Fig. 2 Transmission and reflection characteristics of composite structure described by 4501 and 4502.

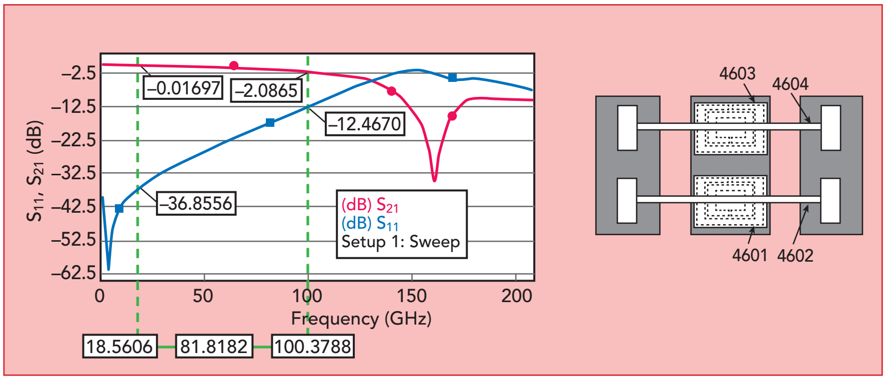

Fig. 3 Transmission and reflection characteristics of composite structure described by 4601 and 4602.

(e.g., of a signal line contact) and interfaces beam 4402. In this example, the beam is thinner than the metamaterial structure, and is supported by a single support extending from one of the ground planes adjacent the signal line. The unit cell is a transmission type at about 34 GHz (having reflection characteristics of -83.75 dB and transmission characteristics of -0.29 dB). The unit cell is a reflection type at about 120 GHz. Thus, the composite structure in Figure 1 is shown to exhibit metamaterial properties, can be used for the realization of stiction free capacitive (metal-insulator-metal) contact MEMS switch.

The composite structure (4501) shown in Figure 2 is included in a metal layer (e.g., of a signal line contact) and interfaces with beam 4502. In this example, the beam is thinner than the metamaterial structure, and is doubly supported by posts on either side of the signal line. The unit cell is a transmission type at about 40 GHz (having reflection characteristics of -54 dB and transmission characteristics of -0.5 dB). The unit cell is a reflection type at about 140 GHz. Thus, the structure of Figure 2 is shown to exhibit metamaterial properties also, hence can be used for the realization of stiction free capacitive (metal-insulator-metal) contact MEMS switch.

Figure 3 includes two composite structures, 4601 and 4603, positioned at opposing input and output sides of the signal line. Each composite structure is included in a metal layer (e.g., of the signal line contact). Further, doubly supported beams, 4602 and 4604, are positioned above each of the composite structures. As in the example of Figure 2, the beams are thinner than the metamaterial structures. The unit cell is a transmission type at about 8 GHz (having reflection characteristics of -60 dB and transmission characteristics of -0.01 dB). The unit cell is a reflection type at about 160 GHz. Thus, the structure of Figure 3 is shown to exhibit metamaterial properties too, hence can be used for the realization of stiction free capacitive (metal-insulator-metal) contact MEMS switch.

Another example of a capacitive MEMS switch is shown in ***Figure 4***.

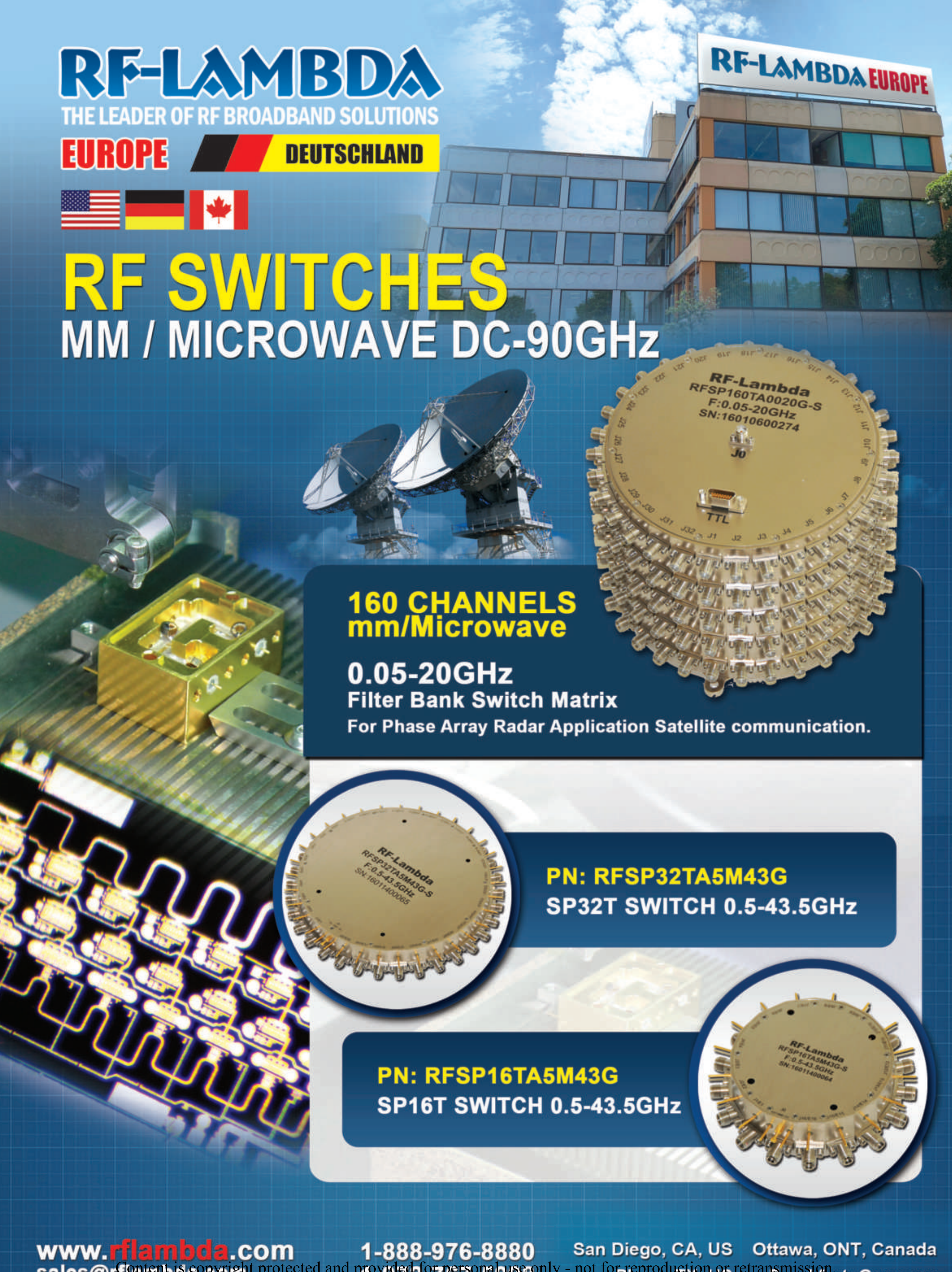
RF-LAMBDA
THE LEADER OF RF BROADBAND SOLUTIONS
EUROPE
DEUTSCHLAND
RF-LAMBDA EUROPE
RF SWITCHES
MM / MICROWAVE DC-90GHz
RF-Lambda
RFSP160TA0020G-S
F:0.05-20GHz
SN:16010600274
J0
TTL
160 CHANNELS
mm/Microwave
0.05-20GHz
Filter Bank Switch Matrix
For Phase Array Radar Application Satellite communication.
PN: RFSP32TA5M43G
SP32T SWITCH 0.5-43.5GHz
PN: RFSP16TA5M43G
SP16T SWITCH 0.5-43.5GHz
www.rflambda.com
sales@rflambda.com
1-888-976-8880
1-972-767-5998
San Diego, CA, US
Plano, TX, US
Ottawa, ONT, Canada
Frankfurt, Germany

As illustrated in Figure 4, the switch includes a structure formed over a signal line having an input side 4712 and an output side 4714. A metamaterial structure having an outer split ring 4722 and inner split ring 4724 is formed in the signal line contact between the input side 4712 and output side 4714, through which a signal is received (arrow in) and an output port through which the signal is transmitted (arrow out).

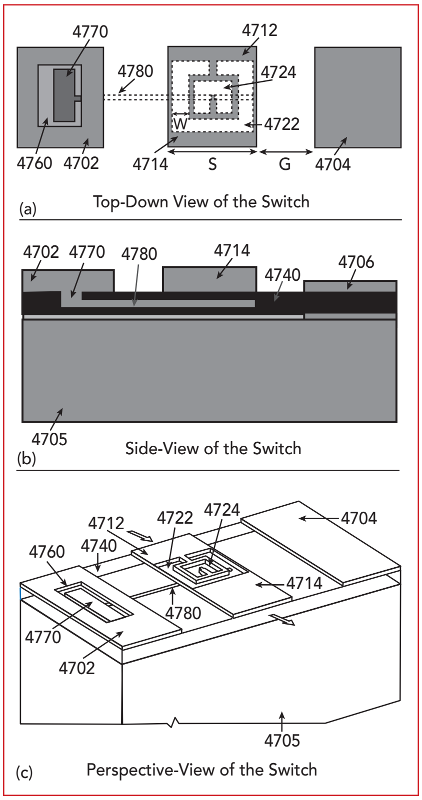

Fig. 4 Diagram of capacitive MEMS switch incorporating metamaterial cells to provide a repulsive Casimir Force between contacts of switch: (a) top-down view, (b) side view and (c) perspective view.

Each of the ground planes 4702, 4704 and the signal line are formed from a conductive material, such as gold, and are formed on top of a dielectric material 4740 such as silicon nitride (Si3N4), which itself is formed on top of a substrate 4705. One of the ground planes 4702 includes a post 4770 extending downward from the ground plane 4702 into the dielectric material 4740, and a beam 4780 extending from the post 4770 in the direction of the signal line 4714. The edge of the beam 4780 is aligned with the opposing edge of the signal line 4712, 4714, such that the end of beam 4780 is positioned underneath the metamaterial structures 4722, 4724, of the signal line 4712, 4714. In Figures 4a and 4c, the post 4770 can be seen through an opening 4760 in the ground plane 4702.

In the example of Figure 4, the ground planes and the signal line may each have a width (in the direction of the beam 4780 length) of about 73 μm and the beam may have a length of about 168 μm. The metamaterial structure formed on the signal line contact may have a ring width W of about 15 μm, a split width G of about 8 μm and a spacing between rings S of about 5 μm.

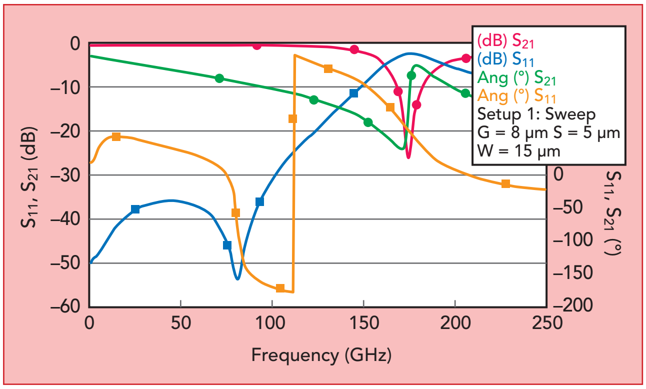

Fig. 5 Transmission and reflection characteristics of capacitive MEMS switch in Figure 4.

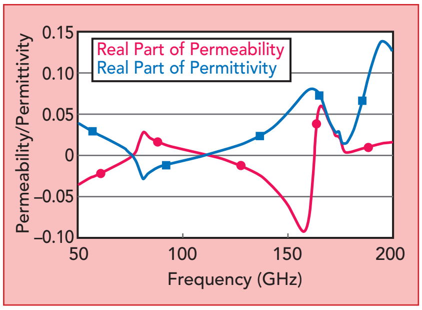

Fig. 6 Plot of permittivity extracted from the S-parameters of the composite structure shown in Figure 4.

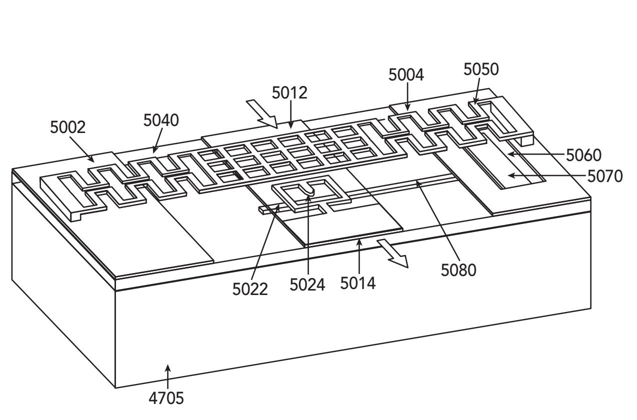

▲ **Fig. 7** **Perspective view of a capacitive shunt MEMS switch utilizing a metamaterial signal line contact to reduce stiction in the switch.**

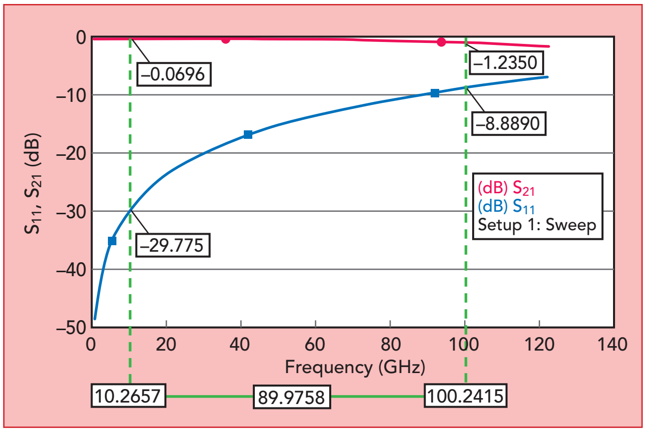

▲ **Fig. 8** **Transmission and reflection characteristics of capacitive MEMS switch shown in Figure 7 in the ON State.**

Transmission and reflection characteristics of the switch over a range of frequencies are shown in ***Figure 5***. The metamaterial is most reflective at about 175 GHz and most transmissive at about 80 GHz. Based on these results, material parameter extraction[10] can be performed to determine the permittivity and permeability of the metamaterial structure. The extraction of the permeability and permittivity are shown over a range of frequencies in ***Figure 6***.

As seen in Figure 6, the metamaterial structure exhibits near zero permittivity and permeability between about 50 and 150 GHz. This indicates that the structure of Figure 4 is suitable for reducing the stiction using the Casimir force of interaction (repulsive) in the desired frequency band.

Figure 7 shows a perspective view of a capacitive shunt MEMS switch utilizing a metamaterial signal line contact to reduce stiction in the switch. Many of the features of switch illustrated in Figure 7 may be compared to the switch described in Figure 4. The switch in Figure 7 also includes a deflectable beam 5050. The beam is comparable to the rectangular beam 510 described in connection with Figure 5 of Part I (May Issue) (e.g., may be made from gold, may have a perforated grid structure, may extend in a serpentine pattern). The deflectable beam 5050 is supported by a pair of posts formed on top of the ground planes 5002 and 5004, respectively, and is configured to deflect downward toward the signal line when actuated by a bias voltage.

In operation, the bias voltage causes the midpoint of the beam 5050 to deflect downward until it comes in contact with the signal line contact, thereby causing the signal line to turn off (or in other cases to turn on). When the bias voltage is removed, the midpoint of the beam 5050 deflects back upward. Because the midpoint of the beam is aligned with the metamaterial structure 5022, 5024 of the signal line contact, the Casimir effect at the interface between the beam and the signal line contact is diminished or even repulsive, thereby reducing the liability of stiction between the beam 5050 and the signal line.

Although not shown in Figure 7, the signal line contact can include a layer of dielectric material above the metal layer including the metamaterial structure. The dielec-

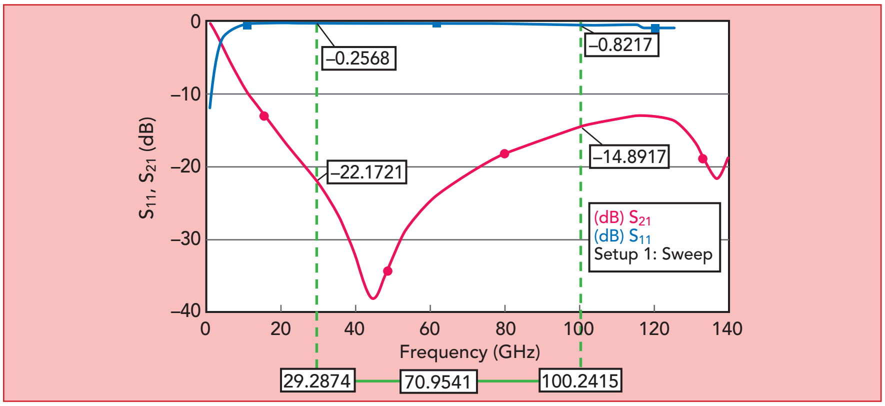

Fig. 9 Transmission and reflection characteristics of capacitive MEMS switch shown in Figure 7 in the OFF State.

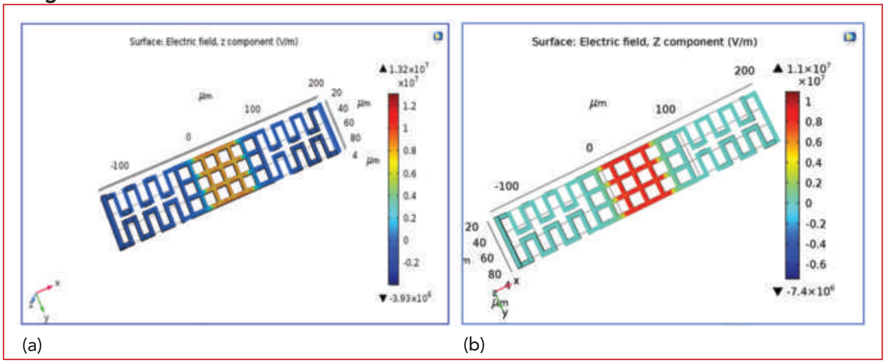

Fig. 10 Electric field distribution of a shunt switch with serpentine signal line and (a) with and (b) without metamaterial.

tric layer can function as an isolation layer to achieve the desired permittivity gradient, as discussed above in connection with Figure 5 (Part II, June Issue). In other words, the beam 5050 can have an infinite permittivity, the isolation layer can have a positive but smaller permittivity and the metal layer including the metamaterial structure in the signal line contact can have a near zero, zero or negative permittivity, thereby satisfying $\varepsilon_1<\varepsilon_2<\varepsilon_3$ condition or vice-versa. The performance of the capacitive MEMS switch (Figure 7) is shown in ***Figures 8*** and ***9*** which are plots of the reflection and transmission characteristics of the switch across a range of high RF frequencies. Figure 8 demonstrates operation of the switch in the ON state (transmitting signals) and Figure 9 demonstrates operation of the switch in the OFF state (cutting off transmission of signals).

In Figure 8, most notably, at 10.3 GHz, return loss is as high as 29.8 dB while insertion loss is as low as about 0.07 dB. Even at 100.2 GHz, return loss is as high as 8.9 dB while insertion loss is only about 1.23 dB. This demonstrates good operation of the switch in the ON state across a wide range of high frequencies, from 10 to 100 GHz.

In Figure 9, the switch is OFF, thus changing to being reflective instead of transmissive. At 29.3 GHz, insertion loss is as high as about 22.2 dB while return loss is as low as about 0.26 dB. Even at 100.2 GHz, insertion loss is as high as 14.9 dB while return loss is only about 0.82 dB. This demonstrates good operation of the switch in its OFF state across nearly the same wide range of high frequencies, from about 20 to 100 GHz.

Good insertion loss and return loss characteristics of the MEMS switch in the ON and OFF states are achieved over 30 to 100 GHz. This makes the presently described switch a good candidate for high frequency switching operations over a wide bandwidth of frequencies. Accordingly, the switches described can improve operation and performance of applications requiring high frequencies over a wide bandwidth. Such technologies may include 5G communications,

Your Smart Partners in RF

Powering the Industry's 5G Solutions

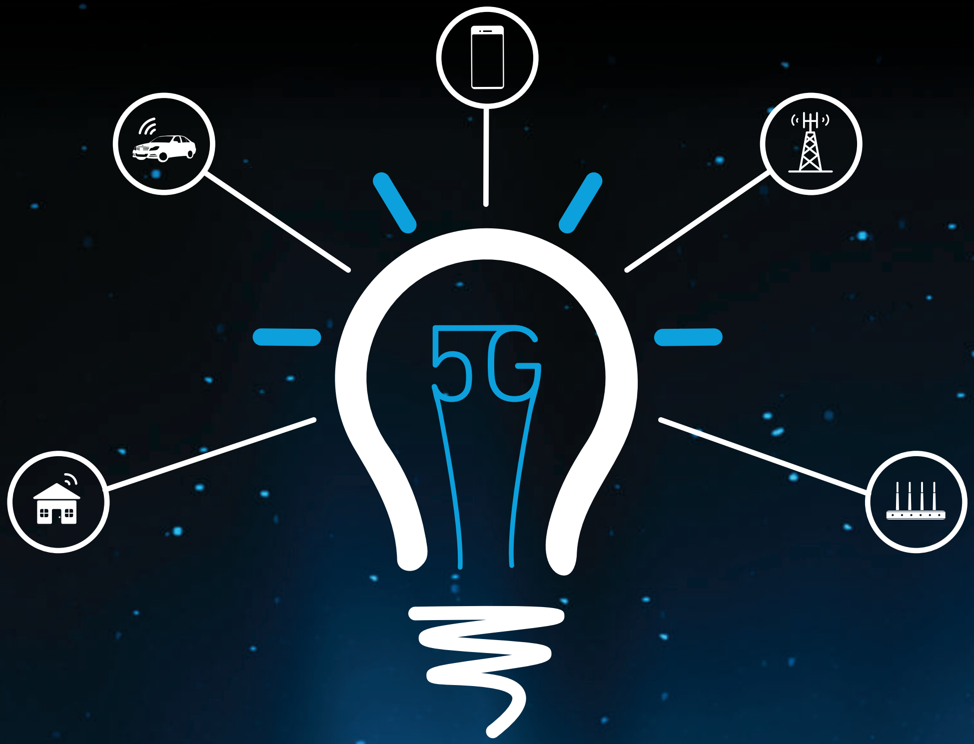

High Gain Driver Amplifier for 5G Massive MIMO

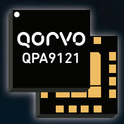

The QPA9121 is a 2.3-5 GHz, high gain and high peak power driver amplifier. Using Qorvo's GaAs HBT process, it provides 27 dBm P3dB with 28 dB gain at 2.6 GHz.

300 Watt GaN RF Transistor for Base Stations

The QPD3640 is a dual-path discrete GaN-on-SiC HEMT for Band 42 and Band 43. This singled stage matched Doherty® transistor delivers P4dB of 389 W at +50 V.

Qorvo® is making 5G deployment a reality and supporting the growth of mobile data with a broad range of RF connectivity solutions. Qorvo offers an industry-leading portfolio of high-performance discrete RF components with the highest level of integration of multifunction building blocks targeted for 5G massive MIMO or TDD macro base stations.

QORVO®

View our robust RF portfolio for both infrastructure & smartphone applications at www.qorvo.com/5g.

RFMW

For more information and product samples, visit our distribution partner, RFMW, at www.rfmw.com/qorvo.

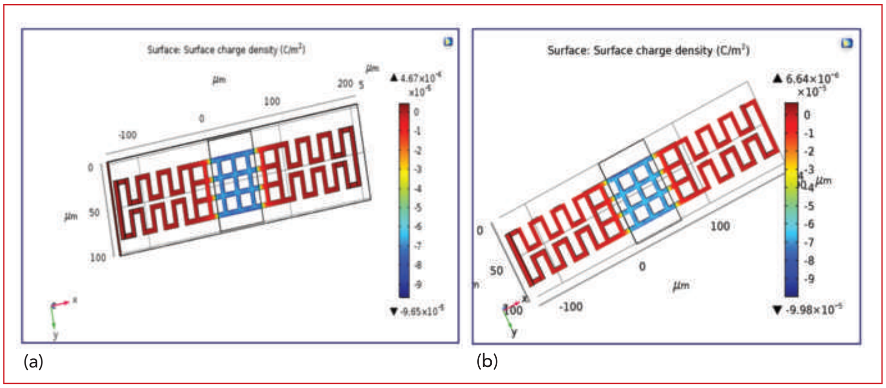

▲ Fig. 11 Surface charge density of a shunt switch with serpentine signal line and (a) with and (b) without metamaterial.

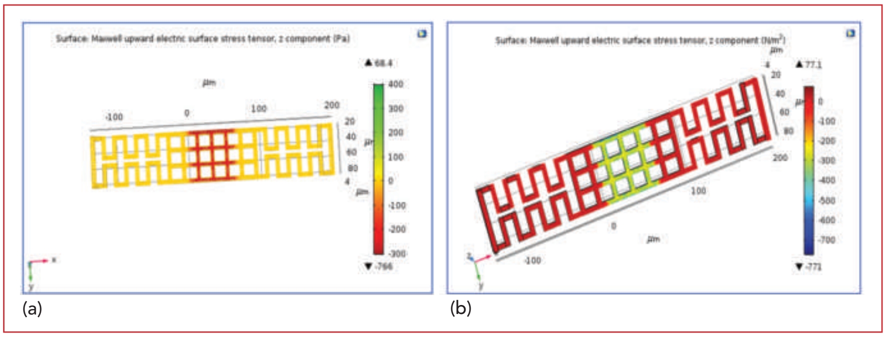

▲ Fig. 12 Electric surface stress tensor of a shunt switch with serpentine signal line and (a) with and (b) without metamaterial.

switching networks, phase shifters (e.g., in electronically scanned phase array antennas) and IoT applications.

CASIMIR FORCE STUDY

In Part I (May Issue), it is shown that a combination of a primary shunt switch, DGS structures and secondary shunt switches behave like a metamaterial. In Part II (June Issue), improvement of resistance to stiction of the MEMS switch using metamaterial layers within the design of resistive switch contact is covered. Here in Part III, the metamaterial layers are used as part of the signal line contacts to realize capacitive switch to improve stiction and hence reliability.

To get more insight into the repulsive Casimir forces generated in these structures, a detailed study of a shunt switch with serpentine signal line with and without metamaterial underneath was carried out using COMSOL software. ***Figures 10*** to ***12*** show electric field distribution, surface charge distribution and electric surface stress tensor of a shunt switch with serpentine signal line with and without metamaterial underneath.

From these results, one can estimate Casimir force. The estimated Casimir force of a shunt switch with serpentine signal line with and without metamaterial underneath is shown in ***Figure 13*** and ***Table 1*** shows key parameters for the serpentine structure with and without the metamaterial. As observed, the structure with metamaterial underneath exhibits Casimir repulsive force.

To verify the accuracy of the simulations, sample structures were fabricated using the PolyMUMPs process and characterized. As an example, the metamaterial inspired MEMS shunt switch shown in Figure 15 (Part I, May Issue) was fabricated and characterized. The SEM and optical microscope images of the fabricated structure are shown in ***Figure 14***. Both primary and secondary switches were experimentally characterized and Eigen frequency, CV characteristics, profiling and LDV plotted. It was observed that the results obtained from the simulations matched with measured data.

Figure 15 and ***16*** show the mea-

Superposition.

XFdtd® Makes it Super Easy.

XFdtd's superposition simulation enables highly sophisticated array analysis.

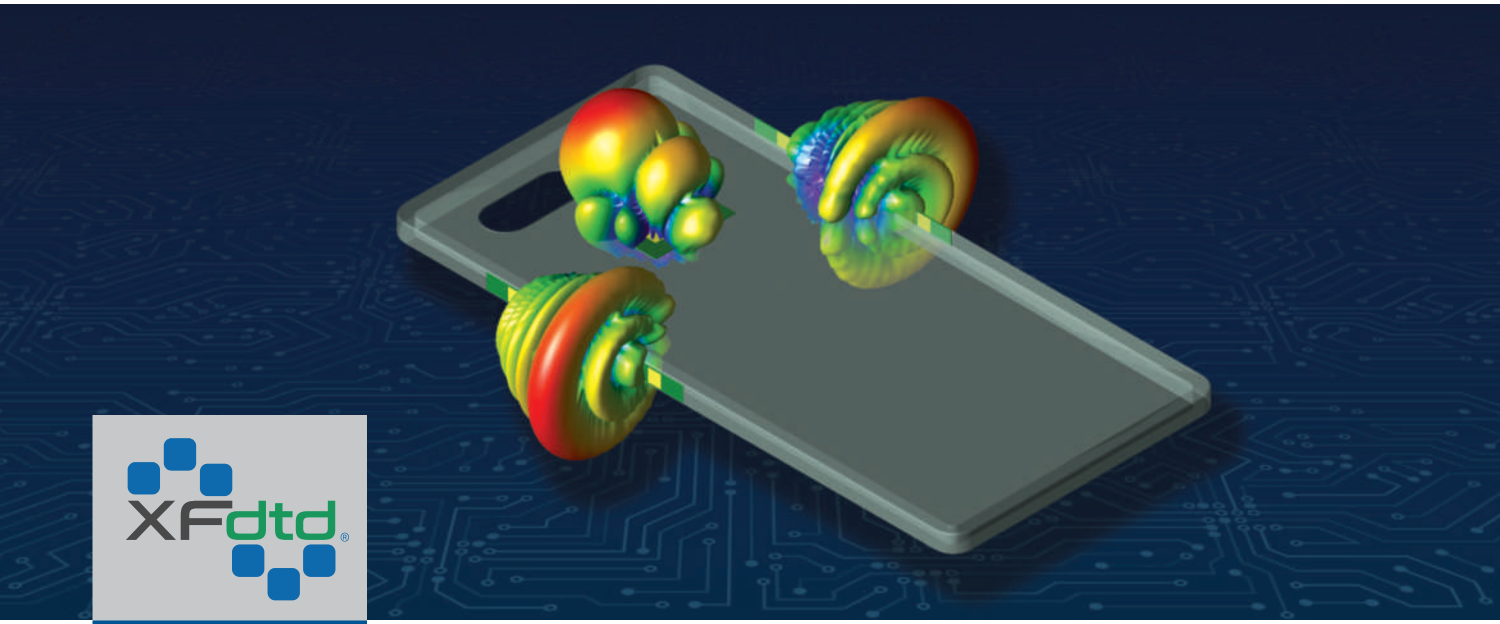

XFdtd®

Electromagnetic
Simulation Software

Designing high-frequency MIMO and 5G devices for optimized performance requires intensive, yet efficient, analysis. Beamforming applications increase complexity due to hundreds or even thousands of beam states that must be analyzed.

XF overcomes these challenges using superposition simulation.

XF leverages the EM principle of superposition to quickly analyze port phase combinations with a single simulation and identifies the ones that maximize far zone coverage in each direction.

The result? Simplified MIMO beamforming array analysis and a greatly streamlined workflow.

Learn more and request a demonstration at | **www.remcom.com/xf7**

REMCOM®

+1.888.7.REMCOM (US/CAN) | +1.814.861.1299 | **www.remcom.com**

Improve the design process | Reduce development costs | Deliver superior results

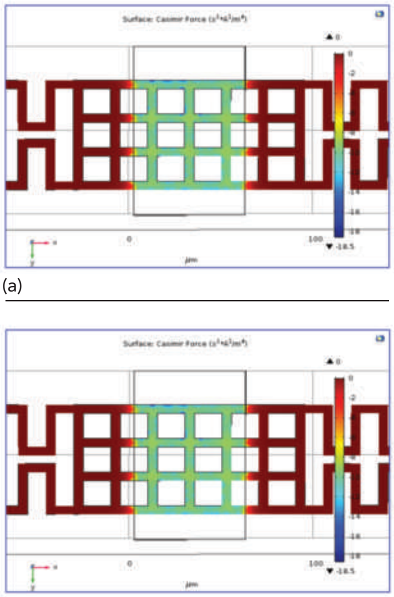

(a)

(b)

▲ Fig. 13 Estimated Casimir Force of a shunt switch with serpentine signal line and (a) with and (b) without metamaterial.

TABLE 1

KEY PARAMETERS FOR SERPENTINE STRUCTURE WITH AND WITHOUT METAMATERIAL IN THE SWITCH

No.	Parameter	Serpentine Structure with Metamaterial Underneath	Serpentine Structure without Metamaterial Underneath
1	Electric Field (V/m)	1.32×10^7	1.1×10^7
2	Electric Charge (C)	-9.65×10^{-5}	-9.98×10^{-5}
3	Electric Surface Tensor (Pa)	-766	-771
4	Calculated Force (10^{-5}N)	-18.5	1,980

sured results (all the measurements were done on bare die). It was observed that by using serpentine beam, pull in voltage reduced by 9 V. Work on different packages suitable for the present application was also done separately.[11-12] Using these techniques, measurements were carried out after packaging without noticing significant changes in the switch performance.

SUMMARY

RF-MEMS switches can provide new solutions for the 5G and IoT applications in which reconfigurable broadband and frequency-agile devices, like high-order switching components, tunable filters, multi-state

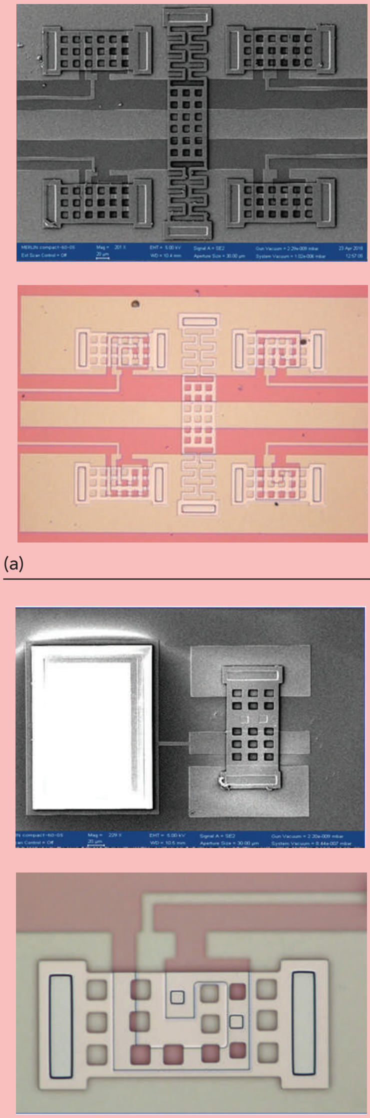

(a)

(b)

▲ Fig. 14 SEM image and Optical Microscope images of (a) primary and (b) secondary shunt switches.

ACHIEVE FAST & ACCURATE DESIGNS.

Accelerate your high frequency designs with ***Modelithics scalable, parasitic simulation models*** *and* ***3D Geometry models*** *in* ***Ansys® HFSS.***

Request a **FREE** trial
www.Modelithics.com/MVP/HFSS

3D Geometry Models

- Substrate Independent
- Measurement Validated
- Physical Geometry-based
- Full Wave 3D EM simulation
- Including over **200** 3D Models

Microwave Global Models for Ansys HFSS EM Co-Simulation

- Substrate Scaling
- Part Value Scaling
- Equivalent Circuit Based
- Statistical Analysis
- Seamless EM Co-Simulation
- Featuring **30** vendors representing more than **18,000** components, including over **300** circuit models

Vector E field in plane perpendicular to length of parts

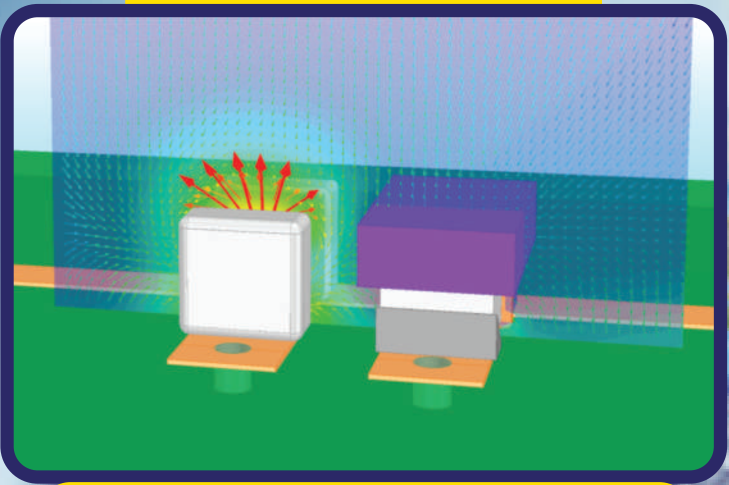

Pictured are encrypted 3D component models of a Johanson R14S chip capacitor and a CoilCraft 0603CS wire-wound chip inductor, included in the Modelithics COMPLETE+3D Library for Ansys HFSS.

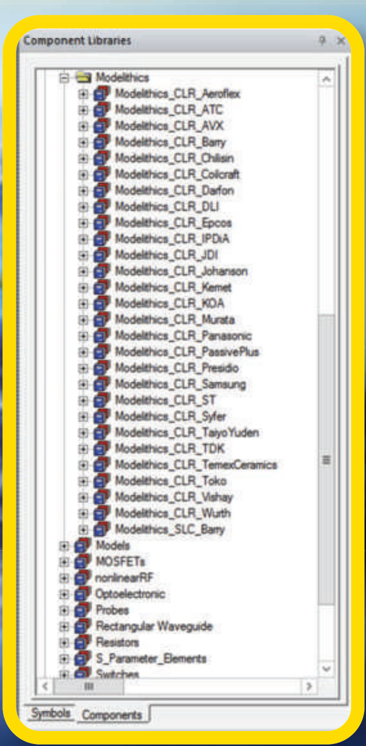

Modelithics®
World's Best RF & Microwave Simulation Models
www.Modelithics.com

Ansys
www.Ansys.com

attenuators and phase shifters will be necessary to enable mmWave communications, small cells and advanced beamforming.[13-14]

As discussed in Part I and Part II of this series, reliability, packaging and integration with standard technologies, were the primary aspects that restricted the usage of MEMS devices in commercial markets.[15-18] Part III highlighted the research efforts that targeted the reliability concerns by exploiting Casimir effect in metamaterial inspired MEMS switch, resulting noteworthy improvement in switch characteristics for 5G and IoT applications.[19]

In this three-part article, the metamaterial structures described are split rings. However, other metamaterial structures can be used, provided those structures provide similar permittivity and permeability characteristics within the desired range of frequencies. For instance, a topology inspired Möbius transformation MTM (metamaterial) structures (meaning a structure that forms a continuous closed path that maps onto itself) can be considered advantageous for generating repulsive Casimir forces.[9] Although this series of articles described specific new configurations of MEMS switches,

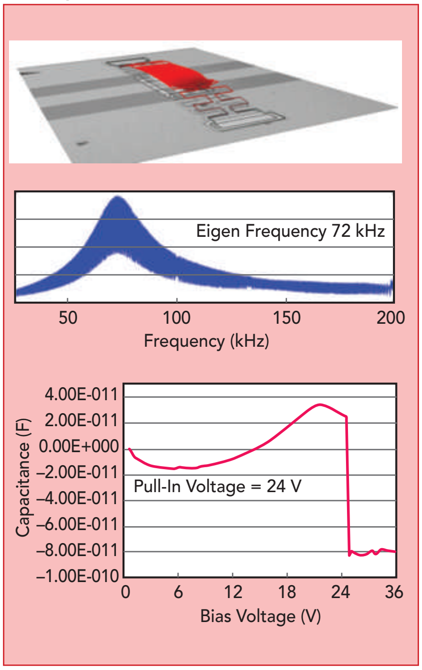

▲ Fig. 15 Plots of measured Eigen frequency and pull-in-voltage of the primary shunt switches.

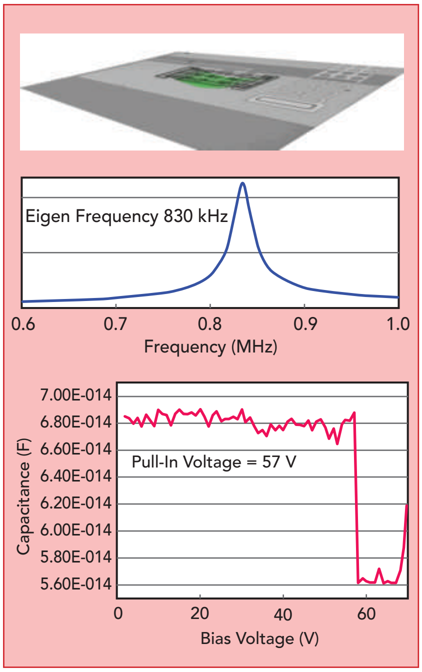

▲ Fig. 16 Plots of measured Eigen frequency and pull-in-voltage of the secondary shunt switches.

DELTA
Electronics Mfg. Corp.
SMP - SMPM - SMPS
High Performance
Connectors to 65 GHz
SMP
SMPM
SMPS
Interconnects
that Guide &
Protect us
978-927-1060
sales@deltarf.com
deltarf.com

these are just some embodiments of designs that are merely illustrative of the principles and applications of the present invention.[1] It is therefore to be understood that numerous modifications can be made to these designs that utilize the same principals demonstrated here.■

References

1. Shiban Koul, Ajay Poddar, Ulrich Rohde, "Microelectromechanical Switch with Metamaterial Contacts," *US Patent Pub. No. 02161415A1.*
2. Astrid Lambrecht, "The Casimir Effect: a Force from Nothing," *Physics World September 2002.*
3. F. Intravaia and C. Henkel, *New Frontiers of Casimir Force*, Santa Fe, New Mexico, 2009.
4. U. Leonhardt and T. G. Philbin, "Quantum Levitation by Left-Handed Metamaterials," *New J. of Physics*, August 2007.
5. Mercado et. al, "A Mechanical Approach to Overcome RF MEMS Switch Stiction Problem," *ECTC 2003.*
6. Chaitanya Mahajan, "Design and Analysis of RF MEMS Switches (70 Ghz to 130 GHz), M. Tech dissertation, *CARE*, IIT Delhi, May 2018.
7. J. Sun, X. K. Hua and L. Gao, "Repulsive and Attractive Casimir Forces between Magnetodielectric Slabs," *Solid State Commun.*, Vol. 152, No. 17, September 2012, pp. 1666–1669.
8. V. Yannopapas and N. V. Vitanov, "First-Principles Study of Casimir Repulsion in Metamaterials," *Phys. Rev. Lett.*, Vol. 103, No. 12, September 2009, pp. 120401.
9. Ulrich Rohde, Ajay Poddar and Shiban Koul, "MTM: Casimir Effect and Gravity Wave Detection" *APMC 2016.*
10. Xudong Chen et. al," Robust Method to Retrieve the Constitutive Effective Parameters of Metamaterials," *Phy. Rev. E70*, 016608, July 2004.
11. S. Chaturvedi, S. Bhalke, M. Bhat K., G. Sai Saravanan, R. Muralidharan and Shiban K. Koul, "EM Simulation and Development of Wafer Level Micro-Packaging Technique for GaAs-based RFMEMS Switches," *Compound Semiconductor Manufacturing Techniques (CSMANTECH) Conference*, May 17-20, 2010, Portland, Ore., U.S., pp. 303-305.
12. S. Chaturvedi, "Modelling of Packages for MMICs and MEMS, Ph.D. Thesis, IIT Delhi under the supervision of Shiban K Koul," *CARE*, IIT Delhi, 2012.
13. L.-Y. Ma et al, "Comprehensive Study on RF-MEMS Switches Used for 5G Scenario," *IEEE Access*, Vol. 7, pp. 107506–22, 2019.
14. J. Iannacci et. al, "RF-MEMS Monolithic K and Ka Band Multi-State Phase Shifters as Building Blocks for 5G and Internet of Things (IoT) Applications," *MDPI Journal*, Sensors, 2020.
15. S. Dey, S. K. Koul, A. K. Poddar and U.L. Rohde, "RF MEMS Switches, Switching Networks and Phase Shifters for Microwave to Millimeter Wave Applications," *ISSS Journal of Micro and Smart Systems*, April 2020.
16. G.S. Karthikeya, S. K. Koul, A. K. Poddar and U.L. Rohde, "Ultra-compact Orthogonal Pattern Diversity Antenna Module for 5G Smartphones," *Microwave and Optical Technology Letters*, March 2020.
17. S. Dey, S. K. Koul, A. K. Poddar and U.L. Rohde, "Compact, Broadband, and Reliable Lateral MEMS Switching Networks for 5G Communications," *PIERS*, pp. 163–171, January 2019.
18. S. Dey, S. K. Koul, A. K. Poddar, U.L. Rohde, "Reliable and Compact 3- and 4-Bit Phase Shifters Using MEMS SP4T and SP8T Switches," *Journal of Micromechanical Systems*, pp. (99):1-12, January 2018.
19. A. K. Poddar, "Slow Wave Resonator Based Tunable Multi-Band Multi-Mode Injection-Locked Oscillator," *Dr.-Ing.-Habil Thesis*, BTU Cottbus, Germany, 2014.

INVITED PAPER

RLC Parameter Extraction Using the Transfer Matrix

Brian Walker
Copper Mountain Technologies, Indianapolis, Ind.

The intuitive understanding of an RF network is only possible if its behavior can at least be understood in first order terms. To aid this understanding, RLC parameter extraction can be very enlightening.

To illustrate, knowing that a 0.1 pF effective capacitance exists between the nodes of a lowpass filter might lead to a superior design: shielding between the nodes, resulting in greater stopband isolation. ***Figure 1*** plots the response of a three element, 500 MHz Butterworth filter, showing the effect of 0.1 pF stray capacitance across an ideal inductor. Above 4 GHz, the isolation is clearly compromised by the stray capacitance.

While this simple example assumes ideal components, it is reasonable to say that stray capacitance between the nodes of a lowpass filter is detrimental—which is why high isolation, lumped-element lowpass filters have shields between sections, where the capacitors to ground are implemented with a feedthrough capacitor in the wall of each shield.

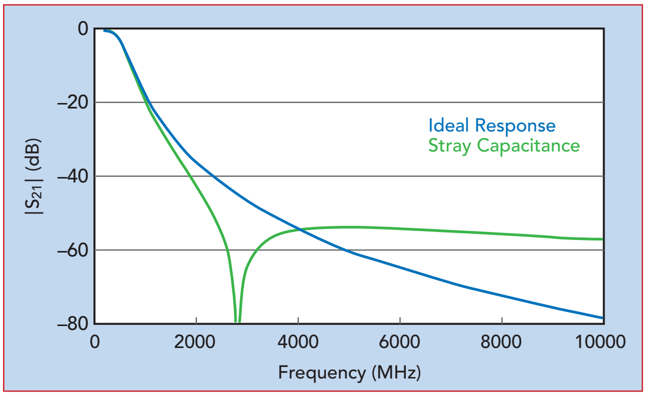

Fig. 1 **$|S_{21}|$ response of a 500 MHz Butterworth lowpass filter, showing the effect of a 0.1 pF stray capacitance in parallel with the ideal inductor.**

ABCD PARAMETERS

Actual components are never ideal, making mathematical extraction useful to understand their limitations. ABCD parameters, which are also known as cascade, chain or T parameters, are particularly useful for this purpose. For a two-port network, the ABCD parameters are defined as[1]:

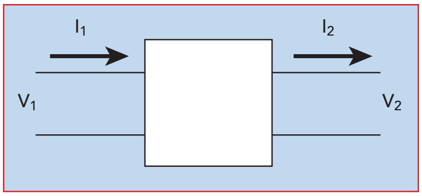

Fig. 2 **Two-port network signal flow for ABCD parameters.**

$$\begin{bmatrix} v_1 \\ i_1 \end{bmatrix} = \begin{bmatrix} A & B \\ C & D \end{bmatrix} * \begin{bmatrix} v_2 \\ i_2 \end{bmatrix} \quad (1)$$

where v_1 and v_2 are the input and output voltages, i_1 flows into the network on the left side and i_2 flows out of the network on the right side (see ***Figure 2***). i_2 is sometimes shown flowing into the right side to preserve symmetry; in that case, its sign is reversed.

Applied to π and T networks (see ***Figure 3***), with some algebra on the voltages and currents of the networks, the ABCD parameters for the π network are:

$$\begin{bmatrix} A & B \\ C & D \end{bmatrix} = \begin{bmatrix} 1+ZY_2 & Z \\ Y_1+Y_1Y_2Z+Y_2 & 1+ZY_1 \end{bmatrix} \quad (2)$$


EXODUS
ADVANCED COMMUNICATIONS
Best in Class RF Amplifier SSPA's
High Power Solid State Power Amplifiers
Chip & Wire Hybrid Assemblies, Modules & Systems
Broadband, CW, Pulse & Linear Applications
10kHz to 51GHz, 3KW CW, 10KW Pulse
Medium Power Amplifiers
10kHz to 51GHz, 2W P1dB and below
Low Noise Amplifiers
Block Up Converters
New! Synthesizers
Exodus, Your Solution Provider 10kHz to >51GHz!
3674 E. Sunset Road, Suite 100
Las Vegas, Nevada 89120 USA
Tel : 1-702-534-6564
Fax : 1-702-441-7016
Email : sales@exoduscomm.com
EXODUS ADVANCED
COMMUNICATIONS

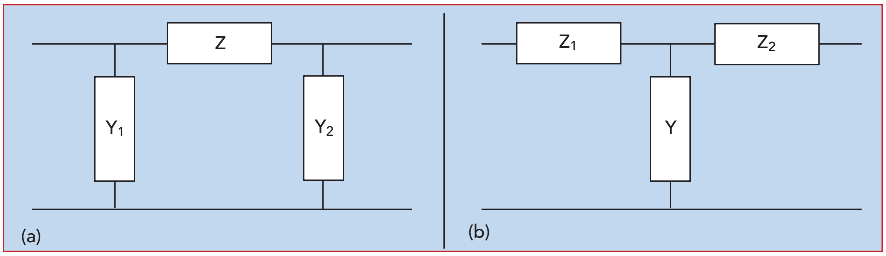

Fig. 3 π (a) and T (b) networks.

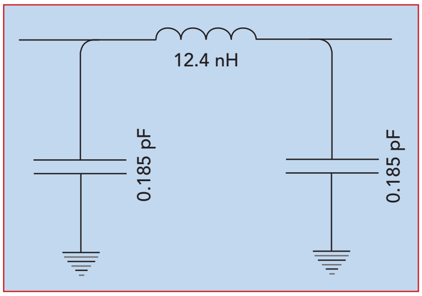

Fig. 4 The π circuit model for a 12.5 nH air core inductor.

Here, the Z term is determined by inspection, and Y_1 and Y_2 are easily derived from A and D. Z needs to be un-normalized, i.e., multiplied by 50. To un-normalize the Y terms, multiply by 0.02.

For the T network, the ABCD parameters are:

$$\begin{bmatrix} A & B \\ C & D \end{bmatrix} = \begin{bmatrix} 1+YZ_1 & Z_1+Z_1Z_2Y+Z_2 \\ Y & 1+YZ_2 \end{bmatrix} \quad (3)$$

Again, the Y term is obvious, and the Z terms are easily derived.

The conversion from 50 Ω S-parameters to the equivalent ABCD matrix is given by:

$$A = \frac{(1+S_{11})(1-S_{22})+S_{12}S_{21}}{2S_{21}} \quad (4)$$

$$B = \frac{(1+S_{11})(1+S_{22})+S_{12}S_{21}}{2S_{21}} \quad (5)$$

$$C = \frac{(1-S_{11})(1-S_{22})-S_{12}S_{21}}{2S_{21}} \quad (6)$$

$$D = \frac{(1-S_{11})(1+S_{22})+S_{12}S_{21}}{2S_{21}} \quad (7)$$

INDUCTOR EXAMPLE

To apply the concept, consider a 12.5 nH air core inductor, such as the Coilcraft A04T MiniSpring. For RF applications, the Spring series are high Q inductors, although the footprint may be too large for some designs. Using parameter extraction, we would like to know the equivalent circuit for the inductor, including its parasitics. The inductor's S-parameters at 200 MHz, available from Coilcraft's website, are:

$$S = \begin{bmatrix} 0.0246+0.1411i & 0.9751-0.1644i \\ 09751-0.1644i & 0.0246+0.1411i \end{bmatrix} \quad (8)$$

Converting the S-parameters to the ABCD (T) parameters:

$$T = \begin{bmatrix} 0.9963+1.723E-07i & 0.001629+0.3130i \\ 9.696E-08+0.02327i & 0.9963+3.790E-05i \end{bmatrix} \quad (9)$$

One might expect symmetry, yet with more digits of accuracy, S_{11} is not precisely equal to S_{22}, and S_{21} is not precisely equal to S_{12}. The actual value of Z is:

$$Z = 50*B = 50*(0.001629+0.3130i) = 0.0814+15.65i \quad (10)$$

Dividing the imaginary part by 2π*200 MHz gives 12.4 nH, which is close to the expected inductance of 12.5 nH.

Y_1 and Y_2 are given by:

$$Y_1 = \frac{D-1}{Z} = 6.042\times10^{-5}+0.0116i \quad (11)$$

$$Y_2 = \frac{A-1}{Z} = -6.042\times10^{-5}+0.0116i \quad (12)$$

The real parts are effectively zero, and the un-normalized admittance is 0.02* 0.0116 = 2.33 × 10^{-4} mhos, equivalent to a 0.185 pF capacitor to ground at 200 MHz (see ***Figure 4***).

To obtain the S-parameters, the

MiCable

T26 Series High Reliable & Durable Test Cable

After 150K Bending Cycles

@26.5GHz

- Phase Stability vs. Flex. <±2° ✓
- Amplitude Stability vs. Flexure <±0.04dB ✓
- Insertion Loss <2.53dB/m ✓
- VSWR <1.25:1 ✓

In Stock !
1 day to 1 week

T26 Cable Assembly Test (90°Connectors)

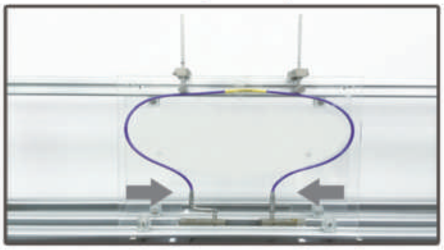

T26 Cable Assembly Test (Straight Connectors)

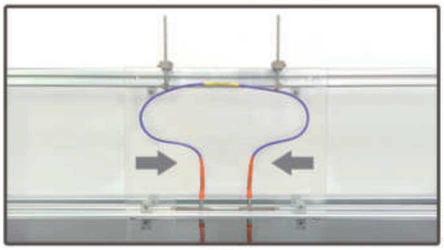

T26 Series DC~26.5GHz

DC~ 26.5GHz（SMA M - SMA MRA, 3FT）

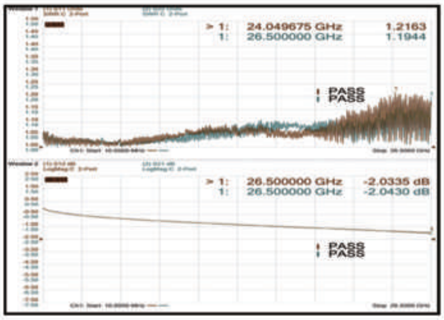

(3.5mm M - 3.5mm M, 1 Meter)

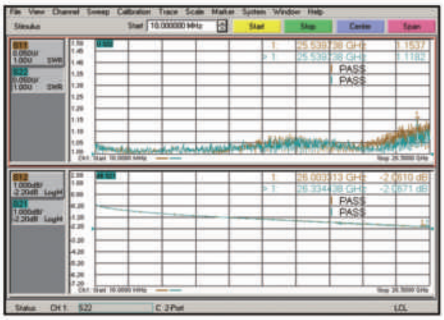

More Information-
Scan the QR Code

affiliated with SSi Cable Corp.

Fuzhou MIcable Electronic Technology Co., Ltd,
Tel: +86-591-87382856 Email: sales@micable.cn Website: www.micable.cn

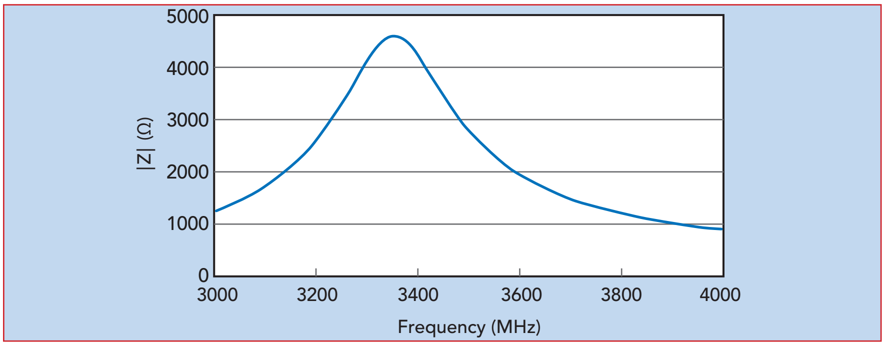

▲ Fig. 5 The |Z| response vs. frequency shows the inductor's self-resonance at 3350 MHz.

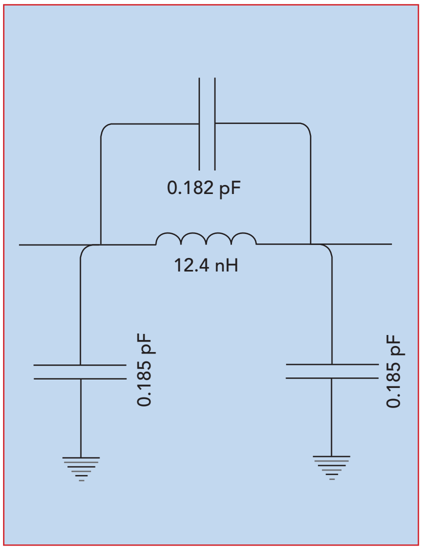

▲ Fig. 6 Adding the inter-winding capacitance to the π model for the inductor.

inductor was likely measured on a printed circuit board with the recommended land pattern, such that each pad contributed 0.185 pF. This is an important result, as the variation in PCB dielectric properties and thickness of the PCB will result in different values of this shunt capacitance.

Examining the magnitude of Z versus frequency from the B term shows the self-resonance at 3,350 MHz (see ***Figure 5***). To resonate at this frequency with the 12.4 nH inductance, the inter-winding capacitance must be approximately 0.182 pF. Updating the LC model for the inductor gives the equivalent circuit shown in ***Figure 6***.

With a little mathematics, it was straightforward to derive a π network model of this inductor. Applying this concept to an unknown component, the ABCD parameters can be examined to see if the reactance of the first series element of the T network or the admittance of the first shunt element of the π network is directly proportional to f or 1/f. Finding this relationship drives the choice of a π or T network. For instance, the equivalent T model derived from the ABCD parameters of an amplifier IC can be examined to determine the bond wire inductance, which can be tuned out with a judicious selection of coupling capacitor.

For reference, the ABCD parameters of a shunt admittance Y are


The Right RF Parts.
Right Away.
Having the correct RF parts shipped to you the same day can mean the difference between project success and failure. We're certain we've got the parts you need, with more than one million components in-stock and available to ship today.
We've Got That!
Available for Same-Day Shipping.
fairviewmicrowave.com
+1-800-715-4396
+1-972-649-6678
Fairview Microwave™
an INFINITE brand

given by:

$$\begin{bmatrix} A & B \\ C & D \end{bmatrix} = \begin{bmatrix} 1 & 0 \\ Y & 1 \end{bmatrix} \quad (13)$$

The ABCD parameters of a series impedance are given by:

$$\begin{bmatrix} A & B \\ C & D \end{bmatrix} = \begin{bmatrix} 1 & Z \\ 0 & 1 \end{bmatrix} \quad (14)$$

The π and T matrices are then easily derived using simple matrix multiplication.

UNKNOWN NETWORK

For the decomposition of an unknown network, examine the Z_1 of the T model and the Y_1 of the π model for proportionality to f or 1/f. The equivalent value of resistance, capacitance or inductance can then be recorded and mathematically removed from the network by pre-multiplying by the inverse ABCD matrix for the shunt or series term:

$$\begin{bmatrix} A & B \\ C & D \end{bmatrix}' = \begin{bmatrix} 1 & -Z \\ 0 & 1 \end{bmatrix} * \begin{bmatrix} A & B \\ C & D \end{bmatrix} \text{ or } \begin{bmatrix} A & B \\ C & D \end{bmatrix}' = \begin{bmatrix} 1 & 0 \\ -Y & 1 \end{bmatrix} * \begin{bmatrix} A & B \\ C & D \end{bmatrix} \quad (15)$$

where

$$\begin{bmatrix} 1 & 0 \\ Y & 1 \end{bmatrix}^{-1} = \begin{bmatrix} 1 & 0 \\ -Y & 1 \end{bmatrix} \text{ and } \begin{bmatrix} 1 & Z \\ 0 & 1 \end{bmatrix}^{-1} = \begin{bmatrix} 1 & -Z \\ 0 & 1 \end{bmatrix} \quad (16)$$

After removing the first series term, the remaining ABCD matrix should be evaluated in terms of the equivalent π model, the leading shunt term analyzed, fitted to R, L and C values and then removed by pre-multiplying again. If the first term of the unknown network is a shunt value, then start with the Y_1 value of the π model followed by the Z_1 value of the T model. Clearly, small errors will accumulate quickly, so it is unrealistic to expect this method will work well for a long network.

Measuring circuits and components is straightforward using a vector network analyzer (VNA), and a transmission line probe de-embedded from the measurement makes it easy. The de-embedding feature is built into the software of the Copper Mountain Technologies VNAs.■

Reference

1. Emerole Kelechi C, Matthew Gabriel Chinedum, A-B-C-D Parameter Model for Two-Port Networks, *International Journal of Advanced Engineering Research and Technology (IJAERT)*, Vol. 3, Issue 10, October 2015, ISSN No.: 2348–8190.

Software Analyzes Complex Beam Steering Antenna Arrays

Remcom
State College, Pa.

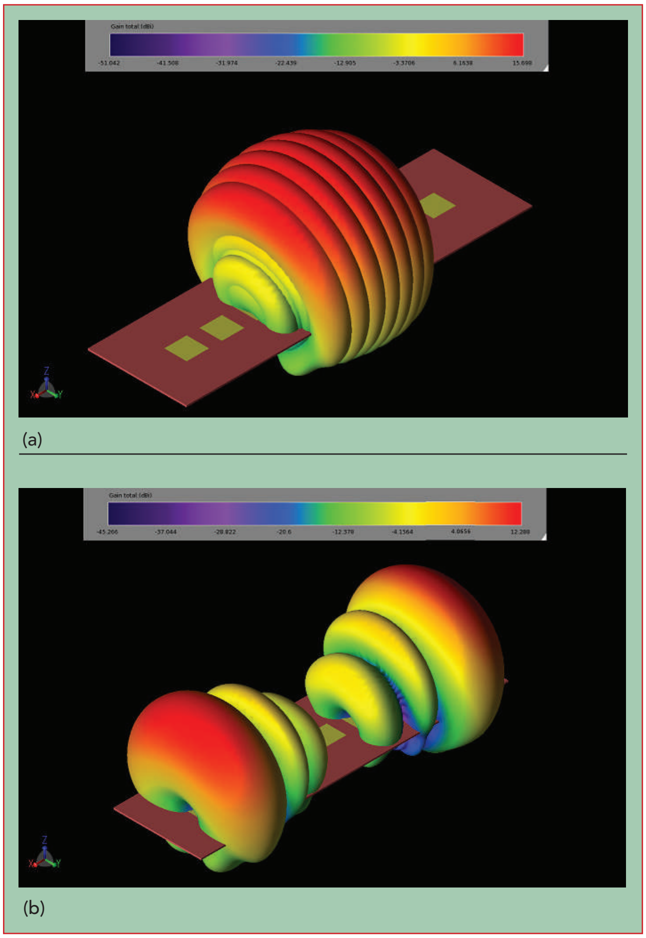

▲ **Fig. 1** **Patterns of a 1 x 8 linear array (a) and two, 1 x 4 linear arrays (b) of patch elements, simulated using the superposition feature in XFdtd.**

As telecommunications standards have shifted to higher frequencies, such as mmWave, system designers have incorporated arrays of antennas into communication systems. These sophisticated arrays enable higher gain and smaller beamwidth patterns that can overcome the high path losses inherent at these frequencies, to deliver the higher throughput promised by these new standards. Even for small arrays with a few elements, fully understanding the coverage possible with different power and phasing combinations can be difficult. When arrays grow larger to contain tens or hundreds of elements, advanced tools are required to fully describe the operation and effectiveness of the design.

The latest release of Remcom's XFdtd® Electromagnetic Simulation Software contains analysis tools for rapidly characterizing the performance of arrays of antennas for beamforming and beam steering applications. Superposition enables the rapid synthesis of complex problems using basic data from an electromagnetic (EM) simulation, quickly overlaying the data in a linear space.

For example, consider multiple antennas in a problem space. The requisite data—S-parameters, efficiency and far-zone—are computed once in an EM simulation for each antenna of interest. These may be quickly combined with complex scaling to yield the radiation pattern and associated active S-

Planar Monolithics Industries, Inc.

0.5 to 18.0 GHz High Performance Digital I/Q Vector Modulators with 360° Phase Shift & Amplitude Control

- Amplifiers - Solid State
- Attenuators - Variable/ Programmable
- Bi-Phase Modulators
- Couplers (Quadrature, 180, Directional)
- Detectors - RF / Microwave
- DLVAs, ERDLVAs & SDL-VAs
- Filters & Switched Filter Banks
- Form, Fit, Functional Products & Services
- Frequency Converters
- Frequency Sources
- Frequency Discriminators & IFM
- Frequency Synthesizers
- Gain & Loss Equalizers
- Integrated MIC/MMIC Assemblies (IMAs)
- IQ Vector Modulators
- Limiters - RF / Microwave
- Log Amps
- Miscellaneous Products
- Monopulse Comparators
- Multifunction Integrated Assemblies (IMAs)
- Phase Shifters & Bi-Phase Modulators
- Power Dividers/Combiners (Passive & Active)
- Pulse Modulators - SP1T
- Rack & Chassis Mount Products
- Receiver Front Ends & Transceivers
- Single Side Band Modulators
- SMT & QFN Products
- Switch Matrices
- Switch Filter Banks
- Switches - Solid-State
- Systems - Radar Sense & Avoid
- Systems - Fly Eye Radar
- Threshold Detectors
- USB Products

Model: PIQ-0R5G2G-360-20-CD-1 (0.5 to 2 GHz)

https://www.pmi-rf.com/product-details/piq-0r5g2g-360-20-cd-1

RF Connectors: SMA (F)
Switching Speed: 500 ns Max
DC Voltage: +15 VDC @ 87 mA, -15 VDC @ 24 mA

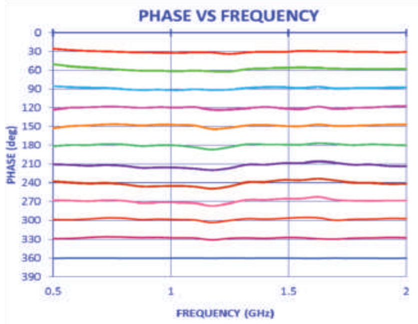

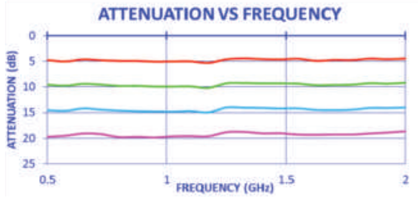

Frequency	0.5 to 2.0 GHz
Dynamic Range	20 dB & 360°
RF Input Power	+5 dBm CW, 1.0 Watt Max
Insertion Loss	11.0 dB Max - Measured 10.54 dB
VSWR	2.2:1 Max - Measured 1.59:1
Attenuation vs Frequency	±1.5 dB Typ - Measured ±1.3 dB
Phase vs Frequency	±10.0° Typ - Measured ±3.5°
Digital Control	2 x 12 Bit Monotonic TTL
Temperature	-10 °C to +60 °C Operating

Model: PIQ-2G18G-360-16-CD-1 (2 to 18 GHz)

https://www.pmi-rf.com/product-details/piq-2g18g-360-16-cd-1

RF Connectors: SMA (F)
Switching Speed: 500 ns Max
DC Voltage: +15 VDC @ 65 mA, -15 VDC @ 76 mA

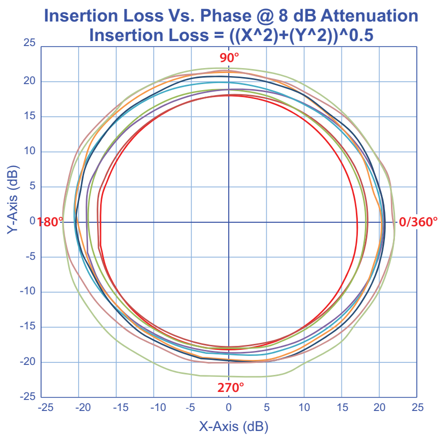

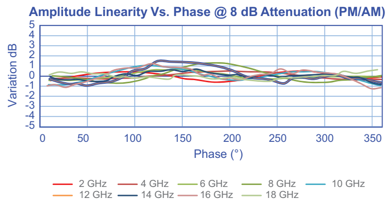

Frequency	2.0 to 18.0 GHz
Dynamic Range	16 dB & 360°
RF Input Power	+10 dBm CW, 1.0 Watt Max
Insertion Loss	18.0 dB Max - Measured 14.74 dB
VSWR	2.2:1 Max - Measured 1.86:1
Attenuation vs Frequency	±3.5 dB Typ Measured ±1.19 dB @ 0 dB Attenuation ±1.41 dB @ 8 dB Attenuation ±2.91 dB @ 16 dB Attenuation
Phase vs Frequency	±20.0° Typ Measured ±9.66° @ 0 dB Attenuation ±12.35° @ 8 dB Attenuation ±18.23° @ 16 dB Attenuation
Digital Control	2 x 12 Bit Monotonic TTL
Temperature	-10 °C to +60 °C Operating

West Coast Operation:
4921 Robert J. Mathews Pkwy, Suite 1
El Dorado Hills, CA 95762 USA
Tel: 916-542-1401, Fax: 916-265-2597

East Coast Operation:
7311-F Grove Road
Frederick, MD 21704 USA
Tel: 301-662-5019, Fax: 301-662-1731

sales@pmi-rf.com • www.pmi-rf.com

ISO 9001-2015 REGISTERED

parameters and efficiency for any desired antenna power and phasing combination. For situations where specific port power and phasing options are known, the resulting far-zone pattern can be computed immediately in post-processing.

A second situation is where the specific beam directions are known in advance, and the power and phasing of the ports is desired to maximize the effective isotropic radiated power (EIRP) in those directions. Using statistical analysis, the coverage provided by the array for all possible directions may be determined by calculating the cumulative distribution function (CDF) of the EIRP, which shows the percent of the spherical far-zone volume with positive gain for a given input power.

To illustrate, we consider a 1 × 8 array of 28 GHz patch antenna elements, where the phasing between elements is swept using the superposition feature from -90 to +90 degrees in 30 degree steps. Seven unique beams will be created, which focus a fan beam between -30 and +30 degrees (see ***Figure 1a***). Alternatively, if the array is used in a configuration with two adjacent 1 × 4 subarrays, the superposition feature can be used to generate separate patterns for each subarray (see ***Figure 1b***).

Alternatively, where the desired beam directions are known and the port settings are desired, an array optimization feature is available. A large, two-dimensional array, such as an 8 × 8 patch array at 28 GHz, will create narrow beams that can be swept over a broad range of directions above the array. ***Figure 2*** shows the "max hold" pattern created with the array optimization

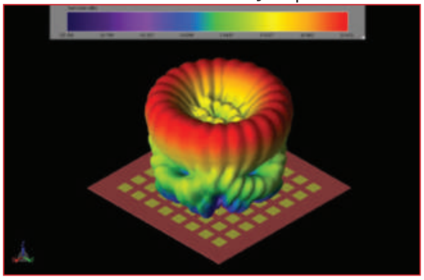

Fig. 2 Patterns of an 8 x 8 array of patch elements, simulated using the array optimization tool in XFdtd.

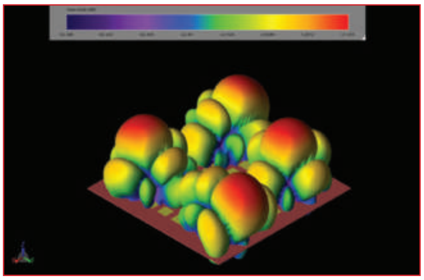

Fig. 3 Patterns of an 8 x 8 array of patch elements structured as four 4 x 4 independent subarrays, simulated using the array analysis tools in XFdtd.

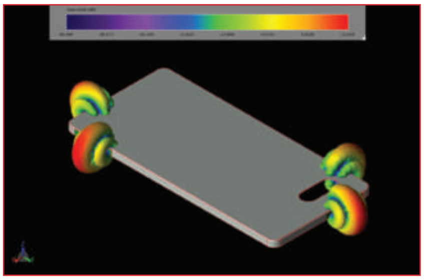

Fig. 4 Four, 1 x 4 patch arrays distributed in a mobile phone to enable wide spatial coverage.


ANALOG DEVICES
AHEAD OF WHAT'S POSSIBLE™
The Trust and Agility to Win the New Space Race.
Reach on-orbit faster by leveraging our 40 years of space heritage, coupled with our rapidly expanding space-qualified portfolio.
End-to-End Signal Chain
Class S & K/QMLV Technologies
Commercial Space Solutions
Get on-orbit faster at analog.com/space

tool, where the beams are desired at every 15 degrees in the azimuth direction and an elevation angle 30 degrees down from normal. Following the calculation, the required port power and phasing requirements for the elements to form each beam are available.

A large array may also be operated as a set of smaller subarrays functioning independently. ***Figure 3*** shows the same 8 × 8 array configured as four, 4 × 4 arrays, each with their own unique power and phasing to communicate with four receivers. Using the array analysis tools, the subarrays are defined and their operating characteristics can be explored.

Multiple arrays on a single device are used for spatial diversity, to provide coverage over a wider range of angles—more than a single array could produce. An example of this is a 5G mobile phone incorporating multiple arrays around the edge of the phone. ***Figure 4*** shows four arrays located on the sides, top and bottom of the phone case. Each are four element patch arrays that can produce a steerable beam covering a wide region normal to the array. When used in combination, the arrays can provide coverage in multiple directions, which is best demonstrated with the CDF of the EIRP. This one-dimensional function describes the percentage of the far-field sphere covered by an array for a given input power. In ***Figure 5***, the CDF of EIRP is plotted for different combinations of the four arrays along the edges of the phone. The single arrays used individually provide positive gain for about 66 percent of the directions (i.e., 1–0.34 from the CDF plot), assuming a typical 23 dBm input power to each array. The coverage improves to about 90 percent when two arrays in one of the corners are used in combination, and full coverage results when the arrays on opposite sides of the phone are used together.

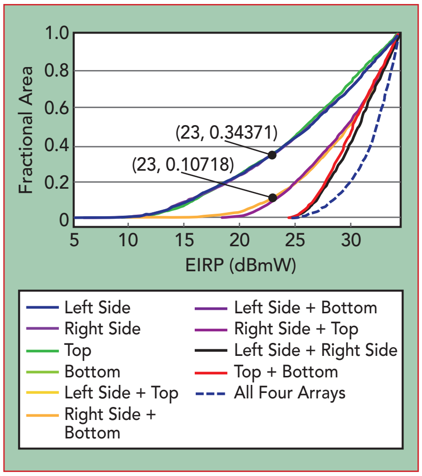

Fig. 5 **EIRP CDFs of the patch arrays in the mobile phone.**

As device performance is pushed to new levels by the increasing demands of 5G mmWave systems, the need for more comprehensive analysis tools for complex antenna systems grows. XFdtd's new features simplify the process of understanding device performance by providing efficient ways to analyze and validate array coverage.

VENDORVIEW

Remcom
State College, Pa.
www.remcom.com

L to K Band Ultra-Wideband

Voltage Controlled Oscillators

Model Number	Frequency	Phase Noise @ 10 kHz offset	Phase Noise @ 100 kHz offset	Tuning Voltage	Output Power
	(GHz)	(dBc/Hz)	(dBc/Hz)	(V)	(dBm)
DCO100200-5	1 - 2	-95	-117	0 - 24	+1
DCYS100200-12	1 - 2	-105	-125	0 - 28	+4
DCO200400-5	2 - 4	-90	-110	0 - 18	-2
DCYS200400P-5	2 - 4	-93	-115	0 - 18	0
DCO300600-5	3 - 6	-75	-104	0 - 16	-3
DCYS300600P-5	3 - 6	-78	-109	0 - 16	+2
DCO400800-5	4 - 8	-75	-98	0 - 15	-4
DCO5001000-5	5 - 10	-80	-106	0 - 18	-2
DCYS6001200-5	6 -12	-70	-94	0 - 15	> +10
DCYS8001600-5	8 - 16	-68	-93	0 - 15	> +10
DCYS10002000-5	10 - 20	-65	-91	0 - 18	> +10

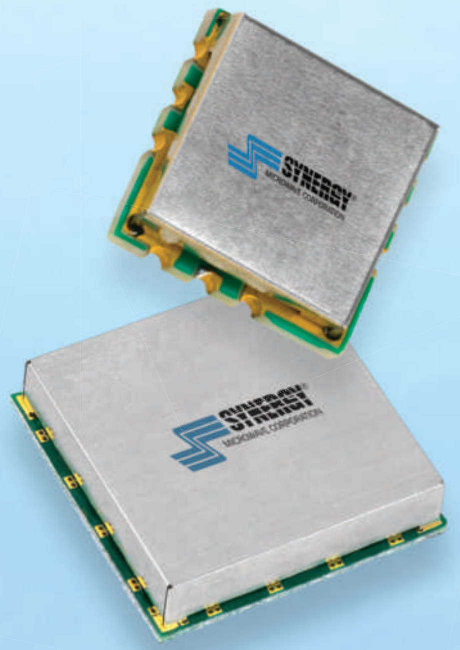

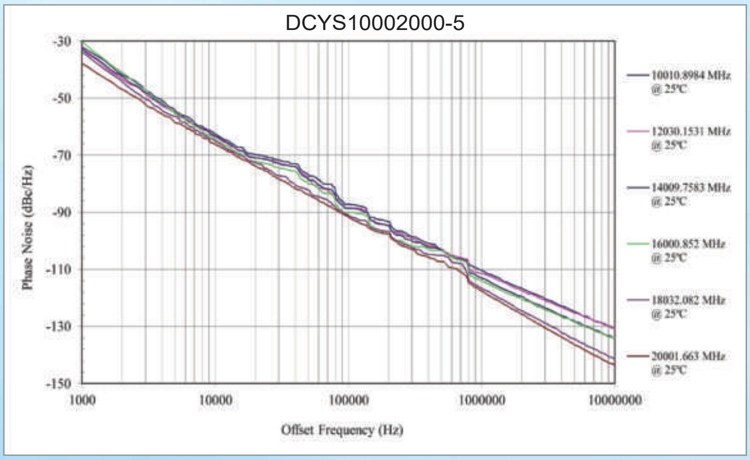

Features:

> Superior Phase Noise
> High Output Power
> Small Size Surface Mount Package
> Vcc: 5 volts
> Future models up to 30 GHz

Talk To Us About Your Custom Requirements.

SYNERGY® MICROWAVE CORPORATION

Phone: (973) 881-8800 | Fax: (973) 881-8361
E-mail: sales@synergymwave.com | Web: www.synergymwave.com
Mail: 201 McLean Boulevard, Paterson, NJ 07504

Comprehensive Model Libraries Help Designers Achieve First-Pass Design Success

Modelithics, Inc.
Tampa, Fla.

A circuit or system simulation is only as good as the component models used in the simulation. Simulating a design with insufficient models will produce simulation results that do not accurately predict the performance of the design when built and tested. Various real world factors associated with RF/microwave components can affect performance, including substrate-dependent parasitics and higher-order resonances. So, component models must capture these effects to assure design accuracy.

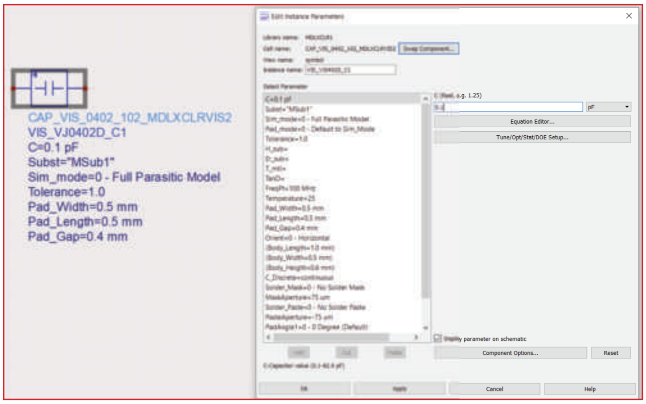

Fig. 1 The Microwave Global Model for the Vishay VJ0402 capacitor family, which has a capacitance range from 0.1 to 82 pF.

Modelithics® specializes in developing accurate measurement-based simulation models for RF/microwave components. The company's premier product, the Modelithics COMPLETE Library™, consists of models for everything: passive components, transistors, diodes and more. Every model Modelithics provides is intended to be a value-add for designers, enabling accurate simulations leading to first-pass design success. Modelithics' model libraries are available for six RF/microwave simulation software platforms, Keysight Technologies' PathWave Advanced Design System, Keysight Technologies' PathWave RF Synthesis (Genesys), Cadence AWR Design Environment, Ansys HFSS, Sonnet Suites and Cadence Virtuoso

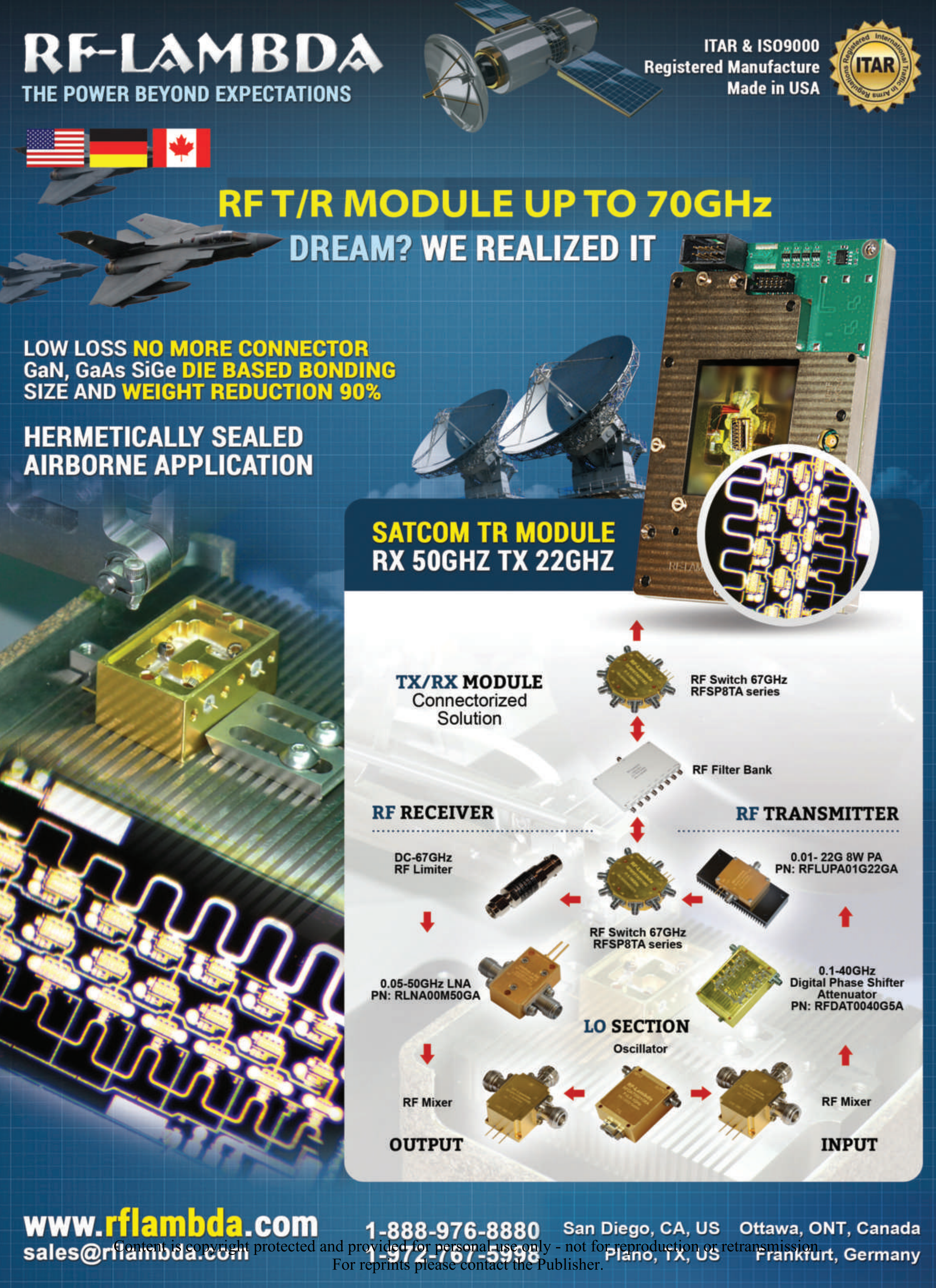
RF-LAMBDA
THE POWER BEYOND EXPECTATIONS
ITAR & ISO9000
Registered Manufacture
Made in USA
ITAR
RF T/R MODULE UP TO 70GHz
DREAM? WE REALIZED IT
LOW LOSS NO MORE CONNECTOR
GaN, GaAs SiGe DIE BASED BONDING
SIZE AND WEIGHT REDUCTION 90%
HERMETICALLY SEALED
AIRBORNE APPLICATION
SATCOM TR MODULE
RX 50GHZ TX 22GHZ
TX/RX MODULE
Connectorized
Solution
RF Switch 67GHz
RFSP8TA series
RF Filter Bank
RF RECEIVER
RF TRANSMITTER
DC-67GHz
RF Limiter
0.01- 22G 8W PA
PN: RFLUPA01G22GA
RF Switch 67GHz
RFSP8TA series
0.05-50GHz LNA
PN: RLNA00M50GA
0.1-40GHz
Digital Phase Shifter
Attenuator
PN: RFDAT0040G5A
LO SECTION
Oscillator
RF Mixer
RF Mixer
OUTPUT
INPUT
www.rflambda.com
sales@rflambda.com
1-888-976-8880
1-972-767-5998
San Diego, CA, US
Plano, TX, US
Ottawa, ONT, Canada
Frankfurt, Germany

Spectre RF. The Modelithics COMPLETE Library contains over 750 models from nearly 70 suppliers, representing more than 18,000 components.

The Modelithics COMPLETE Library contains various sub-libraries: the CLR Library, which is a collection of capacitor, inductor and resistor models and the NLT and NLD libraries, comprising nonlinear transistor and nonlinear diode models, respectively. The Modelithics

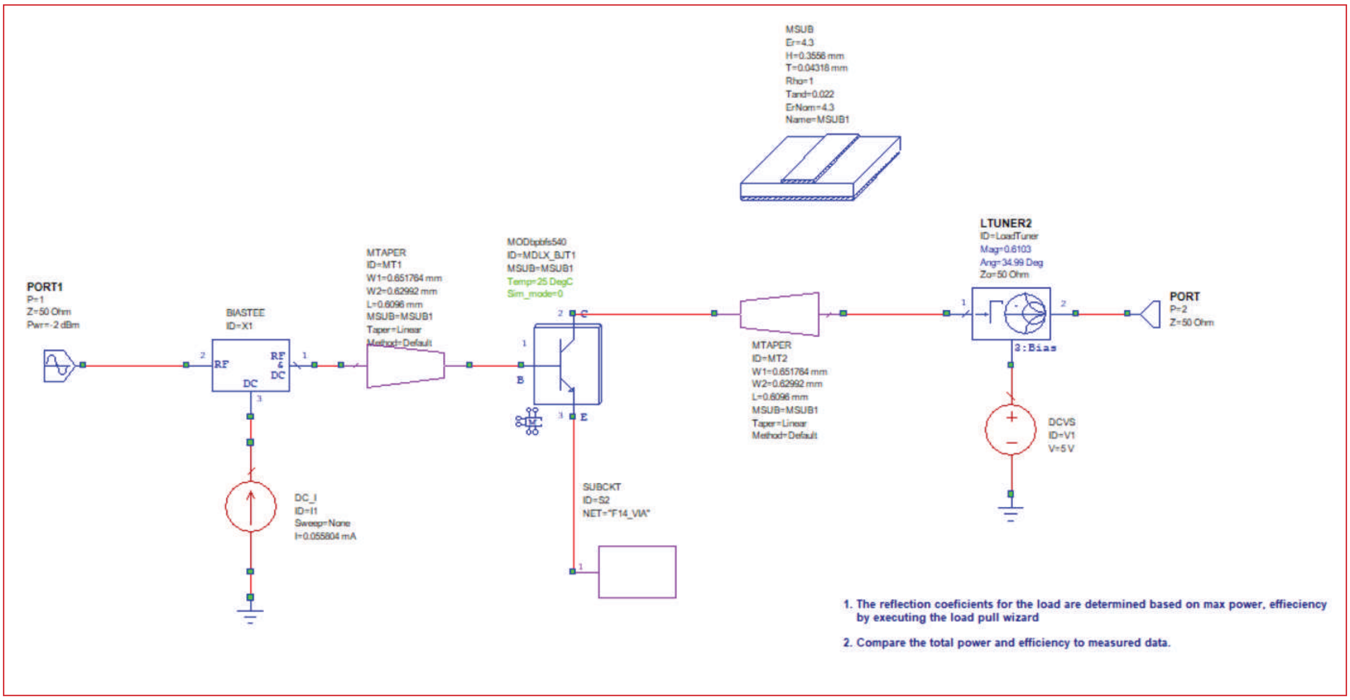

Fig. 2 Example schematic for load-pull analysis.

COMPLETE Library also includes the SLC, SPAR and Substrate libraries. The SLC Library contains linear and nonlinear models for system-level components like amplifiers and filters, while the SPAR Library is a collection of S-parameter, file-based models. The Substrate Library holds substrate property definition blocks for many popular substrates. The CLR, NLT, NLD and SLC libraries contain measurement-based equivalent-circuit models—not just simple S-parameter files—and the Modelithics COMPLETE Library includes various example projects, demonstrating how to use the models.

CLR LIBRARY FOR PASSIVE COMPONENTS

The CLR library contains capacitor, inductor and resistor models from AVX, Coilcraft, Vishay and many other suppliers. This library features Modelithics' Microwave Global Models™, advanced models developed by Modelithics that are part-value scalable. A single Microwave Global Model covers the full range of part values for a component series (see ***Figure 1***). In addition to part-value scalability, Microwave Global Models scale with substrate and solder pad dimensions, to provide designers with flexibility, and the models accurately capture substrate-dependent parasitic behavior. Since a single Microwave Global Model covers the full range of part values for a component series, they are useful for tuning and optimizing a design.

NONLINEAR TRANSISTOR AND DIODE MODELS

The Modelithics COMPLETE Library contains the NLT Library, a collection of nonlinear transistor models for high-power and low-noise devices. This library comprises models for various HEMT, MOSFET and BJT transistors, as well as other technologies. The devices represent products from Qorvo, Mitsubishi, California Eastern Laboratories and others. Common device model features in the NLT Library include temperature and bias dependence. Model datasheets may include S-parameter data over temperature and varying bias conditions, and they typically have the DC current-voltage (IV) characteristics.

Using NLT Library device models, designers can simulate gain compression, power-added efficiency, noise (i.e., low-noise models) and other parameters, with the corresponding data found in the model datasheets. Certain model datasheets also have load-pull performance and some of the models are substrate scalable. The example projects with the Modelithics COMPLETE Library help users learn how to use NLT Library models to perform various simulations. For instance, example schematics are available that demonstrate simulations using different substrates and bias conditions and how to perform simulations analyzing load-pull and harmonic performance (see ***Figure 2***).

The NLD Library comprises a collection of nonlinear diode models

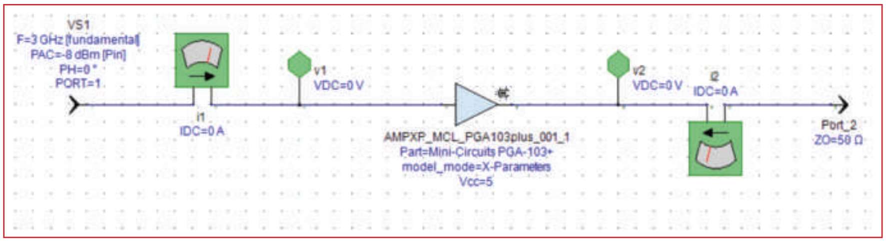

Fig. 3 Example schematic for analysis of a Mini-Circuits amplifier using a nonlinear behavioral model.

for various Schottky, varactor, PIN and step-recovery diodes from Infineon, MACOM, Skyworks and other suppliers. Substrate scalability, temperature dependence and bias dependence are three significant features of the NLD Library models. They are featured in example schematics that demonstrate simulations with varying substrates and bias conditions, with additional schematics illustrating simulations including S-parameters, power compression and harmonics.

SLC AND SPAR LIBRARIES

To complement the CLR, NLT and NLD libraries of active and passive equivalent-circuit models, the Modelithics COMPLETE Library includes the SLC and SPAR libraries. The SLC Library provides models for system-level components such as amplifiers, filters, attenuators, switches and transformers. The amplifier models in this library are nonlinear behavioral models that enable more than S-parameter simulation (see ***Figure 3***): designers can analyze parameters such as 1 dB compression (P_{1dB}) and the third-order intercept point (IP3). The models are validated over frequency and power ranges, which are listed in the datasheets. The SLC Library contains more than amplifiers, including filters, attenuators and switches. Again, substrate scalability is a significant attribute of these models. Among the suppliers represented in the SLC Library are Mini-Circuits, International Manufacturing Services and Barry Industries.

The SPAR Library is a collection of S-parameter, file-based models for components like amplifiers and splitters. These models are more advanced than traditional S-parameter files; many of them contain multiple S-parameter data files activated with user-defined model settings. Multiple data files within a single model correspond to either different part values in a component series, different substrates or different bias conditions (i.e., for amplifiers), depending on the model. SPAR Library models are useful for tuning and optimization.

VENDORVIEW
Modelithics Inc.
Tampa, Fla.
www.modelithics.com
sales@modelithics.com

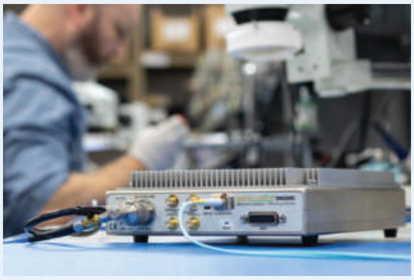

10 GbE-Connected Spectrum Analyzer Offers Performance and Value

Signal Hound's new SM200C is a high performance spectrum analyzer and monitoring receiver with a 10 Gigabit Ethernet (GbE) SFP+ port that enables the instrument to communicate with a PC over long distances using a fiber optic cable—not USB—for data transfer and control.

The SM200C tunes from 100 kHz to 20 GHz and sweeps at 1 THz/s at 30 kHz resolution bandwidth (RBW). It has 110 dB dynamic range, ultra-low phase noise and a GPIO port for antenna switching. The monitoring receiver was designed to provide remote RF data analysis with the highest accuracy and lowest possible cost. With its SFP+ port enabling fast, long-distance communication via optical cable, the SM200C achieves 160 MHz instantaneous bandwidth I/Q streaming over 10 GbE.

The instrument comes with all software required for operation. As with other Signal Hound devices, Spike™ software provides device controls, signal display and data export tools. Spike offers a variety of analysis modes, including tools for EMC pre-compliance testing, interference hunting and digital demodulation. For TSCM applications, the SM200C is compatible with third-party software packages, such as Kestrel™ and SCEPTRE™, for the most affordable and powerful countermeasures solutions.

Signal Hound designs and builds powerful, affordable spectrum analyzers and signal generators for RF professionals around the globe. Whether the need is EMC pre-compliance capability in a two-person shop or spectrum monitoring on a national scale, Signal Hound's test equipment is designed to be accurate and powerful enough for mission-critical applications, while priced to be accessible to most. All Signal Hound products are supported by a talented group of engineers committed to what they do, believing their test equipment offers unrivaled value.

Signal Hound
Battle Ground, Wash.
www.signalhound.com

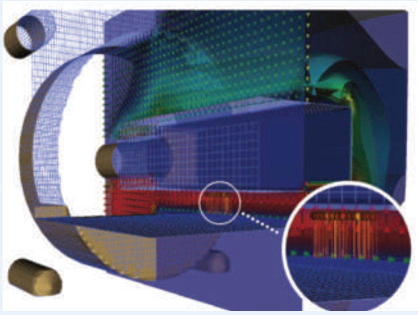

Computation EM Software Predicts Multipacting

Tech-X has released VSim 10.1, the newest version of the VSim computational electromagnetic (EM) software. Built on its powerful Vorpal physics engine, which was designed for the rigorous high performance computing needs of U.S. government research laboratories, VSim 10.1 provides highly accurate analysis, whether running on a laptop or supercomputer. Cross-platform, VSim is flexible and customizable; users can select up to four modules to meet their design needs.

The VSim for Microwave Devices (VSimMD) module is an effective tool for designing, analyzing and optimizing the performance of RF devices, including magnetrons, traveling wave tubes and klystrons. Multipacting, the resonant buildup of secondary electrons, is one of the biggest concerns facing microwave designers working with electron beam devices. When the secondary electron yield is too large, it will trigger an electron avalanche that leads to significant power loss. Designers need to predict this effect; however, not all software products simulate it well. With proprietary algorithms, VSimMD accurately accounts for multipacting, so designers can focus on maximizing power and efficiency. VSimMD comes with an extensive list of example problems, such as multipacting resonances in a waveguide and multipacting growth in a spherical, perfect electric conductor cavity. These examples give users starting points to quickly learn the modeling workflow.

Among the new features in VSim 10.1 are creating rectangular arrays of design geometries enable engineers to quickly test various geometric features on their RF devices and improved particle emitter functionality offers greater control over electron beam simulations. An important addition to VSimMD is the capability to accurately simulate the behavior of particles interacting with transparent materials in microwave devices. With these new features, informative examples and a friendly user interface, VSim 10.1 is a powerful tool. A free, 30 day trial evaluation is available.

Tech-X Corporation
Boulder, Colo.
www.txcorp.com/vsim.

SIX DAYS ■ THREE CONFERENCES ■ TWO FORUMS ■ ONE EXHIBITION

EUROPE'S PREMIER MICROWAVE, RF, WIRELESS AND RADAR EVENT

EUROPEAN MICROWAVE WEEK

JAARBEURS UTRECHT THE NETHERLANDS

10-15 JANUARY 2021

www.eumweek.com

The European Microwave Exhibition

(12th - 14th January 2021)

- 10,000 sqm of gross exhibition space
- Around 5,000 attendees
- 1,700 - 2,000 Conference delegates
- In excess of 300 international exhibitors (including Asia and US as well as Europe)

INTERESTED IN EXHIBITING?

For International Sales:
Richard Vaughan,
International Sales Manager
E: rvaughan@horizonhouse.co.uk
Tel: +44 20 7596 8742

or visit www.eumweek.com

ATC Product Selection Guide

The ATC Product Selection Guide is an abridged catalog that features a complete overview for the full line of ATC products. It provides easy selection through color-coded frequency ranges, giving the user a handy reference for quick and accurate selection of all ATC products by providing key information for each product offering. It includes a capabilities listing for ATC's Thin Film Products. Contact information for Inside Sales and Field Sales Offices is provided on ATC's website.

ATC

https://atceramics.com/

HUBER+SUHNER Extends Antenna Portfolio for Critical Communication

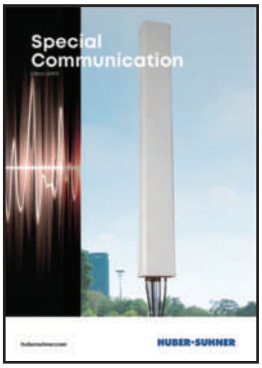

HUBER+SUHNER offers a complete portfolio with its brand SENCITY Special Communications for the area of secure communications within private/professional mobile radio networks including antennas and related installation equipment. A particular focus is placed on broadband products and products combining TETRA and professional LTE and others. Its solutions support the establishment of secure communication networks both indoors and outdoors. The products offer high performance, quality, reliability and long life. Suitable modules for building a secure network architecture can be selected from the new catalogue.

HUBER+SUHNER AG

www.hubersuhner.com

New Product Guide

Rosenberger provides a comprehensive product portfolio of highly reliable interconnect components and devices which is in accordance with the stringent requirements of MIL-PRF 39012, DIN EN 9100 or ESCC Certification of the European Space Agency. A new brochure showcases Rosenberger's wide product range qualified for aerospace, security and defence applications: RF coaxial components, microwave components and cable assemblies, RF test and measurement products or fiber optic connectivity components. A PDF version is available for download from the Rosenberger website, print copies can be ordered at marketing@rosenberger.com

Rosenberger

https://www.rosenberger.com/en/products/aerospace_defence/

General Microwave's Frequency Sources Short Form Catalog

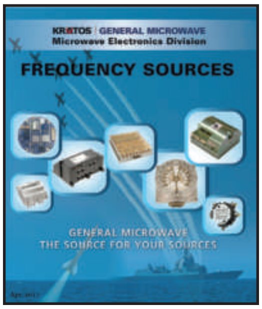

General Microwave Corporation has designed and manufactured cutting edge microwave frequency sources since 1987. This short form catalog includes sources ranging from free running voltage and digitally controlled oscillators to fast (1 usec) indirect synthesizers, company profile and a wideband frequency modulation applications and techniques tutorial. Specially featured is the Series SM60 family of fast indirect synthesizers capable of analog and digital frequency modulation while center frequency remains in the pure locked mode.

General Microwave Corporation

www.kratosmed.com

Download K&L Microwave's Product Catalogs Today

K&L Microwave designs and manufactures a full line of RF and microwave filters, duplexers and subassemblies, including ceramic, lumped element, cavity, waveguide and tunable filters. K&L supplies many of today's most significant military and homeland security electronics programs. Applications include space flight, radar, communications, guidance systems and mobile radio base stations, as well as air traffic communication and control. Visit www.klmicrowave.com to download today!

K&L Microwave

www.klmicrowave.com

Teledyne e2v's New DAC Provides Leap Forward for RF Softwarization

At any band up to Ka-Band, system designers will soon be able to migrate more RF hardware to digital code than ever before. Enabling unprecedented levels of dynamic RF system reconfiguration on the fly. EV12DD700 dual-channel DACs are capable of operating up to Ka-Band frequencies and support beamforming applications.

Teledyne e2v

https://www.teledyne-e2v.com/products/semiconductors/dac/ev12dd700/

NEW PRODUCTS

FOR MORE NEW PRODUCTS, VISIT WWW.MWJOURNAL.COM/BUYERSGUIDE
FEATURING VENDORVIEW STOREFRONTS

COMPONENTS

Double Ridge Waveguide Switches

VENDORVIEW

Fairview Microwave Inc. has introduced a new series of double ridge waveguide electromechanical relay switches that perform over broader frequency bands. They are ideal for applications involving electronic warfare, electronic countermeasures, VSAT, radar, microwave radio, research and development and test instrumentation. Fairview's new comprehensive line of double ridge waveguide electromechanical switches includes 12 models that feature broadband multi-octave frequency coverage spanning 6.5 to 40 GHz, latching self-cut-off actuators, TTL logic and position indicators with manual override.

Fairview Microwave Inc.
www.fairviewmicrowave.com

Digital Phase Shifter

Kratos General Microwave manufactures a complete line of broadband fast switching phase shifters. Model 7929 offers a full tuning range of 360° covering a frequency range of 18 to 40 GHz. Excellent phase accuracy and PM/AM performance are achieved by utilizing double balanced bi-phase linear amplitude modulators. Standard unit designed to operate over -54°C to +95°C. Its small size and high reliability make it ideal for use in demanding shipboard/airborne environmental conditions. Optional optimized performance is available over a narrower frequency range.

Kratos General Microwave
www.kratosmed.com

Four-Way Power Divider

VENDORVIEW

MECA expanded offering of 5G mmWave products. Featuring four-way power dividers covering 26 to 34 GHz with 2.92 mm interfaces. Typical specifications of 1.2:1 VSWR, 19 dB isolation, 2 dB insertion loss and 1 dB amplitude balance. Also available are attenuators, terminations, bias tee's, DC blocks and adapters. Additionally, octave and multi-octave models covering up to 50 GHz built by J-Standard certified assemblers and technicians. Made in U.S. with a 36-month warranty!

MECA Electronics Inc.
www.e-MECA.com

Accuracy Digital Programmable Attenuator

020-180-120-DT is a 2 to 18 GHz 120 dB high resolution and accuracy digital programmable attenuator. It has 1 dB min. attenuation step, ±0.5 dB max. attenuation accuracy, 11 dB max. insertion loss and 2:1 max. VSWR. Input/output connectors are SMA female and power handling is 1 W CW. The component can be controlled through USB and Ethernet. Operating temperature is 0 to 70°C. The size including power supply (110 to 220 V AC) is 227 × 114 × 50 mm.

Fuzhou MIcable Electronic Technology Co. Ltd.
www.micable.cn

Four-Way Divider

VENDORVIEW

Mini-Circuits' model ZC4PD-V1854+ is a four-way, 0° power splitter/combiner with broad frequency range of 18 to 50 GHz. The 50 Ω DC-pass splitter/combiner handles as much as 16 W input power as a power divider with low insertion loss and excellent amplitude and phase unbalance. The typical insertion loss (above the 6 dB power split) is 1.1 dB from 18 to 40 GHz and 1.6 dB from 40 to 50 GHz with typical isolation of 29 dB from 18 to 40 GHz and 30 dB from 40 to 50 GHz.

Mini-Circuits
www.minicircuits.com

MMIC Splitter/Combiner

VENDORVIEW

Mini-Circuits' model EP2-561+ is a two-way, 0-deg. power splitter/combiner fabricated with GaAs IPD technology for applications from 12.0 to 43.5 GHz, including 5G and radar systems. Supplied in a 2 × 2 mm surface-mount-technology (SMT) housing, the 50-Ω power splitter/combiner has full-band VSWR of 1.70:1 or better at all ports. Insertion loss (above the 3 dB split) is typically 1.1 dB from 12 to 24 GHz, 1.3 dB from 24 to 30 GHz, and 1.4 dB from 30.0 to 43.5 GHz. Isolation is typically 15 dB from 12 to 24 GHz, 23 dB from 24 to 30 GHz, and 16 dB from 30.0 to 43.5 GHz. The splitter/combiner provides outstanding amplitude and phase balance, with typical full-band amplitude unbalance of 0.2 dB or better and typical full-band phase unbalance of 1.7 deg. or better. The SMT MMIC handles as much as 0.5 W power as a splitter or combiner and has an operating temperature range of -55° to +105°C.

Mini-Circuits
www.minicircuits.com

Vector Modulator

VENDORVIEW

PMI Model No. PIQ-85M18G-36020-CD-2 is a vector modulator covering the frequency range of 85 MHz to 18 GHz. This unit provides an attenuator resolution of 0.1 dB and a phase shift resolution of 0.8°. The attenuation is phase invariant and the phase is amplitude invariant making it ideal for nulling unwanted signals. The unit can be specifically calibrated for any number of 100 MHz bands within the full operating frequency range of 85 MHz to 18 GHz.

Planar Monolithics Industries Inc.
www.pmi-rf.com

Fixed Attenuator

Response Microwave Inc. announced the availability of its new DC to 8.5 GHz, 50 W fixed attenuators for telecom specific product platform use. The family includes 1 to 40 dB attenuation values that operate between DC to 8.5 GHz. Electrical performance offers typical insertion loss of 0.5 dB and VSWR of 1.25:1 max. Impedance value is 50 Ω power handling is 50 W CW and package size is 0.45 mm OD by 0.110 mm length.

Response Microwave Inc.
www.responsemicrowave.com

High Linearity SP6T Switch

VENDORVIEW

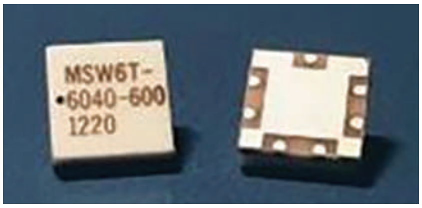

RFMW announced design and sales support for a high power, SMT RF switch. The RFuW Engineering model number MSW6T-6040-600 is a single-pole, six-throw switch capable of handling 400 W of CW RF power over the range of 30 to 512 MHz. Peak power handling is up to 1,000 W. The MSW6T-6040-600 utilizes PIN diodes for high reliability and low insertion loss of <0.7 dB. Hybrid manufacturing processes yield superior performance offering IP3 >65 dBm.

RFMW
www.rfmw.com

Bias Tees

RLC Electronics manufactures both narrow band and broad band bias tees from 5 MHz to 40 GHz that provide excellent performance over the full band. This unit is used to inject a DC current or voltage into an RF circuit without affecting the flow of RF through the main transmission path. Typical applications include biasing amplifiers, DC return, DC blocking, as well as other various digital and analog uses, including in airborne applications.

RLC Electronics Inc.
www.rlcelectronics.com

CABLES & CONNECTORS

Vertical Launch Connectors

VENDORVIEW

HASCO's vertical launch connectors, manufactured by Southwest Microwave, provides optimal signal integrity, are reusable and can be installed without soldering. Suitable for various board materials and thicknesses. These vertical launch connectors reduce footprint without sacrificing performance, resulting in design and installation convenience. With vertical launch connectors from HASCO, enjoy low VSWR, insertion loss and FR leakage, along with high temperature, rugged durability and excellent repeat performance.

HASCO
www.hasco-inc.com

Coaxial Cable Assemblies and Connectors

VENDORVIEW

L-com, an Infinite Electronics brand and a preferred manufacturer of wired and wireless connectivity products, announced that it has introduced a new line of RG178 coaxial cable assemblies that are perfect for use in RF communications, data transmission, wireless communication, GPS systems, security equipment, broadcast equipment and lab applications. L-com's new RG178 coax cable assemblies are built using the highest quality bulk cable and connectors to ensure the highest levels of performance.

L-com
www.l-com.com

50 GHz SUCOFLEX®550S Test Cables

Richardson RFPD Inc., an Arrow Electronics company, announced the availability and full design support capabilities for a new family of test cables from HUBER+SUHNER. With a lifetime of more than 100,000 flex cycles, SUCOFLEX 550S is the latest addition to HUBER+SUHNER's SUCOFLEX 500 family and provides a range of benefits, including a high electrical performance with an enhanced mechanical design for durability. The longer service life also results in less testing downtime and improved cost efficiency.

Richardson RFPD Inc.
www.richardsonrfpd.com

2.92 to 3.5 mm Adapters Series

Withwave's precision test adapters are designed based on precision microwave interconnection technologies. These new 2.92 to 3.5 mm types are manufactured to precise microwave specifications and constructed with male and female gender on both sides. The precision microwave connector interfaces ensure an excellent microwave performance up to 34 GHz.

withwave co. ltd.
www.with-wave.com

AMPLIFIERS

Digital Variable Gain Amplifier

The BeRex BVA3143 is a 5 V digitally controlled variable gain amplifier in 6 × 6 mm LGA package for 3,300 to 3,800 MHz. BVA3143 is high performance and high dynamic range makes it ideally suited for use in 5G/LTE wireless infrastructure and other high performance wireless RF applications.

BeRex
www.berex.com

E LEARNING CENTER

Presented by: Microwave Journal

Webinars

Now On Demand

Progress Towards a Low SWaP-C Miniaturized Rubidium Oscillator by Orolia

Sponsored by: orolia

Presented by:
Christian Schori, Project Manager, Serge Grop, R&D Program Manager and Jean-Charles Chen, Product Line Director – Atomic Clock

microwavejournal.com/events/1958

Understanding What Can Affect PCB Dk Variation and Phase Consistency

Sponsored by: ROGERS CORPORATION

Presented by:
John Coonrod, Technical Marketing Manager

microwavejournal.com/events/1959

Satellite Mission Planning – the R&S®SLP Satellite Link Planner and the R&S®GSACSM Communication System Monitoring

Sponsored by: ROHDE&SCHWARZ Make ideas real

Presented by:
Michael Nebel, Product Manager Satellite Communications

microwavejournal.com/events/1957

Optimizing Peak-to-Average Power Ratio for Wireless Systems

Sponsored by: Boonton, TABOR ELECTRONICS

Presented by:
Mark Elo, US General Manager, Tabor Electronics USA and Walt Strickler, VP and General Manager of Boonton Electronics

microwavejournal.com/events/1950

Register to attend at mwjournal.com/webinars

FEATURED

e-Books

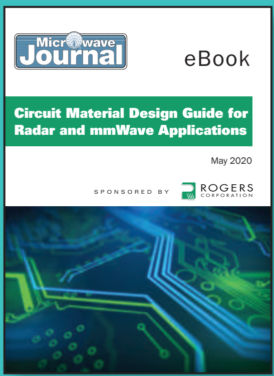

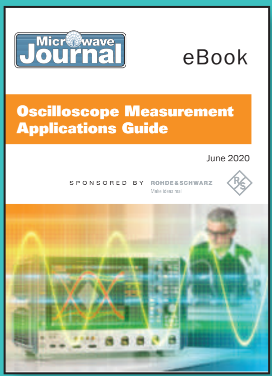

mwjournal.com/ebooks

NewProducts

Thermoelectric Refrigeration Cooling System

VENDORVIEW

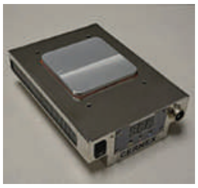

Cernexwave's thermoelectric refrigeration cooling system is the perfect solution to keep your components at optimal temperature. It features an adjustable temperature control with digital readout and a universal mounting plate that is compatible with any amplifier module as well as many other devices. It is an ideal solution for systems where heat dissipation is critical.

Cernexwave
www.cernexwave.com

Solid-State Broadband Amplifier

VENDORVIEW

Exodus Advanced Communication's (AMP4065LC-1) 18.0-26.5 GHz, (AMP4066LC-1) 26.5 to 40.0 GHz, 20 W+ solid-state amps are designed for general EMC testing applications as well as Mil-Std 461 (RS103) standards. Models AMP4065LC-1 and AMP4066LC-1 are compact designs that provide superb RF performance with unprecedented P1dB power as compared to TWT's. The units incorporate its Quiet-Cool Technology with 44 dB min-gain, monitoring parameters for FWD/RFL power, VSWR, voltage, current and temp sensing with outstanding reliability and ruggedness.

Exodus Advanced Communications
www.exoduscomm.com

SOURCES

VCO with Extremely Low Power Consumption

VENDORVIEW

The SMV0912B-LF is a high performance VCO that operates from 865 to 960 MHz within the Vtune range of 0 to 2.5 VDC. It saves precious energy by consuming less than 20 mW of power while at the same time delivering +3 dBm of output power into a 50 Ω load. The SMV0912B-LF has exceptional low phase noise of -100 dBc/Hz at 10 kHz offset and operates off a 3 VDC supply while drawing a mere 6 mA of current.

Z-Communications
www.zcomm.com

SOFTWARE

SignalShark Real Time Spectrum Analyzer

The SignalShark real time spectrum analyzer is designed to be an open platform. By integrating a powerful computer with Windows 10, Narda has decided to remove system limitations of the SignalShark family. The software for most applications runs exclusively on Windows computers—and therefore runs on the SignalShark, too. Regardless of any specific file formats, users can analyze, archive, visualize and export their measurement results. They can load their own software packages on to the analyzer to handle user-specific services.

Narda Safety Test Solutions
www.narda-sts.com

MICRO-ADS

ANTENNAS

Antennas

VENDORVIEW

Pasternack, an Infinite Electronics brand, has introduced a new line of GPS timing antennas, vehicular antennas and a 118 to 174 MHz tunable, telescopic antenna to address mobile wireless, portable instrumentation and wireless monitoring applications. Pasternack's new GPS/GLNSS antennas provide precise reception of satellite timing signals and reference frequencies for use in advanced mobile and base station network applications. The GPS, vehicular and portable UHF antennas are all in stock and available for same-day shipping with no minimum order requirement.
Pasternack
www.pasternack.com

TEST & MEASUREMENT

Oscillating Linear Actuator

VENDORVIEW

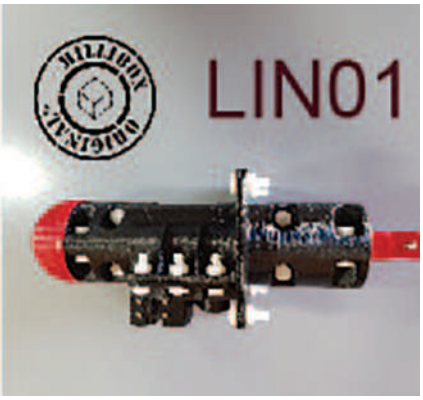

LIN01 is a new accessory for MilliBox chambers especially useful for mmWave radar testing. It is an oscillating linear actuator for mmWave trihedral corner reflectors. Travel distance 30 mm, speed ranges from 0 to 2.5 Hz. Daisy chain up to 10 units with individual speed control. Python controller in source code. Mounts through MilliBox chamber absorber panels.
Milliwave Silicon Solutions, Inc.
www.millibox.org

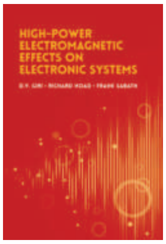

High-Power Electromagnetic Effects on Electronic Systems

D.V. Giri, Richard Hoad, Frank Sabath

This is the first book that comprehensively addresses the issues relating to the effects of radio frequency (RF) signals and the environment of electrical and electronic systems. It covers testing methods as well as methods to analyze radio frequency. The generation of high-powered electromagnetic (HPEM) environments, including moderate band damped sinusoidal radiators and hyperband radiating systems is explored. HPEM effects on component, circuit, sub-system electronics, as well as system level drawing are discussed. The effects of HPEM on experimental techniques and the standards which can be used to control tests are described. The validity of analytical techniques and computational modeling in a HPEM effects context is also discussed.

Insight on HPEM effects experimental techniques and the standards that can be used to control tests is provided, and the validity of analytical techniques and computational modeling in a HPEM effects context is discussed. This book dispels myths, clarifies good experimental practices and ultimately draws conclusions on the HPEM interaction with electronics. Readers will learn to consider the importance of HPEM phenomena as a threat to modern electronic based technologies which underpin society and to therefore be pre-emptive in the consideration of HPEM resilience.

To order this book, contact

Artech House
www.artechhouse.com
Email: artech@artechhouse.com
US 800-225-9977
UK +44 (0)20 70596 8750

https://us.artechhouse.com/High-Power-Electromagnetic-Effects-on-Electronic-Systems-P2076.aspx

ISBN: 978-1-63081-588-2
320 pages
$168
£146

Use code GIR25 to receive 25% discount on this title! (expires 08/31/2020)

Advertising**Index**

Sales Representatives

Eastern and Central Time Zones
Carl Sheffres
Publisher
(New England, New York, Eastern Canada)
685 Canton Street
Norwood, MA 02062
Tel: (781) 619-1949
FAX: (781) 769-5037
csheffres@mwjournal.com

Michael Hallman
Associate Publisher
(NJ, Mid-Atlantic, Southeast, Midwest, TX)
4 Valley View Court
Middletown, MD 21769
Tel: (301) 371-8830
FAX: (301) 371-8832
mhallman@mwjournal.com

Pacific and Mountain Time Zones
Brian Landy
Western Reg. Sales Mgr.
(CA, AZ, OR, WA, ID, NV, UT, NM, CO, WY, MT, ND, SD, NE & Western Canada)
144 Segre Place
Santa Cruz, CA 95060
Tel: (831) 426-4143
FAX: (831) 515-5444
blandy@mwjournal.com

International Sales
Richard Vaughan
International Sales Manager
16 Sussex Street
London SW1V 4RW, England
Tel: +44 207 596 8742
FAX: +44 207 596 8749
rvaughan@horizonhouse.co.uk

Germany, Austria, and Switzerland (German-speaking)
WMS.Werbe- und Media Service
Brigitte Beranek
Gerhart-Hauptmann-Street 33,
D-72574 Bad Urach
Germany
Tel: +49 7125 407 31 18
FAX: +49 7125 407 31 08
bberanek@horizonhouse.com

France
Gaston Traboulsi
Tel: 44 207 596 8742
gtraboulsi@horizonhouse.com

Israel
Dan Aronovic
Tel: 972 50 799 1121
aronovic@actcom.co.il

Korea
Young-Seoh Chinn
JES MEDIA, INC.
F801, MisahausD EL Tower
35 Jojeongdae-Ro
Hanam City, Gyeonggi-Do
12918 Korea
Tel: +82 2 481-3411
FAX: +82 2 481-3414
yschinn@horizonhouse.com

China
Shenzhen
Michael Tsui
ACT International
Tel: 86-755-25988571
FAX: 86-755-25988567
michaelt@actintl.com.hk

Shanghai
Linda Li
ACT International
Tel: 86-021-62511200
lindal@actintl.com.hk

Beijing
Cecily Bian
ACT International
Tel: +86 135 5262 1310
cecilyb@actintl.com.hk

Hong Kong, Taiwan, Singapore
Mark Mak
ACT International
Tel: 852-28386298
markm@actintl.com.hk

Japan
Katsuhiro Ishii
Ace Media Service Inc.
12-6, 4-Chome,
Nishiiko, Adachi-Ku
Tokyo 121-0824, Japan
Tel: +81 3 5691 3335
FAX: +81 3 5691 3336
amskatsu@dream.com

Ed Kiessling • Traffic Manager • 685 Canton Street, Norwood, MA 02062 • Tel: (781) 619-1963 FAX: (781) 769-6178 • ekiessling@mwjournal.com

dB Control: Reliability by Design

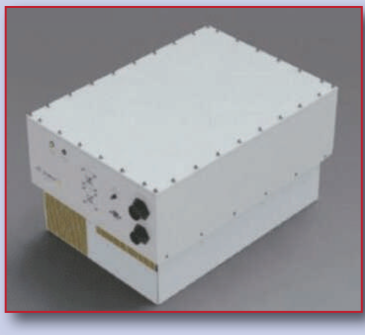

Despite the advances in solid-state technology, many high-power applications remain out of reach and still require tube amplifiers. Only a handful of companies have the heritage and expertise to supply these high-voltage products. dB Control is one of the few, formed in 1990 to repair high-voltage power supplies used on the B-52 long-range bomber. Using this experience, the company expanded its products and services to design and manufacture high-power traveling wave tube amplifiers (TWTA), microwave power modules (MPM), full transmitters with modulators and power supplies.

The TWTAs cover bands from 1 to 96 GHz and support pulsed or CW operation. The MPM family, with a modular design for dense packaging and easy customization, covers bands from 2 to 46 GHz. To complement power amplifiers, dB Control added to its portfolio with the acquisition of TTT-Cubed in 2019, offering custom instantaneous frequency measurement, frequency-locked oscillator, digital control, antenna control and other integrated subassemblies.

Most of dB Control's business serves the U.S. defense market, its products supporting radar, electronic countermeasures and data links. It continues to serve the military's repair depots, repairing or replacing TWTAs, power supplies, printed circuit board assemblies and potted modules. dB Control also applies its high-voltage expertise to commercial systems, providing contract manufacturing of X-ray tubes, power supplies and custom assemblies. Among its specialized capabilities, the firm manufactures custom high-voltage connectors and cable assemblies and both low- and high-voltage transformers, performing the winding, vacuum/pressure encapsulation and high potential (hi-pot) and high altitude testing. To ensure its high-voltage products perform at high altitude without failure, dB Control has developed proprietary materials and mixtures for potting and encapsulation, which also enable dense packaging while maintaining reliability.

With its long heritage supporting defense programs, dB Control's culture and capabilities ensure products are designed and manufactured to withstand harsh environments, whether in the air, on a ship or on land. Its 40,000 square foot facility in Silicon Valley houses design, manufacturing and an extensive test capability, including temperature, altitude, thermal shock, vibration and highly accelerated life testing (HALT). The company is ISO 9001:2015 certified and designs to the AS-9100 quality standard; assembly personnel are certified to the individual processes they perform.

dB Control's suppliers include the leading TWT manufacturers. They supply tubes to its custom specifications: tight limits on current and heater voltages. The company screens incoming TWTs to verify data sheet parameters, then tests hi-pot leakage on all leads. After final electrical test and environmental stress screening, the TWT parameters are retested to ensure no adverse changes. To provide programs with additional confidence in reliability, dB Control can develop a highly accelerated stress screen (HASS) for production HPAs.

Underlying its 30-year tenure is dB Control's expertise in high-voltage electronics and commitment to reliability, reflected by its many subsystems serving on such platforms as the Global Hawk UAV, Fire Scout helicopter and SPQ-9B shipborne radar. Programs have achieved power amplifier MTBFs greater than 12,000 hours, from a population of 400 units in the field. To dB Control, reliability is not an option — it is a requirement.

www.dbcontrol.com

WERLATONE®

NEW E-PLANE COMBINERS

Higher CW Power & Increased Duty Cycle Relative to Radial Combiners

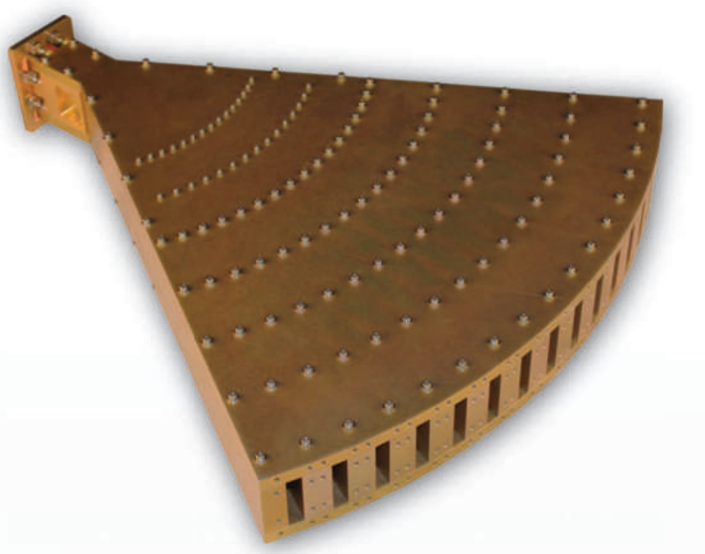

C-Band
E-Plane 16-Way Combiner
5300 - 5900 MHz
12,000 W CW, 2.5 MW Peak
WR159 Output, Half Height WR159 Inputs

- Combine Multiple High Power Solid State Power Amplifiers
- Planar Structures
- N-Way Architectures
- Coaxial or Waveguide Inputs
- Extremely Low Insertion Loss
- Scalable for S, C, X, Ku, Ka Bands
- Patented Werlatone Technology

*** CW & Peak Power of E-Plane Limited by Power Handling of Waveguide Output Connector Rating.**

Frequency	Output Waveguide	Radial Combiners	E-Plane Combiners
S-Band	WR284	≈ 2.0 kW CW	**≈ 36.0 kW CW**
C-Band	WR159	≈ 1.6 kW CW	**≈ 12.0 kW CW**
X-Band	WR90	≈ 0.55 kW CW	**≈ 2.4 kW CW**
Ku-Band	WR62	≈ 0.42 kW CW	**≈ 1.4 kW CW**
Ka-Band	WR28	≈ 0.02 kW CW	**≈ 0.4 kW CW**

Werlatone, Inc. 17 Jon Barrett Road Patterson, NY 12563 845-278-2220 sales@werlatone.com www.werlatone.com